Influence of Coupled Shear Wall Components on Structural Behaviour under Dynamic Loads

Sosena Eshetu

A Thesis Submitted to
The School of Civil and Environmental Engineering
Presented In Partial Fulfillment of the Requirements for the Degree of Master of Science in Civil Engineering (Structures)

Addis Ababa University
Addis Ababa, Ethiopia
June 2017

Addis Ababa University

Addis Ababa Institute of Technology

School of Civil and Environmental Engineering

This is to certify that the thesis prepared by Sosena Eshetu, entitled: *Influence of Coupled Shear Wall Components on Structural Behaviour under Dynamic Loads* and submitted in partial fulfillment of the requirements for the degree of Master of Sciences in Civil Engineering (Structures) complies with the regulations of the university and meets the accepted standards with respect to originality and quality.

Signed by the Examining Committee:

Dr. Shifferaw Taye Advisor	Signature	14/6/2017 Date
Dr. Abrham Gebre External Examiner	Signature	June 12, 2017 Date
Dr. Adil Zekaria Internal Examiner	Signature	13/06/2017 Date
Dr. Agizew Nigussie Chairman	Signature	Date

Dr. Agizew Nigussie
Dean, School of Civil & Environmental Engineering

Director of Postgraduate Program
Addis Ababa University
Addis Ababa Institute of Technology

ACKNOWLEDGMENT

First and foremost I would like to thank the almighty God who gave me health to carry out this research.

I would also like to take this opportunity to thank my sponsor UN for providing this special female Scholarship program and also Addis Ababa institute of Technology (AAit) for supporting me to take this chance.

A very special thanks goes to my advisor Dr. Shifferaw Taye for proposing and inspiring me to do research on this fascinating area of study. I am also grateful for his unreserved assistance, constructive and timely comments at all stages of my work. I should strongly appreciate his patience and full guidance in a lot of discussions we made on various problems I faced during the course of the work.

Finally, I would like to express my warm feeling of appreciation and thanks to my family and friends who believed in me and provided me their support in every aspect.

ABSTRACT

The growth of population density and shortage of land in urban areas are two major problems for all developing countries including Ethiopia. In order to mitigate these two problems, the designers resort to high-rise buildings, which are rapidly increasing in number, with various architectural configurations and ingenious use of structural materials. Shear walls are usually provided in tall buildings to avoid collapse of buildings under seismic forces. More often than not, such walls are pierced by numerous openings for windows, doors, service holes and other purposes. The effects of these openings on the stress distribution in the walls can be neglected if the openings are small. But in the case of larger openings, the wall could not work as one vertical element but as two or more coupled shear walls, depending on the number of rows of openings.

In this paper, a general formulation of the analysis of plane coupled shear walls is presented to investigate the behaviour of coupled shear walls subjected to lateral loads with more than one coupling beam in a story. The continuous medium method of analysis of coupled shear walls is reformulated with an additional beam parameter, number of connecting beams per story (n_b).

First the behaviour of coupled shear wall has been studied and the equations for the system have been reformulated for the beam parameter in consideration. The corresponding charts are also developed for the structural responses in question. Based on the curves plotted an illustrative example is solved and comparisons are made with solution from Extended Three dimensional Analysis of Building Systems (ETABS 2015) output.

Finally the theory of the continuous medium method is extended to give an approximate solution to the natural frequency of the coupled shear wall system.

Key words: Coupled shear walls, Continuous medium method, Generalized Single Degree of Freedom systems, Natural frequency of coupled shear walls.

DECLARATION

I, the undersigned, declare that this thesis is my original work and has not been presented in any other University, and that all sources of materials used for the thesis have been appropriately acknowledged.

Name: Sosena Eshetu Abebe

Signature:

Place: Addis Ababa University

Date of Submission:

TABLE OF CONTENTS

LIST OF FIGURES

LIST OF TABLES

LIST OF SYMBOLS & ABBREVATIONS

$2d_ı$	Width of Wall 1	[m]
$2d_2$	Width of Wall 2	[m]
α	Stiffness factor which depends on width of opening, moment of inertia of walls, height of floor and center to center distance of the walls	[1/m]
$A_ı$	Cross sectional area of Wall 1	[m²]
A_2	Cross sectional area of Wall 2	[m²]
A	Total cross sectional area of Walls	[m²]
A_b	Cross sectional area of the connecting beam	[m²]
b	Span of opening	[m]
c.g	Center of gravity	
E	Modulus of elasticity of the walls	[kN/m²]
E_{ko}	Maximum kinetic energy	
E_{so}	Maximum strain energy	
F_1	Axial force factor in the walls	
F_2	Shear flow factor in the connecting beams	
F_3	Deflection factor of the walls	
$F_ω$	Natural frequency factor of the coupled shear wall	
G_b	Shear modulus of the connecting beams	[kN/m²]
γ	Unit weight	[kN/m^3]
h	Height of story	[m]
H	Total height of the coupled Walls structure	[m]
I_1	Moment of inertia of Wall 1	[m^4]
I_2	Moment of inertia of Wall 2	[m^4]
I	Total moment of inertia of Walls	[m^4]
I_b	Moment of inertia of connecting beams	[m^4]
I_e	Equivalent moment of inertia of connecting beams which contains the shear effect	[m^4]
k	Stiffness factor which depends on cross sectional area of walls, second moment of area of walls and centre to centre distance of the shear walls	
k_1	Percentage of moment carried by individual action of walls	

k_2	Percentage of moment carried by composite action of walls	
λ	Form factor	
l	Center to center distance of wall 1 and 2	[m]
M_1 (z)	Bending moment in wall 1 as a function of height	[kN.m]
M_2 (z)	Bending moment in wall 2 as a function of height	[kN.m]
M_0	Bending moment in the walls due to axial force in the laminae	[kN.m]
m (z)	External bending moment applied on walls as a function of the height due to external loads w and P	[kN.m/m]
N (z)	Axial load in the walls as a function of height	[kN]
n (z)	Axial load in the connecting medium per unit height	[kN/m]
n_b	Number of beams per story	
υ	Poisson ratio of concrete	
ω_n	Natural vibration frequency	[rad./sec.]
P	Point load applied at the top of the walls	[kN]
$\Psi(x)$	Shape function	
q (z)	Shear force in the connecting mediums per unit height	[kN/m]
σ	Stress	[kN/m^2]
T_n	Natural vibration period	[sec.]
w	Uniformly distributed applied load	[kN/m]
t_b	Thickness of the connecting beams	[m]
t_w	Thickness of the shear walls	[m]
x (z)	Lateral deflection of the coupled walls system due to horizontal forces	[m]
z	Height coordinates	[m]
z(t)	Generalized displacement	
δv	Relative displacement at base due to elastic foundation	[m]
$\delta\theta$	Rotational displacement at base due to elastic foundation	
CSW	Coupled shear walls	
FEM	Finite element method	
Mcsw	Mass of Coupled shear walls per unit height	[kg/m]
SDF	Single degree of freedom system	

CHAPTER ONE
INTRODUCTION

1.1. Background

The usefulness of structural walls have been recognized by structural engineers long ago. The efficiency of these walls in resisting lateral loads that originate from dynamic loads such as wind, earthquakes or blast loads increases with the positions they are placed at in a particular building. Provided that the floor slabs are rigidly connected to the walls, they serve in effect as connecting beams to produce a shear interaction between the two inplane cross walls. Also, as cantilevers they are effectively restrained at their foundations, they can accept a major part of, if not all, the lateral load on a building particularly at the lower floors of a multistory building. By doing so they can considerably relieve those structural units which primarily carry gravity loads. Such structures, which consists of walls that are connected by bending-resistant elements, are termed "coupled shear walls" in which the presence of the moment-resisting connections greatly increases the stiffness and efficiency of the wall system.

Functional and often structural requirements make the use of shear walls compulsory in many buildings. Exterior walls with small openings, permanent interior partition or fire walls, and cores encasing lift shafts and stair wells are only a few of the uses of shear walls. More often than not, such walls are pierced by numerous openings for windows, doors, service holes and other purposes. The structural engineer is fortunate enough if these openings are arranged in a systematic pattern. In addition to serving the functional requirements of dividing and enclosing space, and providing fire and acoustic insulation between dwellings, the cross walls are employed as load bearing walls, since their disposition favors an efficient distribution of both gravity and lateral loads to the structural elements.

Though coupled shear walls have been accepted for quite some time as essential structural units of multistory buildings, our understanding of their behavior is not even approaching that of beam-column frames (Paulay, 1969). Earlier investigations considered the effects of both fixed and flexible foundation to predict the stresses and deformation of coupled shear walls. The analysis of coupled shear wall systems may be approached from several directions. The particular approach selected by the structural engineer will depend upon the

desired application and the design stage of the structure. If the need is for preliminary design analysis, it is more amenable to use approximate techniques. Now-a-days, it has become a standard in the design and analysis of coupled shear walls or shear wall systems to use the continuum medium technique. One benefit of this approach is that the differential equation developed, under the continuum approximation, will have a closed form solution.

1.2. Objectives

General Objectives

The analysis of coupled shear walls using continuous medium method is most popular and commonly used approximate method. But for a single coupled shear wall in which the walls' functional requirement enforce the designer to use more than one coupling beam in a single story it is important to advance the analysis method and investigate its effect on structural responses for preliminary design. So this paper aims in finding and generalizing solution method to such system of walls.

Specific Objectives

The specific objectives of this research are:

- ✓ To advance the continuous medium method to give solutions for coupled shear walls with more than one coupling beam in a story.
- ✓ To study the effect of connecting beams' by varying the number of beams in a story on behaviour of the wall's system.
- ✓ To extend the continuous medium method for the dynamics of the coupled shear walls.
- ✓ To advance understanding of behaviour and analysis of coupled shear walls.

1.3. Significance of the Study

In general, the research is concerned primarily with analysis that is suitable for preliminary analysis and design of coupled shear walls, *i.e.* it is pursued as far as it will yield solutions within the framework of the stated objectives. These include that the method would be simple and rapid in giving reasonably accurate results for deflections and internal forces for the CSW system. It would also employ a single unified theory that can be applied to a

wide range of coupled shear wall structural forms. The resulting analysis equations would be in closed form which allows a simple graphical presentation for the responses of the coupled shear walls. This is believed to offer a helpful tool to the design engineer.

1.4. Outline of the Thesis

Six chapters are contained within this study, where, Chapter one deals with introducing the general background and objectives of the thesis work.

In the second chapter, the theoretical background for the behaviour of the coupled shear walls with one row of opening supported on rigid foundation will be reconsidered based on continuous medium method. In addition, literatures will be reviewed to figure out the basic assumptions of previous works on the continuous medium method and dynamics of the coupled shear walls.

Chapter three deals with modifying and giving solutions to the equation of the coupled shear walls with more than one connecting beam in a story and investigating their effect on the structural response of the system. In addition, an illustrative analysis example is presented and comparison of the results of the continuous medium method with finite element method analysis is made to determine the accuracy of the results obtained from the continuous medium method.

Chapter four highlights the theoretical basis for the dynamics of the coupled shear wall system and tries to formulate a simpler mechanism to obtain the natural vibration frequency of the structure using factors from the previous chapter. Based on the proposed method, illustrative example and comparison of the results of the continuous medium method with finite element method is made.

Chapter five presents summary of outputs with their respective discussion.

The last chapter of this thesis is made to address the conclusion drawn from the results and discussion section and recommendations are put forward on the basis of the findings.

1.5. The Scope of the Study

As this research is concerned with extending the basic continuous medium theory for coupled shear wall structures of multiple connecting beam number in a story and its effects on structural behaviour, it is limited to only the coupled shear walls by itself and not on

interaction with other structural systems like frames. As continuous medium approach is used, the analysis is concerned with coupled shear walls on rigid foundation with single row of opening subjected to lateral loadings only. It is believed that point loads, triangularly and uniformly distributed loads represent the dynamic loads that could arise due to blast, wind or earthquake loads.

CHAPTER TWO

LITERATURE REVIEW

2.1. General Background

In this section the theory that lies behind the behaviour and analysis of coupled shear walls is presented. The assumptions and the formulation of equations to obtain the structural responses based on the continuous medium method is also presented. Note that the approach and the notations which have been used in this section are based on the study of Stafford and Coull (1991).

2.1.1. Behaviour of Coupled Shear Wall Structures

If a pair of inplane shear walls is connected by pin-ended links that transmit only axial forces between them, any applied moment will be resisted by individual moments in the two walls, the magnitudes of which will be proportional to the walls' flexural rigidities. The bending stresses are then distributed linearly across each wall, with maximum tensile and compressive stresses on opposite edges (Fig. 2.1(d)).

If, on the other hand, the walls are connected by rigid beams to form a dowelled vertical cantilever, the applied moment will be resisted by the two walls acting as a single composite unit, bending about the centroidal axis of the two walls. The bending stresses will then be distributed linearly across the composite unit, with maximum tensile and compressive stresses occurring at the opposite extreme edges (Fig. 2.1(c)).

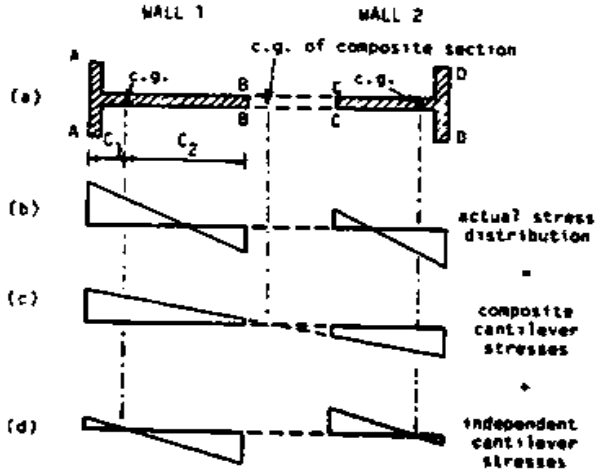

Figure 2.1 Superposition of stress distributions due to composite and individual cantilever actions to give true stress distribution in walls. Stafford and Coull (1991)

The practical situation of a pair of walls connected by flexible beams will lie between these two extreme cases, which may be regarded as bounds on the structural behaviour of a coupled wall system. The stiffer the connecting beams, the closer the structural behaviour will approach that of a fully composite cantilever. The efficiency of the system may be assessed by the degree to which it approaches the optimum behaviour of a composite cantilever.

When the walls deflect under the action of the lateral loads, the connecting beams ends are forced to rotate and displace vertically, so that the beams bend in double curvature and thus resist the free bending of the walls (Fig. 2.2). The bending action induces shears in the connecting beams, which exert bending moments, of opposite sense to the applied external moments, on each wall. The shears also induce axial forces in the two walls, tensile in the windward wall and compressive in the leeward wall. The applied moment M at any level is then resisted by the sum of the bending moments M_1 and M_2 in the two walls at that level, and the moment of the axial forces N*l*, where N is the axial force in each wall at that level and *l* is the distance between their centroidal axes.

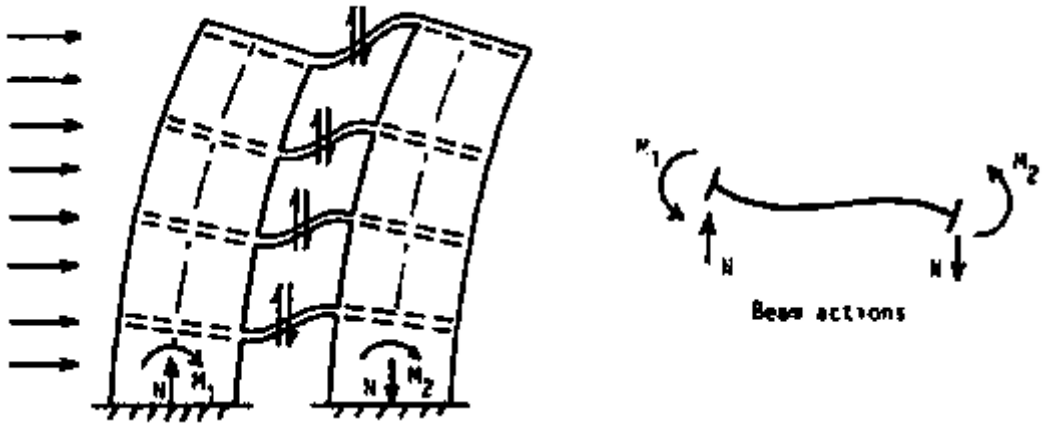

Figure 2.2 Behaviour of laterally loaded coupled shear walls. Stafford and Coull (1991)

$$M = M_1 + M_2 + Nl \qquad (2.1)$$

The last term N*l* represents the reverse moment caused by the bending of the connecting beams which opposes the free bending of the individual walls. This term is zero in the case of linked walls, and reaches a maximum when the connecting beams are infinitely rigid.

2.1.2. Derivation of the Governing Differential Equation Based on Continuous Medium Method

One of the important methods to analyze coupled shear walls is the continuous medium method Stafford and Coull (1991). The Continuous method is an approximate method which has been used since 1962. In this method, the horizontal connecting beams will be replaced by equivalent continuous mediums over the height of the building which connects the coupled walls as illustrated in Fig. 2.3. Furthermore, the basic assumptions made in the analysis are as follows:

- Each element of the coupled shear wall behaves as a perfectly elastic, homogeneous & isotropic body. The elastic properties of the material are the same throughout the structure.
- The dimensions of the walls and connecting beams will not change throughout the height of the structure.
- The floor heights are uniform so that the coupling beams are equally spaced.
- The axial deformation of the coupling beams are neglected.
- The shear deformations in the walls are neglected.

- The effect of gravity load on the coupling beam is not taken into account.
- The stiffness of the walls are so much larger than those of coupling beams, that their slopes are locally not affected by the discrete beams. Consequently the slopes and the deflections of the two walls are identical at every point over the height of the structure. Therefore, each of the coupling beams will have a point of contraflexure at its mid span.
- The stiffness of the topmost beam is one half of that of the other coupling beams.

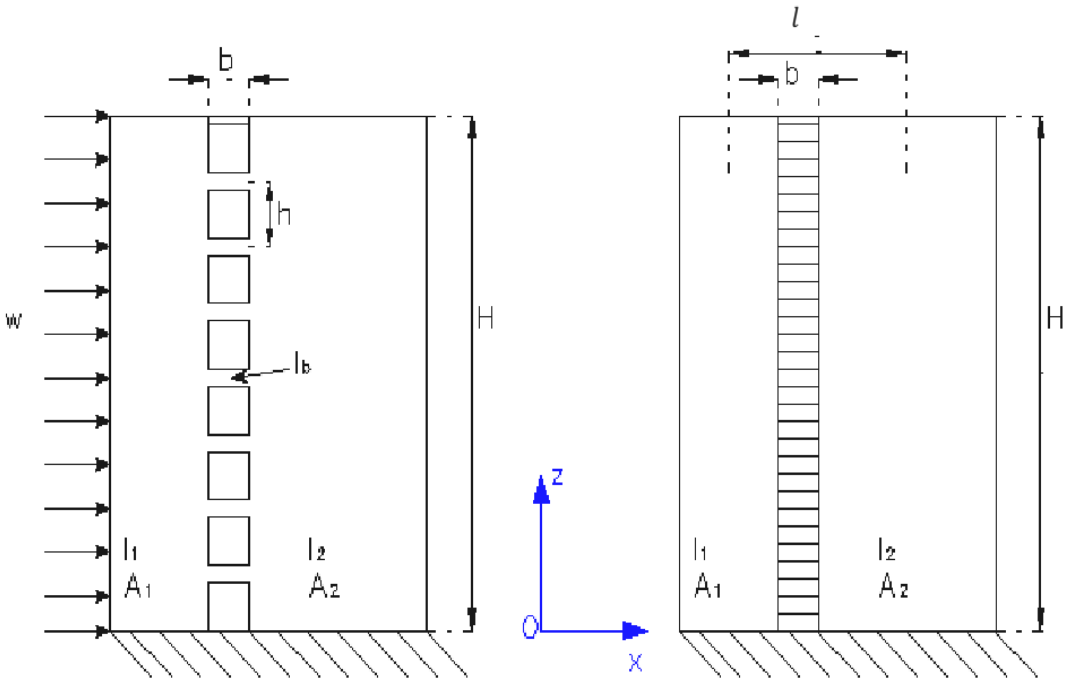

Figure 2.3 Coupled shear walls according to continuous method model

Consider the coupled shear walls system shown in Fig. 2.3. The connecting beams will be replaced by equivalent continuous mediums. To derive the equations related to internal forces in the beams and walls, the connecting medium will be cut along the vertical line of contra flexure (See Fig. 2.4). As has been mentioned in the assumptions, the point of contra flexure in the medium is identical to the midpoint of the clear span of each connecting beam. The applied forces on the shear walls and the connecting mediums will be as following:

- n(z) is axial force in the connecting mediums (per unit height)
- q(z) is the shear flow per unit height applied in the connecting mediums
- $M_1(z)$ is the bending moment in Wall 1

- $M_2(z)$ is the bending moment in Wall 2
- N(z) is the axial force in walls namely, tension in Wall 1 and compression in Wall 2
- w is the uniform distributed load
- m(z) is the external bending moment applied on walls system due to external load w

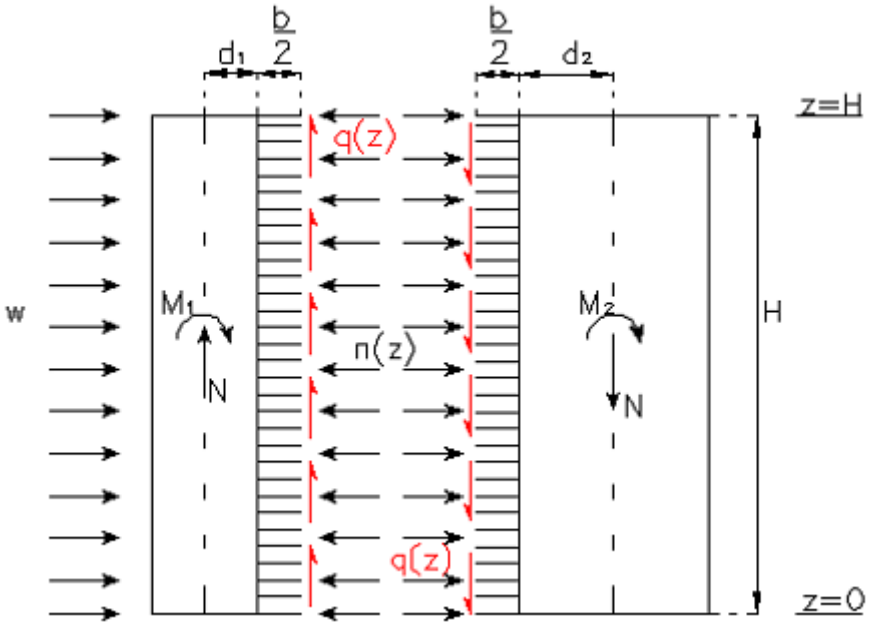

Figure 2.4 Internal forces in coupled shear walls

Since the cantilevered laminas have been cut along the line of contra flexure some relative displacements as have been shown in Fig. 2.5 to Fig. 2.8 will occur at the cut ends due to the following four basic actions. [In the derivation, positive relative displacements are taken to mean that the end of the left hand connecting beam(1) move downward relative to the end of the right end beam(2).]

1) Rotation of the wall cross section due to bending (Fig. 2.5). Due to the applied bending moment on the walls, the cross sections will rotate. It is worth to mention that there are two bending moments which act on the walls, first the bending moment due to external load and second the bending moment due to the shear force in the connecting laminas.

$$\delta_1 = \left(\frac{b}{2} + d_1\right) \times \frac{dx}{dz} + \left(\frac{b}{2} + d_2\right) \times \frac{dx}{dz} = l \times \frac{dx}{dz} \qquad (2.2)$$

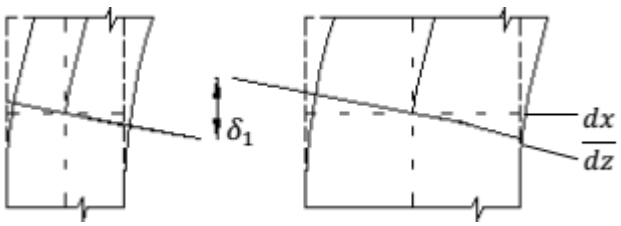

Figure 2.5 Relative displacements of the laminas due to applied bending moment on the walls

2) Deformation of the connecting mediums due to shear flow (Fig. 2.6). By considering a small part of the connecting medium with depth of dz and the flexural rigidity of EI_e the deformation of the laminas due to shear flow can be derived.

$$\delta_2 = -q\frac{b^3 h}{12EI_e} \tag{2.3}$$

In which E is the modulus elasticity of the beams and EI_e is the equivalent flexural rigidity of the connecting beams. Note that I_e includes the effect of shearing and bending deformation of the beams and can be expressed as:

$$I_{e=}\frac{I_b}{1+r} \tag{2.4}$$

$$r = \frac{12EI_b}{b^2 GA_b} \times \lambda \tag{2.5}$$

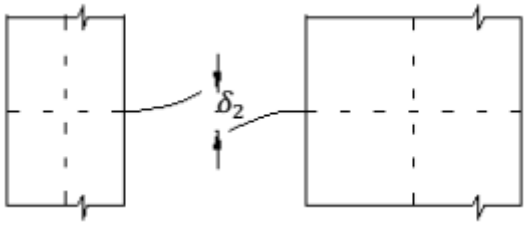

Figure 2.6 Relative displacements of the laminas due to shear flow in the connecting mediums

3) Deformation of the walls due to axial force (Fig. 2.7). As can be seen, due to the deflection of the connecting beams, the applied load will introduce a tensile force in wall 1 and a compressive force in wall 2. Note that in this equation, the modulus of elasticity for both beams and walls is assumed to be equal which defines by E.

$$\delta_3 = -\frac{1}{E}\left(\frac{1}{A_1} + \frac{1}{A_2}\right)\int_0^z N(z)dz \tag{2.6}$$

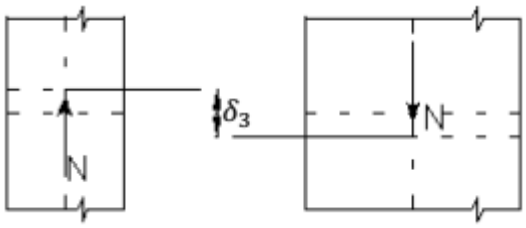

Figure 2.7 Relative displacements of the laminas due to axial force in the walls

4) Vertical and rotational relative displacements, at the base which will occur in the case of elastic foundation and it depend on the modulus of sub-grade reaction (Fig. 2.8 a & b). As has been mentioned before, in the first part of this thesis, the walls on rigid foundation will be considered which means that, relative displacement (δ_v) and rotation (δ_θ) at base will be zero.

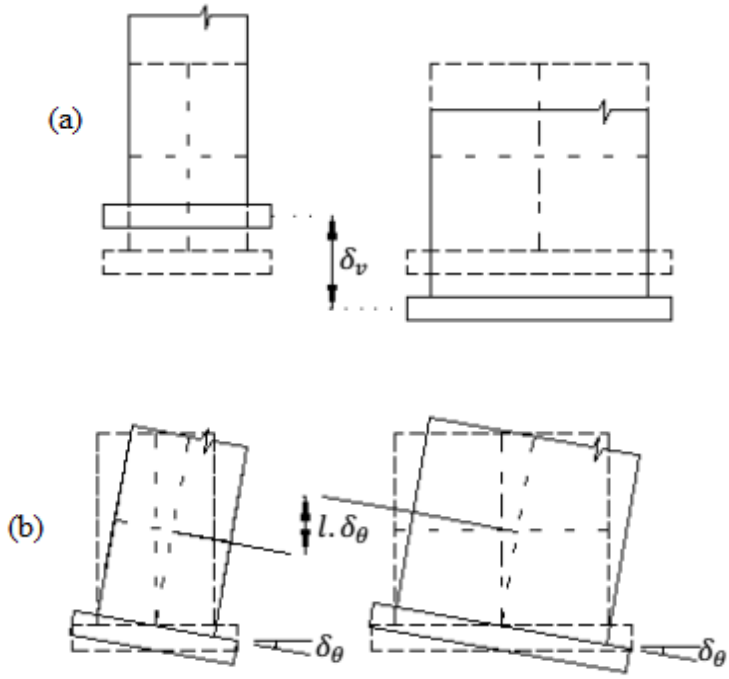

Figure 2.8 Relative displacements of the laminas due to flexible foundations

As is known, in reality there is no relative displacement at the point of contra flexure in the connecting mediums. If it is assumed that the summation of the relative displacements is equal to δ, then it can be concluded that δ is equal to zero.

$$\delta = \delta_1 + \delta_2 + \delta_3 = 0 \qquad (2.7)$$

$$\delta = l\left(\frac{dx(z)}{dz}\right) + \frac{1}{12}\frac{\left(\frac{d}{dz}N(z)\right)b^3h}{EI_e} - \frac{\left(\frac{1}{A_1}+\frac{1}{A_2}\right)\left(\int_o^z N(z)dz\right)}{E} = 0 \qquad (2.8)$$

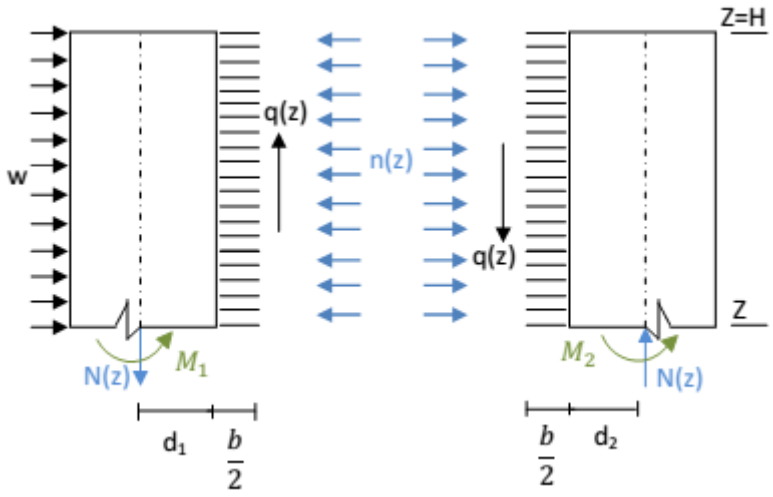

Figure 2.9 Internal forces in coupled shear walls

Considering the vertical force equilibrium in the walls (Fig. 2.9), it can be concluded that the axial force in the walls at each level is equal to the integral of the shear flow in the connecting medium from that particular level to the top.

$$\left(\int_z^H q(z)dz\right) = N(z) \qquad (2.9)$$

By differentiating from the above equation, shear flow in the mediums can be obtained.

$$q = -\frac{dN}{dz} \qquad (2.10)$$

On considering both the free bending due to the externally applied moment *M* and the reverse bending due to the shears and axial forces in the connecting medium (Fig. 2.1.9), the moment curvature relationships for the two walls are, at any level, as follows:

$$M_1 = m(z) - \left(\frac{b}{2} + d_1\right) \times \int_Z^H q(z)dz - M_0 = EI_1 \times \frac{d}{dz}\left(\frac{dx}{dz}\right) \qquad (2.11)$$

$$M_2 = -\left(\frac{b}{2} + d_2\right) \times \int_Z^H q(z)dz + M_0 = EI_2 \times \frac{d}{dz}\left(\frac{dx}{dz}\right) \qquad (2.12)$$

where M_o is the moment caused by the axial force, n (z), in the connecting beams. M(z) is the applied external moment which is equal to $\frac{w(H-z)^2}{2}$ in case of uniform distributed load. Substituting Eqn. 2.9 into above equations and addition of Eqns. 2.11 and 2.12 gives the overall moment-curvature relationship for the coupled shear walls equal to:

$$M_1 + M_2 = m(z) - l \times N(z) = (EI_1 + EI_2)\left(\frac{d^2x(z)}{dz^2}\right) \qquad (2.13)$$

$$\frac{d^2x(z)}{dz^2} = \left(\frac{m(z) - lN(z)}{E(I_1 + I_{2)}}\right) \qquad (2.14)$$

Differentiating Eqn. 2.8 with respect to z, and combining with Eqn. 2.13 to eliminate the curvature d^2x/dz^2 gives:

$$\frac{d^2}{dz^2}N(z) - k^2a^2N(z) = -\frac{a^2}{l}m(z) \qquad (2.15)$$

This is the governing equation for coupled walls expressed in terms of the axial force N.

The parameters in the equation are defined as:

$$\left(\frac{12I_e l^2}{b^3 hI}\right) = a^2 \qquad (2.16)$$

$$\left(1 + \frac{AI}{A_1 A_2 l^2}\right) = k^2 \qquad (2.17)$$

And

$$I_1 + I_2 = I$$

$$A_1 + A_2 = A$$

Alternatively, eliminating the axial force N from Eqns. 2.8 and 2.13 gives:

$$\left(\frac{d^4x(z)}{dz^4}\right) - \left(\frac{d^2x(z)}{dz^2}\right)k^2a^2 = \left(\frac{1}{EI}\right) \times \left(\frac{d^2}{dz^2}m(z) - m(z) \times (k^2 - 1)\,a^2\right) \qquad (2.18)$$

This is the governing equation for coupled walls expressed in terms of the lateral deflection x(z).

2.2. Previous Works on Coupled Shear Walls

In the subsequent sections, a review of previous works on coupled shear walls is stated that is believed to be in chronological order. The review is restricted to the brief examination of such theories put forward to assess the strength and behaviour of coupled shear walls. Works related to other interesting topics on shear walls, in particular the interaction of a set of shear walls or the interaction of shear walls and rigid jointed frames, are beyond the scope of this review.

2.2.1. Previous Works on Analysis and Behaviour of Coupled Shear Walls

Many researchers have developed analytical or numerical methods to analyze (and mostly to design) coupled shear walls, most of which pertain to the independent manner of behaviour in the two walls.

An approach, by which the statically indeterminate problem of coupled shear walls can be reduced to a relatively simple analysis, seems to originate from Chitty (1947). She studied the behaviour of a number of parallel cantilevers which are rigidly interconnected by cross-bars. These bars are replaced by an equivalent continuous elastic medium which is capable of transmitting the same actions as the cross-bars. The device enables the various actions to be expressed by continuous functions along the cantilever beams. Chitty correctly assessed the equilibrium and compatibility requirements but she neglected the effects of shear. She proposed a differential equation in terms of a continuously varying moment applied by the connecting medium to the cantilever beams. The solution of the problem is completed by satisfying the boundary conditions for the cantilever structure.

A most penetrating work on the elastic behaviour of coupled shear walls originates from Beck (1956). His first publication deals with wall panels containing one or more rows of openings. The Vierendeel girder, with deep horizontal and relatively slender vertical members, is one of the examples on which he introduced his method of analysis.

In an extract of a dissertation, Beck (1958) presented his approach in a more general form. The aim of his study was to replace a very large number of statically indeterminate quantities by a few "mathematically sensible" functions. Instead of setting up a large number of simultaneous linear equations he dealt with a few simultaneous differential equations. In many cases, and the problem of two coupled shear walls is one of these, the solution is obtained from a single second order differential equation. The larger is the degree of static indeterminancy the larger is the appeal of the laminar analysis.

In 1960 appeared the first publication of Rosman, who is the most prolific theoretical worker on the topic of coupled shear walls. Making use of the laminar system and by strain energy considerations, he established the fundamental Eulerian differential equation of the problem. He chose the solution in terms of the axial force on the walls and expressed this by trigonometric series. By applying this approach to a shear wall with two vertical rows of

openings, he showed that simultaneous, nonhomogeneous, second order differential equations with, constant coefficients, yield the required static quantities. In this rather original mathematical approach, Rosman neither allowed for shear deformations nor considered the separation forces which are exerted by the coupling beams.

In a discussion of Rosman's paper, Beck (1960) pointed out the similarity to his mathematical model and showed the complete solution by giving expressions for the laminar separation forces and the singular separation force at the top lamina.

In 1961, Paulay showed both theoretically and experimentally how reinforced Concrete coupling beams would behave and how they could meet the demand for strength and ductility. He has also shown, how the ultimate strength of the structure is attained through a specified sequence of plastification. The equations, giving the intensity of the significant structural actions, the elastic and plastic deformations are presented for each stage of the elasto-plastic behaviour. His work was extended to the experimental evaluation of Concrete coupling beams behavior on how they could meet the demand for strength and ductility.

Later in 1967, Coull and Choudhury attempted to complete the work of Rosman and Beck by introducing a simple and effective approach of analysis of coupled shear walls by the continuous method. The charts given by Coull and Choudhury are more useful than the previous ones since, using these graphs is easier and they are applicable to determine the forces at each level of the walls. As well as the previous work the bending moment, shear and the deflections at each point can be found based on the height ratio and the stiffness parameter. Moreover, Coull and Choudhury considered not only the walls subjected to uniformly distributed load but also walls subjected to the triangularly distributed load and point load.

A number of other publications, also dealing with the analysis, behaviour and strength of shear wall structures, have been reviewed by Coull and Stafford Smith (1966).

2.2.2. Previous works on the Dynamics of Coupled Shear Walls

The dynamic properties of coupled shear wall has attracted less attention from investigators (Skattum, 1971). Kanai, Tajimi, Osawa and Kobayashi (1968) did a dynamic analysis in which they neglected the longitudinal deflections of the walls, and Tani,

Sakurai and Iguchi (1969) have done a dynamic study of a related structure; the core-wall building. In 1971, Tso and chan analyzed the free vibration of coupled shear wall with equal and unequal walls. The axial deformations of the walls were included in the analysis, and dynamic tests of two models have good verification for the theoretical values of the fundamental modes and frequencies.

Shear wall buildings, in which coupled shear walls are major components, have recently been analyzed by coull and Irwin (1970) (static case). Tso and Biswas (1971), and Irwin and Heidebrecht (1971) have studied the dynamic response of such buildings.

Wang et al. (2005) used fourth order Sturm-Liouville differential equation, to determine first two periods of natural vibration of the buildings with uniform coupled shear walls. Skattum(1971) made a study of the free vibrations of planar coupled shear walls by using the variational approach and assuming the spandrels can be replaced by a system of continuous laminae. Skattum method considered the effects of longitudinal motion in an approach, which keep the motion in the longitudinal direction of the wall as separate variables. Skattum's free vibration work was conducted under the assumption of fixed foundation. Mukherjee and Coull (1973) computed the free vibrations of coupled shear walls under the continuum assumption. Their work developed the dynamical equations for a fixed base using force moment equations. The equations of motion were transformed into one sixth order differential equation, which was solved using the Galerkin technique. Mukherjee and Coull (1974) later developed an approximate technique to compute the free vibrations of coupled shear walls on flexible bases. The dynamics of coupled shear walls has not been addressed to near the degree as that of static loading. Most of the work has addressed only the free vibration analysis of the coupled shear wall system. Previous studies conducted free vibration analysis of coupled shear walls using continuum approach on fixed base (Mukherjee et al., 1973) and discrete-continuous approach (Li, 1995).

CHAPTER THREE

INVESTIGATION OF THE BEHAVIOUR OF COUPLED SHEAR WALL WITH VARYING NUMBER OF CONNECTING BEAMS

In this chapter, the coupled shear walls' behaviour is investigated by considering those structures that have more number of connecting beams. In the continuous medium method, the appropriate modification on the governing differential equation is made, solution to the equation is also given and an illustrative example is worked out.

- ✪ It is to be noted that the works are done based on the idealization of the continuous medium method and using the assumptions, notations and solution method of Stafford and Coull (1991) as given in chapter two of section 2.1.2.

3.1. Modification of the Governing Differential Equation

When there exists more than one coupling beam in a story, the difference in deriving the differential equation arises when calculating deformation of the connecting mediums due to shear flow. i.e. the shear force on a single beam, F= q(z).h now becomes $F = \frac{q(z)h}{n_b}$ where n_b is number of beams per story.

3.1.1. Equivalent Flexural Rigidity of the Connecting Beams

Consider a cantilever beam with a length of L, cross sectional area of A_b and second moment of area of I_b. If a point load, F, is applied at the end beam, the beam deflects. The total deflection of a beam subjected to a point load consists of shear and bending deflection.

a. It is known that the bending deflection of a beam due to a point load is;

$$\delta_{b,bending} = \frac{F \times L^3}{3E_b I_b} \qquad (3.1)$$

b. The shearing deflection of a beam due to a point load is:

$$\delta_{b,Shear} = \frac{F \times L}{G_b A_b} \times \lambda \qquad (3.2)$$

E_b and G_b are the modulus of elasticity and shear modulus of the beam, respectively.

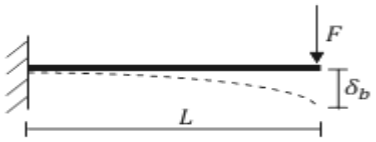

Figure 3.1 Deflection of a cantilever beam due to a point load

It is assumed that the shear flow q(z) is applied at the point of contra flexure (middle point) of the continuous mediums. As a result, each connecting beam is subjected to a shear force of q(z).h, which is assumed to be applied at the midpoint of the span. Note that h is the height of one story. Consequently, F can be substituted by q(z).h in the above equations. Further, the length of the beam is assumed to be equal to b/2 since, the relative displacement at the midpoint of the beams has to be considered. By substituting the following parameter in the above equations, the total deflection of the beam can be obtained.

- F = q(z).h
- L = b/2 is half of the span of the connecting beams
- λ is the form factor of the cross section which is equal to 1.2 for a rectangular cross section
- A_b is the cross sectional area of the connecting beams
- I_b is the second moment area of the connecting beams

As a result the total deformation of the connecting beams could be written as:

$$\delta_2 = -2 \times (\delta_{b,bending} + \delta_{b,shear}) = -2 \times (\frac{q(z) \times h \times b^3}{24 E_b I_b} + \frac{q(z) \times h \times b}{2 G_b A_b} \times \lambda) \qquad (3.3)$$

Note that, the factor 2 has been used because the relative displacement is considered at the midpoint of the beam as shown on Fig. 3.2. Therefore the relative displacement is equal to two times the displacement of half span (Fig. 3.1).

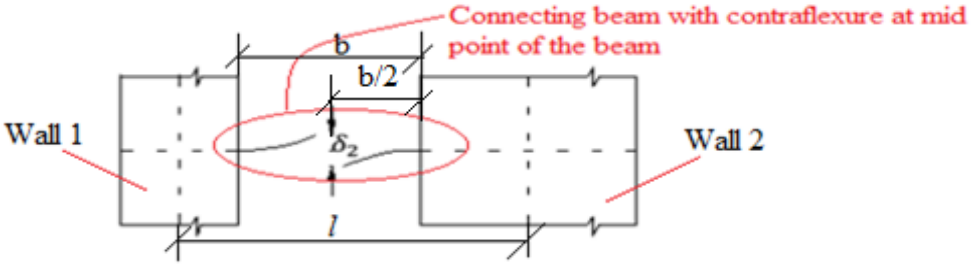

Figure 3.2 Relative displacements of the connecting mediums due to shear flow in the connecting mediums

$$\delta_2 = \left(\frac{b^3}{12E_bI_b} + \frac{b}{G_bA_b} \times \lambda\right) \times h \times q(z) \quad (3.4)$$

$$\delta_2 = -\left(\frac{b}{I_b} + \frac{12E_b}{G_bA_bb^2} \times \lambda\right) \times \frac{b^3h}{12E_b} \times q(z) = -\left(\frac{G_bA_bb^2+12E_bI_b\lambda}{I_bG_bA_bb^2}\right)\frac{b^3h}{12E_b}q(z) \quad (3.5)$$

$$= -\left(\frac{1+\frac{(12E_bI_b)}{G_bA_bb^2}}{I_b} \times \lambda\right) \times \frac{b^3h}{12E_b} \times q(z)$$

Assuming the following parameters:

$$r = \frac{12E_bI_b}{G_bA_bb^2} \times \lambda \; and \frac{1}{I_e} = \left(\frac{1+r}{I_b}\right) \quad (3.6)$$

$$\delta_2 = -\left(\frac{1+r}{I_b}\right) \times \frac{b^3h}{12E_b} \times q(z) = -\frac{1}{I_e} \times \frac{b^3h}{12E_b} \times q(z) \quad (3.7)$$

Now, for number of beams, $n_b > 1$ per story,

a. The bending deflection becomes:

$$\delta_{b,bending} = \frac{F \times L^3}{3E_bI_bn_b} = \frac{q(z) \times h \times \left(\frac{b}{2}\right)^3}{3E_bI_bn_b}$$

$$\delta_{b,bending} = \frac{q(z) \times h \times b^3}{24E_bI_bn_b}$$

b. Accordingly the shearing deflection would also be:

$$\delta_{b,shear} = \frac{F \times L}{G_bA_bn_b}\lambda = \frac{q(z) \times h \times \frac{b}{2}}{G_bA_bn_b} \times \lambda$$

$$\delta_{b,shear} = \frac{q(z) \times h \times b}{2G_bA_bn_b} \times \lambda$$

The total deformation of the connecting beams could also be written as:

$$\delta_2 = -2 \times (\delta_{b,bending} + \delta_{b,shear}) = -2 \times (\frac{q(z) \times h \times b^3}{24E_bI_bn_b} + \frac{q(z) \times h \times b}{2G_bA_bn_b} \times \lambda)$$

$$\delta_2 = -\frac{q(z) \times h \times b^3}{12E_bn_b}\left(\frac{1}{I_b} + \frac{12E_b}{G_bA_bb^2} \times \lambda\right)$$

$$\delta_2 = -\frac{q(z) \times h \times b^3}{12E_bn_b}\left(1 + \frac{12E_bI_b}{G_bA_bb^2} \times \lambda\right)$$

Assuming r and I_e as above, total deformation of the connecting beams will be:

$$\delta_2 = -\frac{q(z)\times h\times b^3}{12E_b I_e n_b} = \frac{dN}{dz}\frac{h\times b^3}{12E_b I_e n_b} \qquad (3.8)$$

where

$$\frac{dN}{dz} = -q(z) \qquad (3.9)$$

In which the equivalent flexural rigidity of the connecting beams for multiple connecting beams per story becomes, $EI_e n_b$.

3.1.2. Equation for the Axial Force and Deflection of the Wall

The vertical compatibility at the cut line of contraflexure from Fig. 2.9 for a coupled shear wall system with more than one coupling beam in a story becomes,

$$\delta = \delta_1 + \delta_2 + \delta_3 = 0, \qquad (3.10)$$

$$l\left(\frac{dx(z)}{dz}\right) + \frac{1}{12}\frac{\left(\frac{d}{dz}N(z)\right)b^3 h}{EI_e n_b} - \frac{\left(\frac{1}{A1}+\frac{1}{A2}\right)+\left(\int_0^z N(z)dz\right)}{E} = 0 \qquad (3.11)$$

where δ_2 is done for n_b>1 as shown on Eqn. 3.8.

The overall moment-curvature relationship for the coupled shear walls is unchanged and differentiating the compatibility equation (Eqn. 3.11) with respect to z and substituting for d^2x/dz^2 (same expression as Eqn. 2.14),

$$\frac{d\delta}{dz} = l\left(\frac{d^2x(z)}{dz^2}\right) + \frac{1}{12}\frac{\left(\frac{d^2}{dz^2}N(z)\right)b^3 h}{EI_e n_b} - \frac{\left(\frac{1}{A1}+\frac{1}{A2}\right)+N(z)}{E} = 0$$

$$l\left(\frac{m(z)-lN(z)}{E(I_1+I_2)}\right) + \frac{b^3 h}{12EI_e n_b}\frac{d^2N(z)}{dz^2} - \frac{1}{E}\left(\frac{A}{A_1A_2}\right)N = 0 \qquad (3.12)$$

Simplifying the above equation and substituting $\alpha^2 = \left(\frac{12I_e l^2}{b^3 hI}\right)$ and $k^2 = \left(1 + \frac{AI}{A_1A_2l^2}\right)$, as in chapter two (Eqn. 2.16 & 2.17), gives a second order differential equation based on the normal force of the shear walls as:

$$\frac{d^2N(z)}{dz^2} - k^2\alpha^2 n_b N(z) = -\frac{n_b\alpha^2}{l}m(z) \qquad (3.13)$$

where: α is a measure of the relative flexibility of the coupling beams and the walls. A low value of α indicates a relatively flexible coupling beam system. In such a case, the overall behaviour of the system will be governed by the flexural response of the

individual wall piers. A higher value of α leads to greater coupling (frame) action between the walls (Kent et.al (2004)). And

k is a measure of the relative flexural to axial stiffness of the wall piers. This parameter has a lower limit of k=1 representing axially rigid wall piers and varies up to values of about k=1.2. It should be noted that a structurally and architecturally practical coupled structure will typically have a k value less than 1.1 (Kent et.al (2004)).

The equation of the lateral deflection of the system can be determined by getting rid of the axial force. As a result, a fourth order differential equation according to the height of the structure will be found.

$$N(z) = \frac{m(z)}{l} - \frac{EI}{l}\frac{d^2x(z)}{dz^2} \qquad (3.14)$$

$$\frac{d^2N(z)}{dz^2} = \frac{d^2m(z)}{dz^2 l} - \frac{EI}{l}\frac{d^4x(z)}{dz^4}$$

$$\frac{d^2m(z)}{dz^2 l} - \frac{EI}{l}\frac{d^4x(z)}{dz^4} - k^2\alpha^2 n_b\left(\frac{m(z)}{l} - \frac{EI}{l}\frac{d^2x(z)}{dz^2}\right) = -\frac{n_b\alpha^2}{l}m(z)$$

Rearranging terms,

$$\frac{d^4x(z)}{dz^4} - k^2\alpha^2 n_b\frac{d^2x(z)}{dz^2} = \frac{1}{EI}\left(\frac{d^2m(z)}{dz^2} - \alpha^2 n_b m(z)(k^2-1)\right) \qquad (3.15)$$

3.1.3. Boundary Conditions

When the coupled walls are fully restrained at their base, to solve the differential equation and find the integration constants, the boundary conditions to be used are:

i. At the top, the axial force is zero:

$$z = H, N(H) = 0$$

ii. At the base of the wall no rotations occur, hence the lowest lamina does not deform and no actions are induced in it. Hence,

$$z = 0, \frac{dN(z)}{dz} = 0$$

iii. At the base of the wall there is no deflection or rotation due to fixed foundation,

$$x(0) = 0 \ \& \ \frac{dx(z)}{dz} = 0$$

iv. At the top, the moment is zero,

$\frac{d^2m(z)}{dz^2} = 0$ *Hence,*

$$\frac{d^3x(z)}{dz^3} - n_b(k\alpha)^2\frac{dx(z)}{dz} = \frac{1}{EI}\left(\frac{dm(z)}{dz} - n_b\alpha^2(k^2-1)\int_0^H m(z)dz\right)$$

3.2. Solution to the Governing Differential Equations

The solution to the differential equations can be obtained by substituting the expressions for the applied moment (m(z)), solving the ordinary differential equation (ODE) and applying the boundary conditions. The case for a coupled shear wall system with applied point load at the top is shown first and based on it, the modifications to the other loads are implicated. Note that the calculations have been made in mathematical software, Maple program, version 18.0 and more details about solving and simplifying the equations can be found in Appendix 1.

As a result, in the following sub sections, the solutions to the governing ODE has been computed and, the results and their outcomes for five structural responses has been illustrated as follows:

3.2.1. Axial Force in the Walls

The normal force in the shear walls for a point load applied at the top can be derived by substituting m(z) = P(H-z) in Eqn. 3.13 and solving the ordinary differential equation (ODE) using the boundary conditions. As a result, the equation of normal force in the shear walls will be:

$$N_{point}(z) = \frac{P\times H}{k^2 l}\left[1 - \frac{z}{H} - \frac{sinh\left(k\alpha H\sqrt{n_b}\left(1-\frac{z}{H}\right)\right)}{cosh\left(k\alpha H\sqrt{n_b}\right)k\alpha H\sqrt{n_b}}\right] \qquad (3.16)$$

Eqn. 3.16 shows that the distribution of the axial force throughout the height depends on the two non-dimensional variables (the relative height z/H and stiffness parameter kαH multiplied by $\sqrt{n_b}$).

- The stiffness parameter kαH may be interpreted as a measure of the stiffness of the coupling beams and is most sensitive to changes in either the stiffness or length of the coupling beam—that is, the α term. If the connecting beams have negligible stiffness (kαH=0) then the applied moment is resisted entirely by bending of the

wall piers. That is, the structure behaves as a pair of linked walls. If the coupling beams are rigid (kαH=∞) the structure behaves as a single cantilever wall. (Kent et.al (2004))

- ✪ Typically, if kαH is less than 1, the structure is considered to have negligible coupling action and behaves as an arrangement of linked walls. For values of kαH greater than about 8, the coupling beams are considered to be stiff and the structural response is dominated by that of the wall piers as described by the factor k. (Kent et.al (2004))

The normal force in the walls can also be rewritten as follows:

$$N_{point}(z) = \frac{P \times H}{k^2 l} \times F_1 \qquad (3.17)$$

where F_1 is the axial force factor in the walls due to the applied external load and can be defined as following:

$$F_1 = 1 - \frac{z}{H} - \frac{sinh\left(k\alpha H\sqrt{n_b}\left(1-\frac{z}{H}\right)\right)}{cosh(k\alpha H\sqrt{n_b})k\alpha H\sqrt{n_b}} \qquad (3.18)$$

The effect of number of beams, n_b, on the variation of the axial force factor in the walls due to point load has been drawn for different height ratio and stiffness factor, kαH in Fig. 3.3, Fig. 3.4 and Fig. 3.5.

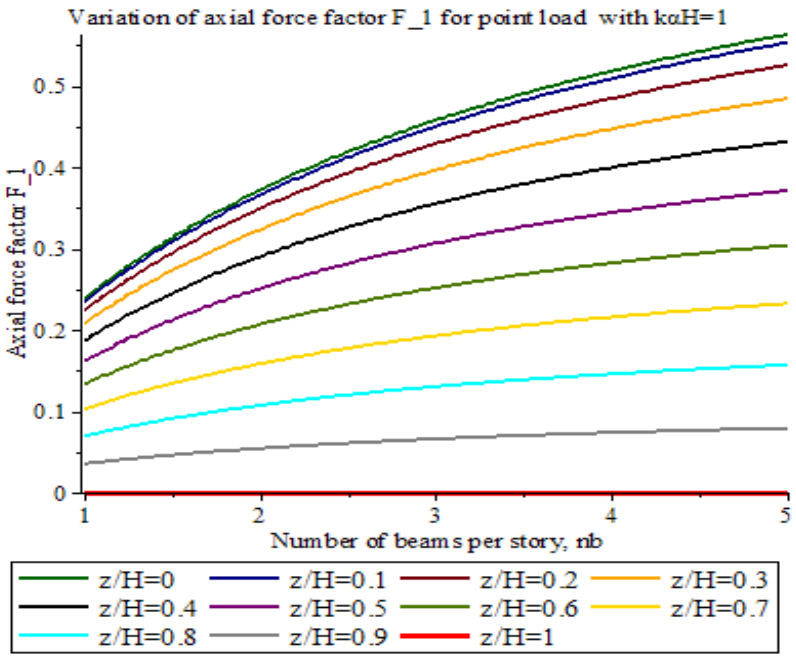

Figure 3.3 Variation of axial force factor F_1 for point load with kαH = 1

As shown in Fig. 3.3 above the value of axial force factor for kαH = 1 decreases on going up the height and increases as the number of beams per story increase from one to multiple.

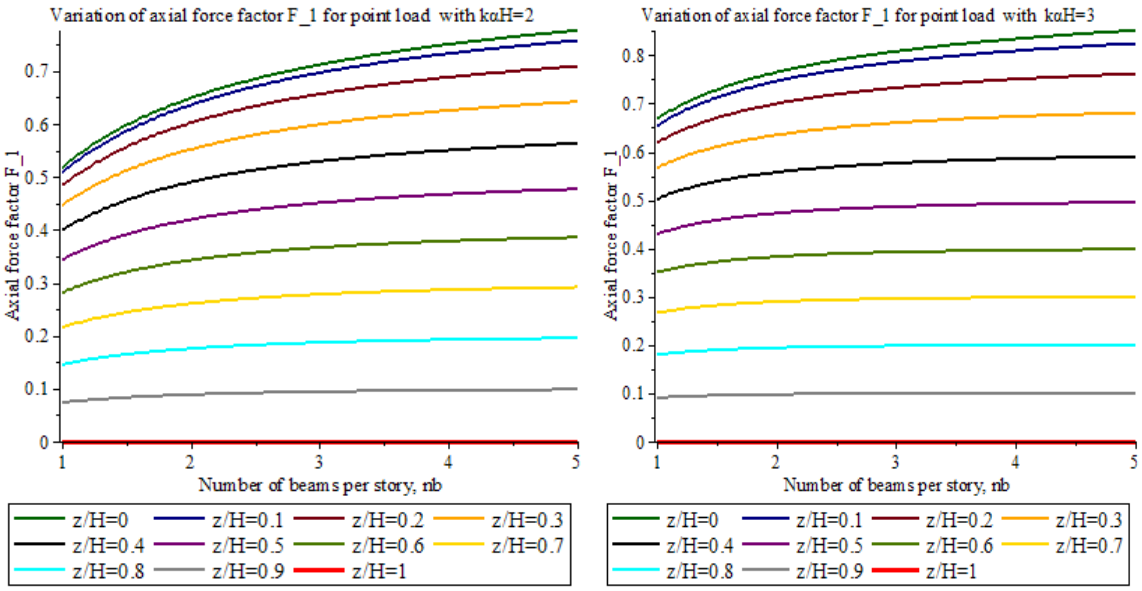

Figure 3.4 Variation of axial force factor F_1 for point load with kαH=2 and kαH= 3

The two figures above (Fig. 3.4) also show that when the stiffness parameter is increased (i.e. relative to that, if a single beam in a story was used) the variation of axial force factor with increasing number of beams is minimized specially for the upper stories.

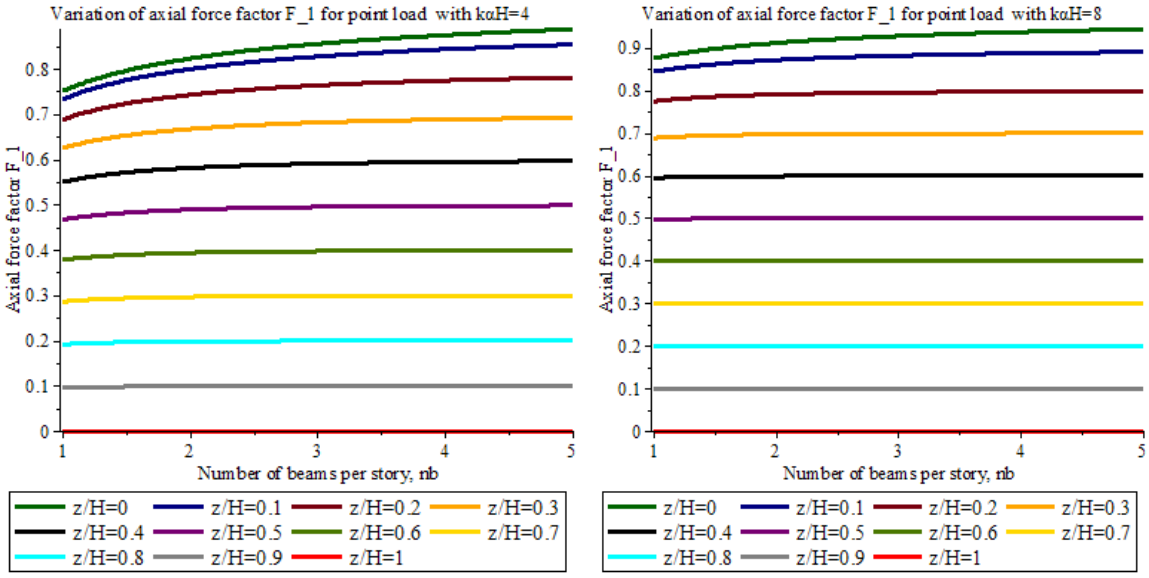

Figure 3.5 Variation of axial force factor F_1 for point load with kαH= 4 and kαH=8

In general the above graphs show that the variation of axial force factor still increases in going down the height but the increment with the beam number for a story effect becomes very small for increased value of kαH.

3.2.2. Shear Force in the Connecting Beams

According to Eqn. 3.9 by differentiating from the axial force in the wall, the shear flow in the connecting mediums can be determined:

$$q_{point}(z) = -\frac{P}{k^2 l}\left(-1 + \frac{cosh\left(k\alpha\sqrt{n_b}(H-z)\right)}{cosh\left(k\alpha H\sqrt{n_b}\right)}\right) \quad (3.19)$$

This may be expressed in a form similar to Eqn. 3.17 as:

$$q_{point}(z) = -\frac{P}{k^2 l} \times F_2 \quad (3.20)$$

In which F_2 is the shear flow factor in the connecting mediums and can be given by the following equation:

$$F_2 = -1 + \frac{cosh\left(k\alpha\sqrt{n_b}(H-z)\right)}{cosh\left(k\alpha H\sqrt{n_b}\right)} \quad (3.21)$$

The variation of shear flow factor F_2 versus the height ratio and the stiffness factor kαH has been illustrated in the Appendix 1 for various beam number. But here since our main concern is variation of shear flow factor for increased connecting beam number per story, the variation of shear flow factor versus n_b for different cases is plotted and is as shown below.

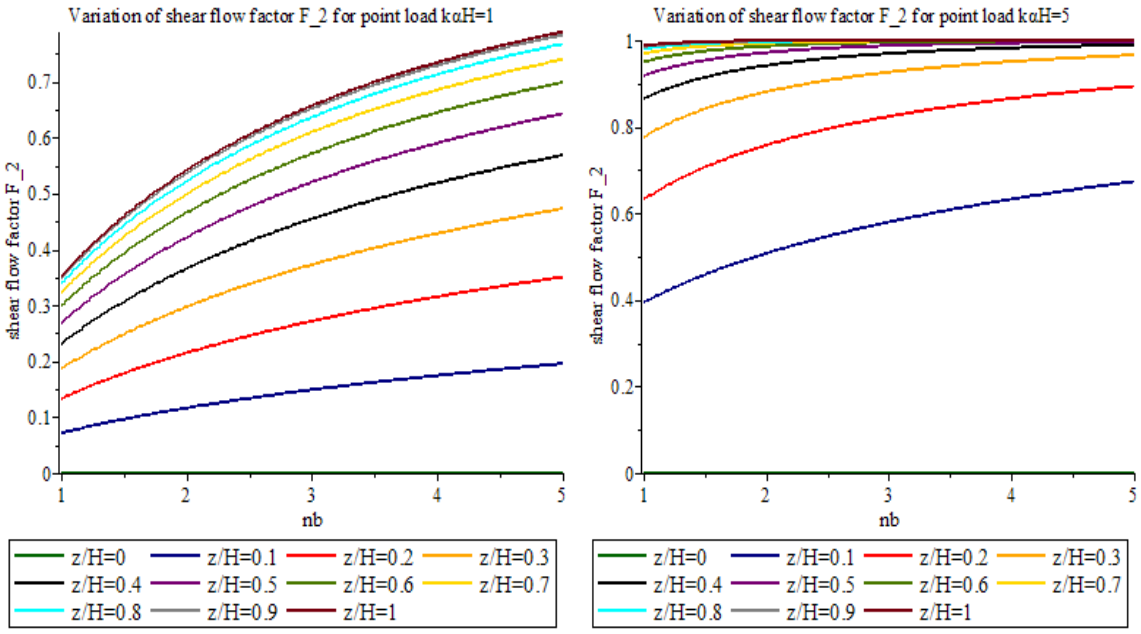

Figure 3.6 Variation of shear flow factor F_2 for point load with kαH=1 and kαH=5

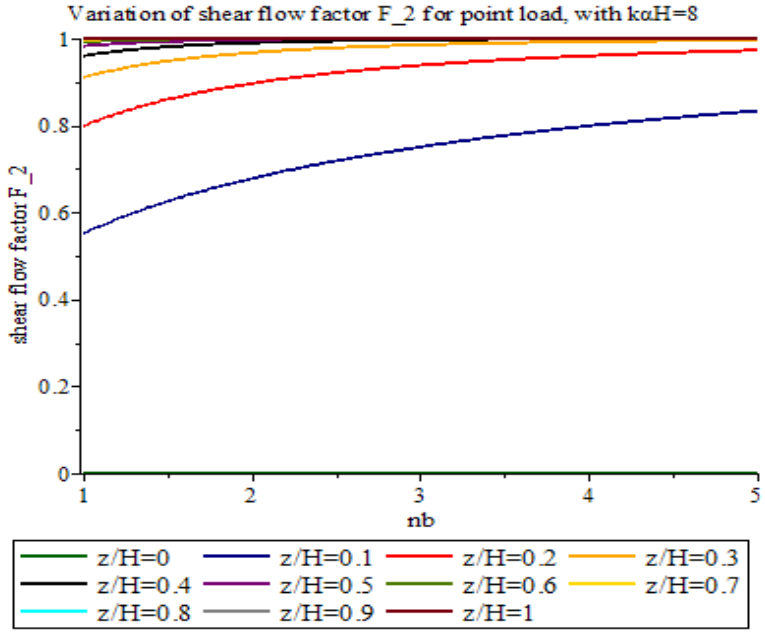

Figure 3.7 Variation of shear flow factor F_2 for point load with kαH= 8

Note: In the above graphs also it can be observed that:

1. As the stiffness parameter, kαH increases the shear flow factor increases for each height ratio despite the number of beams and reaches maximum at the top of the walls since the load is point load applied at top.

2. As number of beams per story is increased the shear flow factor also increases specially at the bottom stories. Which shows as number of beam increases the increment in shear flow is higher in the connecting beams at the lower stories rather than the corresponding upper stories of the coupled shear walls.

Shear force in the individual connecting beams

The shear force in each individual connecting beam can be calculated by integrating the shear flow over the height of each story. But this works when the connecting beam is only one in each story and for more than one story, the integration will be over the height of each story according to their number. Also calculating the area under the shear flow curve for a specified level gives the shear force in that beam.

$$Q_{z,point}(z) = \int_{z_i - \frac{h}{(2)^{n_b}}}^{z_i + \frac{h}{(2)^{n_b}}} q_{point}(z)dz \qquad (3.22)$$

$$Q_{z,point}(z) = \frac{2Ph}{k^2 l 2^{n_b}} - \frac{2P\cosh(ak\sqrt{n_b}z_i)\sinh\left(\frac{ak\sqrt{n_b}h}{2^{n_b}}\right)}{\sqrt{n_b}k^3 la} \qquad (3.23)$$

$$+ \frac{2P\sinh(\sqrt{n_b}akH)\ \sinh(ak\sqrt{n_b}z_i)\sinh\left(\frac{ak\sqrt{n_b}h}{2^{n_b}}\right)}{\sqrt{n_b}k^3 la\cosh(\sqrt{n_b}akH)}$$

3.2.3. Bending Moment in the Walls

By considering moment curvature relation of the walls and the assumption of identical deflection of the walls, it can be concluded that bending moment in each wall is proportional to its flexural rigidity. So for the coupled shear walls subjected to point load, the moment at each level of height (z) will be:

$$M_1 = \frac{I_1}{I} \times (P \times (H - z) - N(z)l) \qquad (3.24)$$

where N(z) is the axial force in the walls and it has been derived earlier.

According to Eqn. 3.17, the bending moment of the walls can be rewritten as follows:

$$M_1 = \frac{I_1}{I} * PH((1 - \frac{z}{H}) - \frac{F_1}{k^2})) \qquad (3.25)$$

$$M_2 = \frac{I_2}{I} * PH((1 - \frac{z}{H}) - \frac{F_1}{k^2})) \qquad (3.26)$$

3.2.4. Deflection

The lateral deflection x may be obtained by substituting m (z) = P (H-z) in Eqn. 3.15 and solving the ordinary differential equation (ODE) using the boundary conditions. As a result, the equation of lateral deflection will be:

$$x(z) = \frac{PH^3}{3EI}\left[\frac{(k^2-1)(3\left(\frac{z}{H}\right)^2-\left(\frac{z}{H}\right)^3}{2k^2} + \frac{3\left(\frac{z}{k^2\alpha^2H^3n_b} - \frac{sinh(k\alpha H\sqrt{n_b})-sinh\left(k\alpha H\sqrt{n_b}\left(1-\frac{z}{H}\right)\right)}{k^3\alpha^3H^3n_b^{\frac{3}{2}}cosh(k\alpha H\sqrt{n_b})}\right)}{k^2}\right] \quad (3.27)$$

According to this equation the deflection depends on the height (z), stiffness parameters α and k and the number of beams per story n_b. Therefore it is not possible to draw a diagram which shows the variation of the deflection against the height ratio. It is known that the maximum deflection occurs at the top of the coupled walls. Therefore, the height level (z) in the above equation will be substituted equal to total height of the wall (H) which gives the maximum lateral deflection of the wall as a function of α and k for different number of beams per story. The variation of the deflection factor is also illustrated in Appendix 1 for number of beams per story one up to five.

$$x(H) = \frac{PH^3}{3EIk^2}\left[1 - 3\left(\frac{1}{3} + \frac{sinh(k\alpha H\sqrt{n_b})}{k^3\alpha^3H^3n_b^{\frac{3}{2}}cosh(k\alpha H\sqrt{n_b})} - \frac{1}{k^2\alpha^2H^2n_b}\right)\right] \quad (3.28)$$

$$x(H) = \frac{PH^3}{3EI} \times F_3 \quad (3.29)$$

where F_3 is the deflection factor of the walls system due to the point load and can be given by the following equation:

$$F_3 = \frac{1}{k^2}\left(1 - 3\left(\frac{1}{3} + \frac{sinh(k\alpha H\sqrt{n_b})}{k^3\alpha^3H^3n_b^{\frac{3}{2}}cosh(k\alpha H\sqrt{n_b})} - \frac{1}{k^2\alpha^2H^2n_b}\right)\right) \quad (3.30)$$

Since variation of deflection factor depends not only on a single parameter kαH but also on k, the variation of this factor with number of beams per story shall be seen for both cases and it is shown as follows:

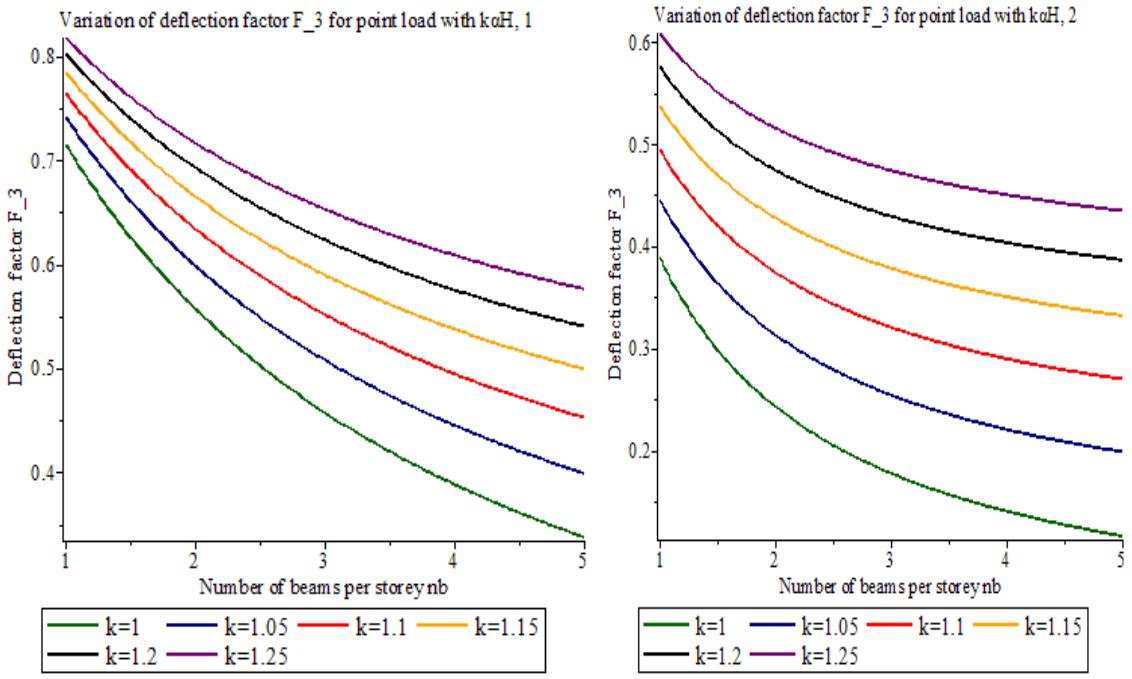

Figure 3.8 Variation of deflection factor F_3 for point load with kαH=1 and kαH=2

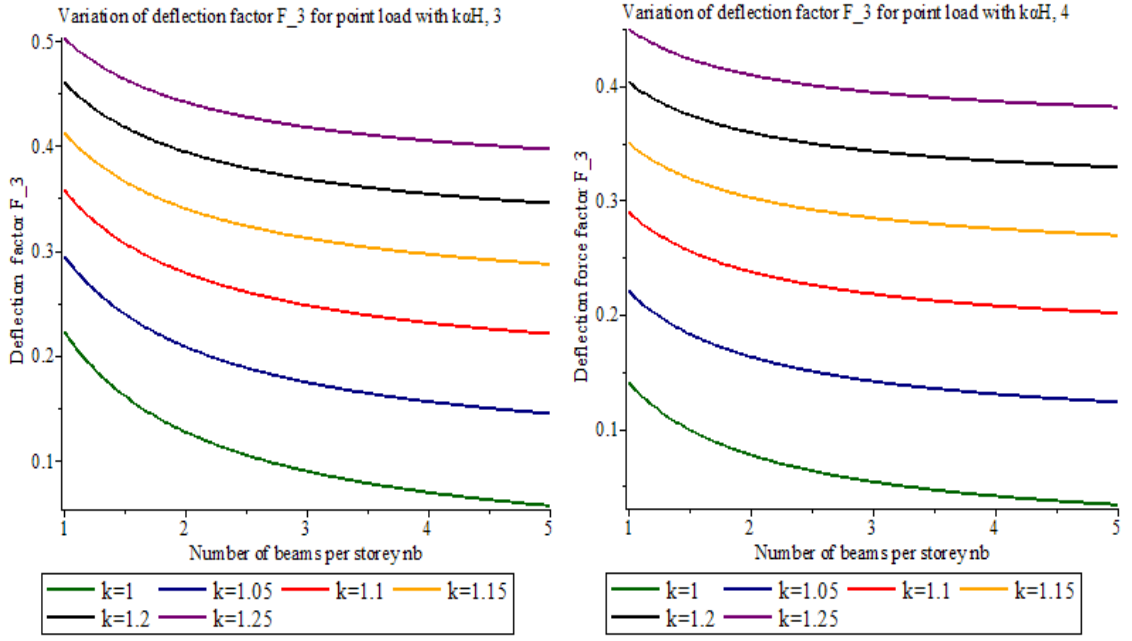

Figure 3.9 Variation of deflection factor F_3 for point load with kαH=3 and kαH=4

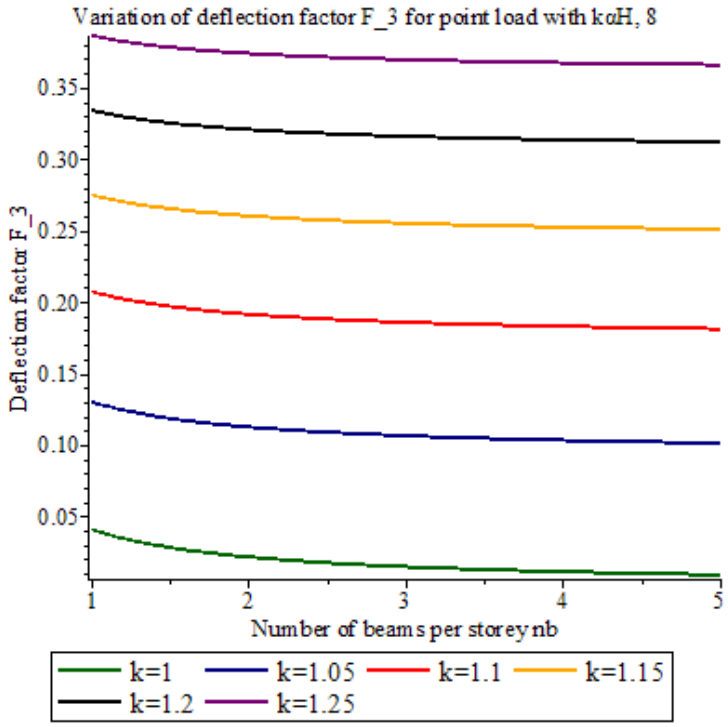

Figure 3.10 Variation of deflection factor F_3 for point load with kαH=8

The above five graphs (Fig. 3.8 up to Fig. 3.10) show that the deflection factor F_3 at top of the walls becomes smoother as number of beams, n_b increase for higher values of kαH, especially as values get closer and higher to value of kαH=8 for all values of the wall parameter k.

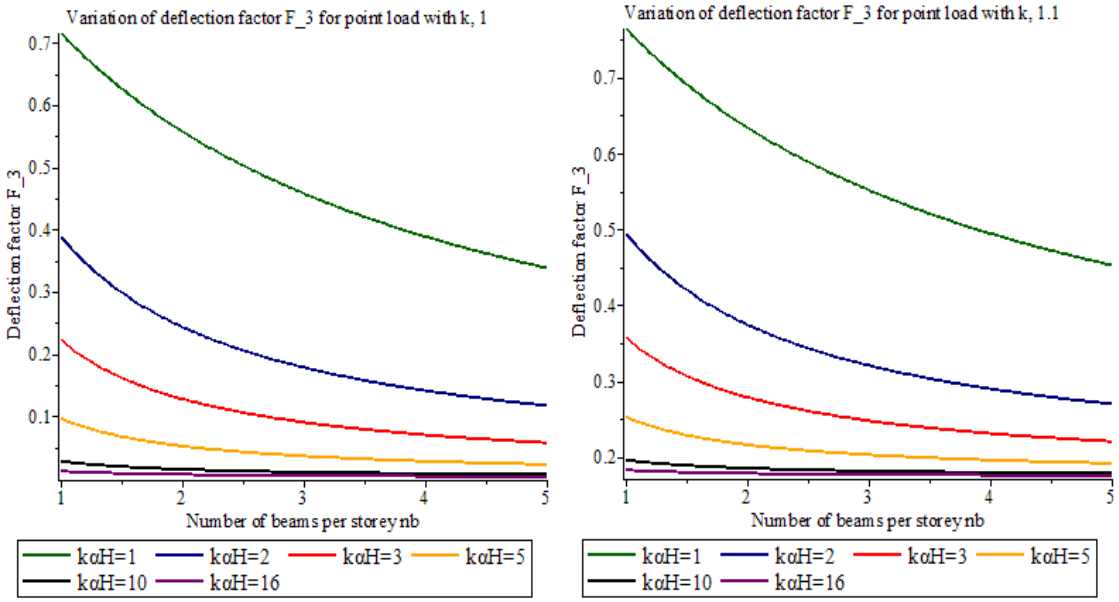

Figure 3.11 Variation of deflection factor F_3 for point load with k=1 and k=1.1

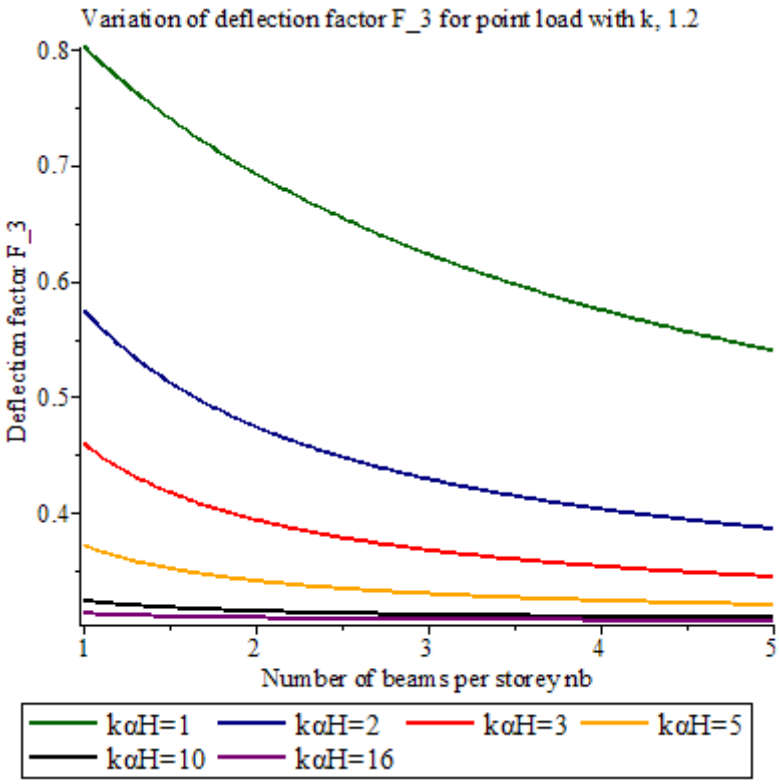

Figure 3.12 Variation of deflection factor F_3 for point load with k=1.2

The second observation that can be made on deflection factor, F_3 is its variation with the wall parameter, k. It can be seen that with increasing number of beams in a story the same pattern is observed for variation of the wall parameter, k. i.e. even though the value of k increases the variation of deflection factor, F_3 for various values of stiffness parameter kαH shows the same pattern (deflection factor F_3 decrease as n_b increase). The only variation is with k value increasing, the margin of the factor F_3, shifts up.

3.2.5. Stress in the Walls

Up to now the internal forces and the deflection of the coupled shear walls have been considered which are depending on the stiffness factor, kαH, number of beams per story n_b and the height ratio, z/H. Another important aspect about the coupled shear walls is the efficiency of the coupling which has a large impact on the design and optimization of the connection. Consider a pair of coupled shear walls. The stress distribution at any section due to the applied load is shown in Fig. 3.13. The actual stress at each section is a superposition of the stress due to axial load on the wall and the stress due to acting bending moment in each wall.

$$\sigma_A = \frac{\left(m(z) - \left(N_{point\ load}\right) \times l\right) I_1 c_1}{I} + \frac{N_{point\ load}}{A_1}$$

$$\sigma_B = \frac{\left(m(z) - \left(N_{point\ load}\right) \times l\right) I_1 d_1}{I} + \frac{N_{point\ load}}{A_1} \qquad (3.31)$$

In which N_{point} (z) is the axial force in the walls. Further, I and A_1 are the summation of second moment of area of the walls 1 and 2 and cross sectional area of wall 1 respectively. Note that, the same expression holds for the stress in wall 2 at point C and D.

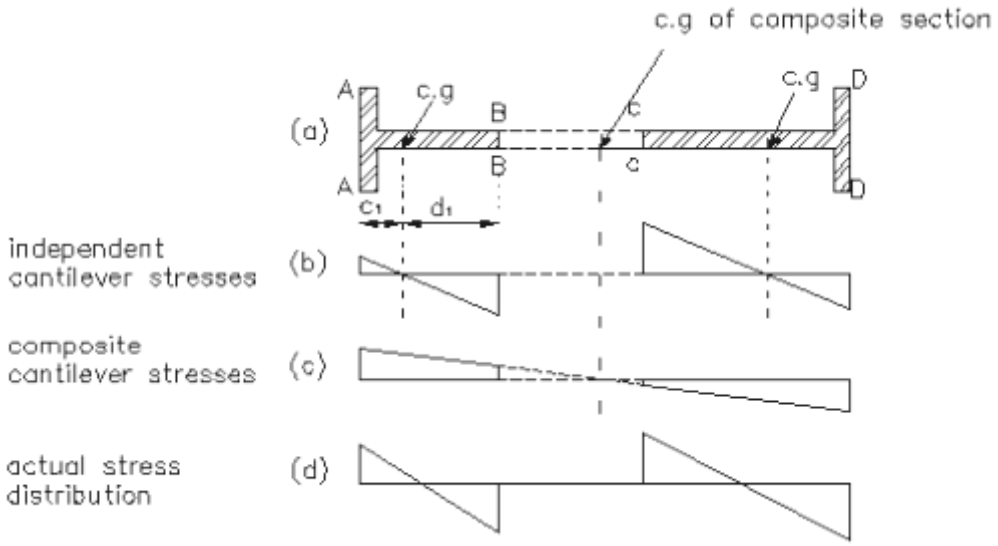

Figure 3.13 Stress distribution due to composite and individual cantilever action

Note that, c.g is used as a notation for center of gravity.

The actual stress distribution can also be derived by an alternative superposition of:

1. Assuming that the coupled walls act as a single composite cantilever system. In this case the neutral axis is situated at the centroidal axes of the wall element, as has been illustrated in Fig. 3.13 (c). If it is assumed that k_2 is the percentage of the bending moment which is resisted by the walls as a composite cantilever system, the total moment which will be carried by the walls is:

$$M_{composite} = m(z) \times \frac{k_2}{100} \qquad (3.32)$$

Consequently the stress distribution at each section will be:

$$\sigma_A = \frac{m(z)}{I + \frac{A_1 A_2}{A} . l^2} . \left(\frac{A_2 l}{A_1} + C_1\right) . \left(\frac{k_2}{100}\right)$$

$$\sigma_B = \frac{m(z)}{I + \frac{A_1 A_2}{A} . l^2} . \left(\frac{A_2 l}{A_1} - d_1\right) . \left(\frac{k_2}{100}\right) \qquad (3.33)$$

2. Assuming that the coupled shear walls act as two completely independent cantilevers. In this case the neutral axis is situated at the center of each wall. If k_1 is the percentage of the bending moment which is resisted by the two independent cantilever system the total moment carried by the walls will be:

$$M_{individual} = m(z) \times \frac{k_1}{100}$$

$$\sigma_A = \frac{M_1 \times c_1}{I_1} = \frac{m(z) c_1}{I} \times \frac{(100 - k_2)}{100}$$

$$\sigma_B = -\frac{M_1 \times d_1}{I_1} = -\frac{m(z) d_1}{I} \times \frac{(100 - k_2)}{100} \qquad (3.34)$$

Substituting summation of Eqn. 3.31, 3.33 equal to Eqn. 3.34, and the value of composite factor k_2 can be determined.

$$k_2 = \frac{100}{(H-z) n_b k\alpha} \times \left(\frac{sinh\left(\sqrt{n_b} k\alpha z - \sqrt{n_b} k\alpha H\right)}{cosh\left(\sqrt{n_b} k\alpha H\right)} + \left((H - z) n_b k\alpha\right)\right) \qquad (3.35)$$

The variation of k_1 and k_2 as a function of height ratio and kαH has been illustrated in Fig. 3.14 & 3.15.

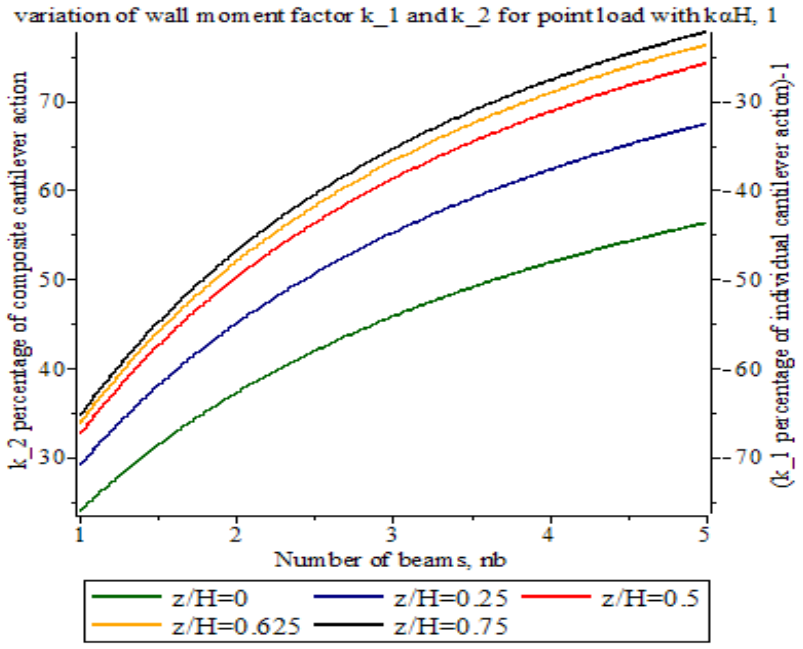

Figure 3.14 Variation of wall moment factor k-1 and k-2 for point load with kαH= 1

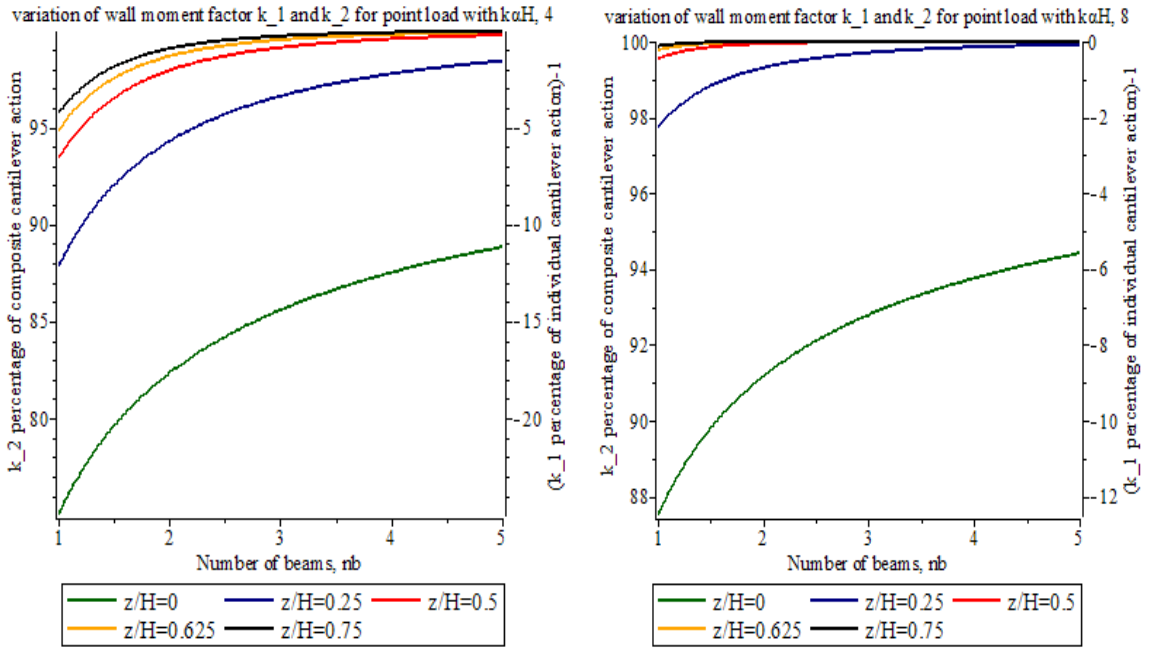

Figure 3.15 Variation of wall moment factor k-1 and k-2 for point load with kαH= 4 and kαH=8

As can be seen, in the higher level of the walls the composite action factor is larger especially for increased value of the stiffness factor kαH. Furthermore, it can be seen that the value of composite action will be increased by increasing the number of beams in a story especially for low values of kαH. Moreover, variation of composite action factor still exists at lower stories even for increased stiffness parameter kαH.

3.3. Numerical Analysis

In this section, first sample coupled shear wall problem is solved numerically. In the second section, a single case of coupled shear wall systems with varying beam number per story is analyzed using the modified continuous medium method and next using Extended Three dimensional Analysis of Building Systems (ETABS) and the results are included in this report which is believed to be self-explanatory.

3.3.1. Illustrative Example

In the analysis example made, coupled shear wall widths of 5m and 7m with a thickness of 0.3m and coupling beam width of 2.5m and 0.4m depth is taken. A point lateral load of 100 kN is applied at the top story.

To determine the stress, bending moment, axial force and the deflection of the walls and connecting beams the curves from the previous sections and from Appendix 1 have been used. The effect of self-weight of the members has been ignored since in the continuous medium method the effect of self-weight is not considered. The following are the various parameters used in the analysis example.

Material:

Concrete: Modulus of elasticity, E=30GPa

Poisson's ratio, υ= 0.2

Shear wall section:

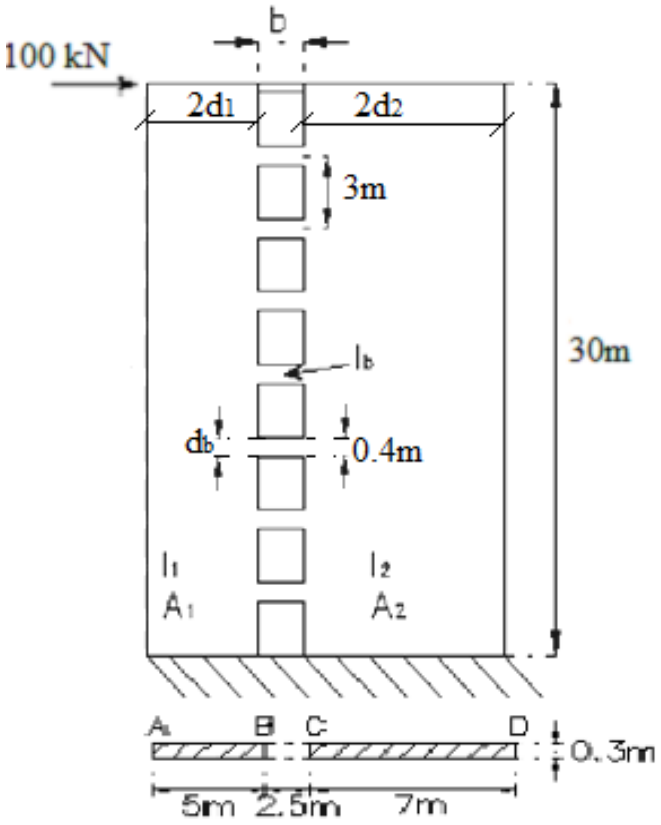

Figure 3.16 Sample CSW structure

Number of beams per story, n_b=2

a. Determine the area and the second moment of area of the connecting beams and the shear walls illustrated in Fig. 3.16. It should be noted that in this example a high modulus of elasticity is used for the walls and beams since the walls system is assumed to be uncracked.

Table 3.1 Properties of the coupled walls

H	[m]	30	**d_b**	[m]	0.4
L	[m]	8.5	**$t_w=t_b$**	[m]	0.3
$2d_1$	[m]	5	**H**	[m]	3
$2d_2$	[m]	7	**E**	[kN/m^2]	30000000
b	[m]	2.5	**G**	[kN/m^2]	12500000
b_e	[m]	2.7			

- In the evaluation of δ_2, it was assumed that the connecting beam is rigidly connected to the wall and thus ignores the effects of local elastic deformation at the beam-wall junction that will increase the flexibility of the connecting beams. Both elasticity and finite element studies have shown that the additional flexibility that arises may be included by the simple expedient of extending the beam length by a further quarter beam depth into the wall at each end. The length b sould thus be taken as b_e= b (the true length)+½ beam depth. Stafford and Coull (1991)

Table 3.2 Cross sectional properties of connected beams and shear walls

A_1 (m^2)	1.5	**A_b(m^2)**	0.12
A_2 (m^2)	2.1	**I_b(m^4)**	0.0016
A (m^2)	3.6	**E (kN/m^2)**	30000000
I_1 (m^4)	3.125	**G**	12500000
I_2 (m^4)	8.575	**r**	0.073728
I (m^4)	11.7	**I_e**	0.00149014

b. Determine the stiffness parameter kαH

k	**α**	**kαH**	**k^2**	**α^2**
1.08861	0.04324	1.41227	1.18507	0.00187

c. By using the curves in the Appendix for n_b=2 and Eqn. 3.17 the axial force at any level of the walls can be determined.

d. The bending moment throughout the height in each wall can be determined according to the Eqns. 3.25 and 3.26. The variation of the axial force and the bending moment for this example has been shown in Fig. 3.17 to indicate the effect of coupling on the magnitude of bending moment in the walls.

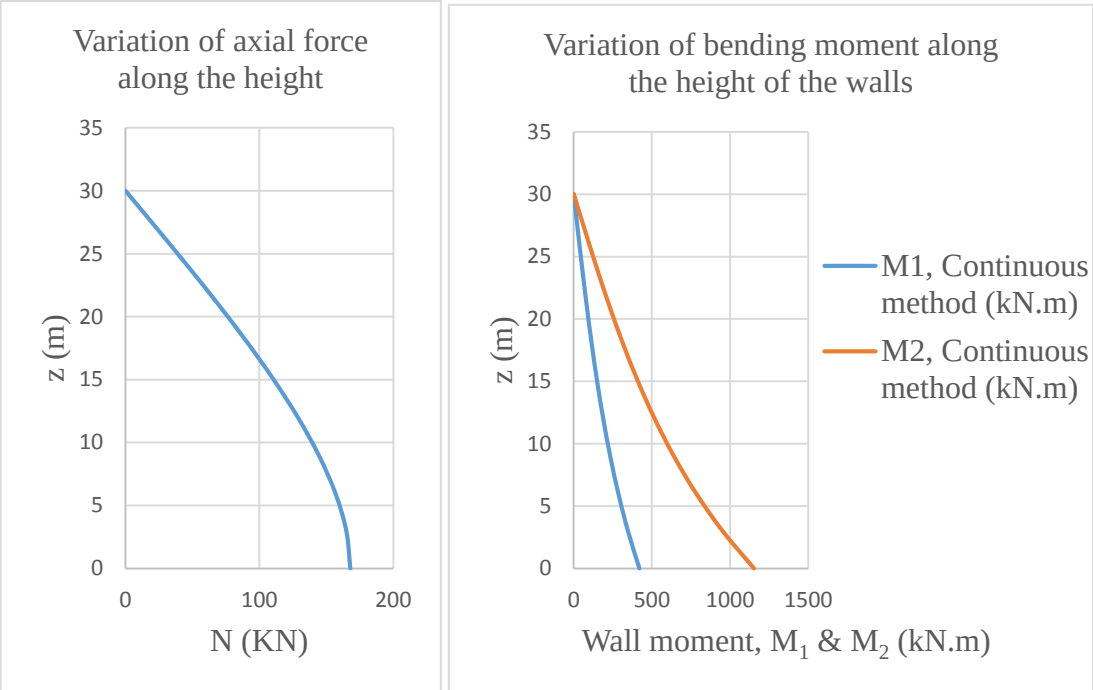

Figure 3.17 Distribution of the axial force and bending moment in the walls along the height

e. To determine the max shear force, the curve from chart in Appendix 1 for shear flow factor with n_b=2 have been used. Since the load is point load, as can be seen from the curve on the figure in Appendix 1, the maximum shear force occurs at the level z/H= 1 in all cases. The maximum shear factor F_2 at this level is about 0.73, as a result the maximum shear flow will be:

$$q_{max} = \frac{P}{k^2 l} \times F_2 = \frac{100}{1.185 \times 8.5} \times 0.73 = 7.251 kN/m$$

Consequently the maximum shear force in connecting beams will be:

$$Q_{max} = q_{max} \times h = 21.753\ kN$$

The maximum possible moment in any connecting beam is:

$$M_{max} = Q_{max} \times \frac{b}{2} = 21.753 \times \frac{2.5}{2} = 27.19\ kN.m$$

It should be noted that, with this method the amount of shear force in the connecting beams can be overestimated. The reason is that here, it is assumed that the maximum shear flow is constant throughout the height of a story though; the accurate shear force in a connecting

beam is equal to the integration of the shear flow from $\frac{h}{(2)^{n_b}}$ above to$\frac{h}{(2)^{n_b}}$under the considered beam.

f. To determine the maximum deflection at the top, figure from Appendix 1 will be used to figure out the deflection factor and then the top deflection will be given by Eqn. 3.29. For k = 1.088 and kαH = 1.412, F_3 is equal to 0.483.

$$x(H) = \frac{PH^3}{3EI} \times F_3 = \frac{100 \times 30^3}{3 \times 30 \times 10^6 \times 11.7} \times 0.483 = 0.00124m$$

As can be seen due to coupling, the maximum deflection at the top is reduced by to 0.483 of its original value, this means that if the walls were not coupled the maximum deflection would be:

$$x(H) = \frac{PH^3}{3EI} = \frac{100 \times 30^3}{3 \times 30 \times 10^6 \times 11.7} = 0.00256$$

g. Now the effect of the coupling will be considered by determining the percentage of moment carrying by individual cantilever action (k_1) and the percentage carrying by composite cantilever action (k_2). Using the curves in Appendix 1 for n_b=2 gives:

$$k_1 = 49\% \ and \ k_2 = \ 51\%$$

It is known that the maximum moment is applied at the base of the wall.

$$M = P \times H = 100 \times 30 = 3000kN.m$$

Part of the moment carried by individual action: $k_1 \times M = 0.49 \times 3000 = 1470 \ kN.m$

The bending moment in each wall is proportional to second moment of area.

$$Moment\ of\ wall\ 1: M_1 = \frac{I_1}{I} \times M \times k_1 = \frac{3.125}{11.7} \times 1470 = 392.62 \ kN.m$$

$$Moment\ of\ wall\ 2: M_2 = \frac{I_2}{I} \times M \times k_1 = \frac{8.575}{11.7} \times 1470 = 1077.38 \ kN.m$$

Part of the moment carried by composite action: $k_2 = 0.51 \times 3000 = 1530 \ kN.m$

h. Having the percentage of the composite cantilever action and the individual cantilever action, the stress at the extreme fiber of the walls can be calculated by using beam theory.

Effective composite second moment of area of the wall system:

$$I_g = I_1 + I_2 + \frac{A_1 \times A_2}{A} \times l^2 = 3.125 + 8.575 + \frac{1.5 \times 2.1}{3.6} \times 8.5^2 = 75\, m^4$$

Centre of the gravity for composite wall system is positioned at a distance of 7.45 m from the left corner of the wall which is shown in Fig. 3.13 (a).

$$\sigma_A = \frac{392.62 \times 2.5}{3.125} + \frac{1530 \times 7.45}{75} = 466.1 \frac{kN}{m^2}$$

$$\sigma_B = -\frac{392.62 \times 2.5}{3.125} + \frac{1530 \times 2.45}{75} = -264.12 \frac{kN}{m^2}$$

$$\sigma_C = \frac{1077.38 \times 3.5}{8.575} - \frac{1530 \times 0.05}{75} = 438.73 \frac{kN}{m^2}$$

$$\sigma_D = -\frac{1077.38 \times 3.5}{8.575} - \frac{1530 \times 7.05}{75} = -583.6 \frac{kN}{m^2}$$

The above illustrative example for a coupled shear wall is believed to be self-explanatory on the analysis of coupled shear walls with more than one beam per story.

3.3.2. Comparisons of results from continuous medium method and computer analysis using finite elements

There are two main methods to analyze the coupled shear walls: the approximate methods and more exact techniques. Up to now the continuous method for the coupled shear walls with one row of opening has been studied. Furthermore, the related equations and the design curves have been derived. In this Section the results obtained from analysis of the coupled shear walls based on the FEM and continuous medium method will be numerically compared.

For the numerical investigation, the system of coupled shear walls which was given in the previous example has been analyzed by using the FEM. For this reason the Extended Three dimensional Analysis of Building Systems (ETABS), has been used. Analyzing structures calls for choosing the type of idealizations that would approximate with satisfactory precision to the real structure behaviour. So the coupled shear walls system has been modeled as plane stress element and appropriate mesh is provided to maintain the modelling errors at as low level as possible considering the will to fast attain to actual results. A representative model with its structural response output has been shown in Appendix 3.

Case I: Number of beams per story, n_b=1

a. Axial force in the walls n_b=1

Table 3.3 Axial force in the walls, n_b=1

z (m)	F_1	$N_{point}(z)$, Continuous method (kN)	$N_{point}(z)$, ETABS (kN)
0	0.41997	125.077	118.316
3	0.41309	123.028	122.877
6	0.39395	117.327	116.525
9	0.36458	108.581	107.677
12	0.32677	97.3204	96.7052
15	0.28208	84.0109	84.022
18	0.23191	69.0674	70.0808
21	0.1775	52.8634	55.374
24	0.12001	35.7409	40.3702
27	0.0605	18.0185	24.5151
30	0	0	-3.5222

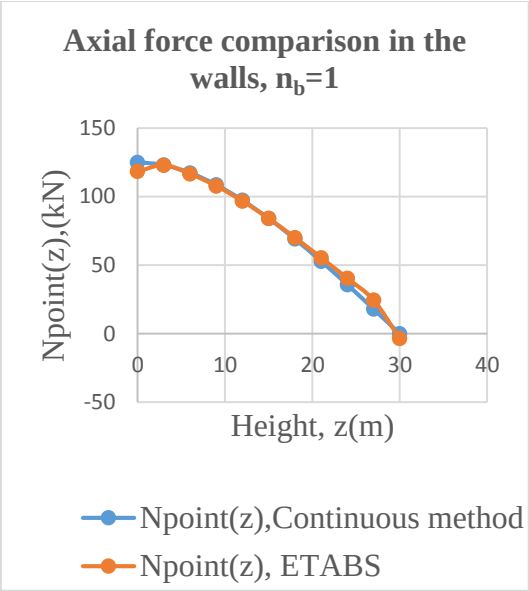

Figure 3.18 Axial force comparison in the walls, n_b=1

b. Bending moment in the walls, n_b=1

Table 3.4 Bending moment in the walls, n_b=1

z (m)	M_1, Continuous method (kN.m)	M_1, ETABS (kN.m)	M_2, Continuous method (kN.m)	M_2, ETABS (kN.m)
0	517.319	568.668	1419.52	1425.647
3	441.844	454.196	1212.42	1208.156
6	374.659	378.015	1028.06	1039.604
9	314.386	315.547	862.675	879.2526
12	259.823	263.732	712.954	726.1406
15	209.911	221.845	575.996	577.7071
18	163.709	190.691	449.218	430.2934
21	120.369	169.707	330.292	282.1009
24	79.1139	150.733	217.089	139.6398
27	39.2207	108.638	107.622	29.1288
30	9.5E-14	8.1114	2.6E-13	9.9938

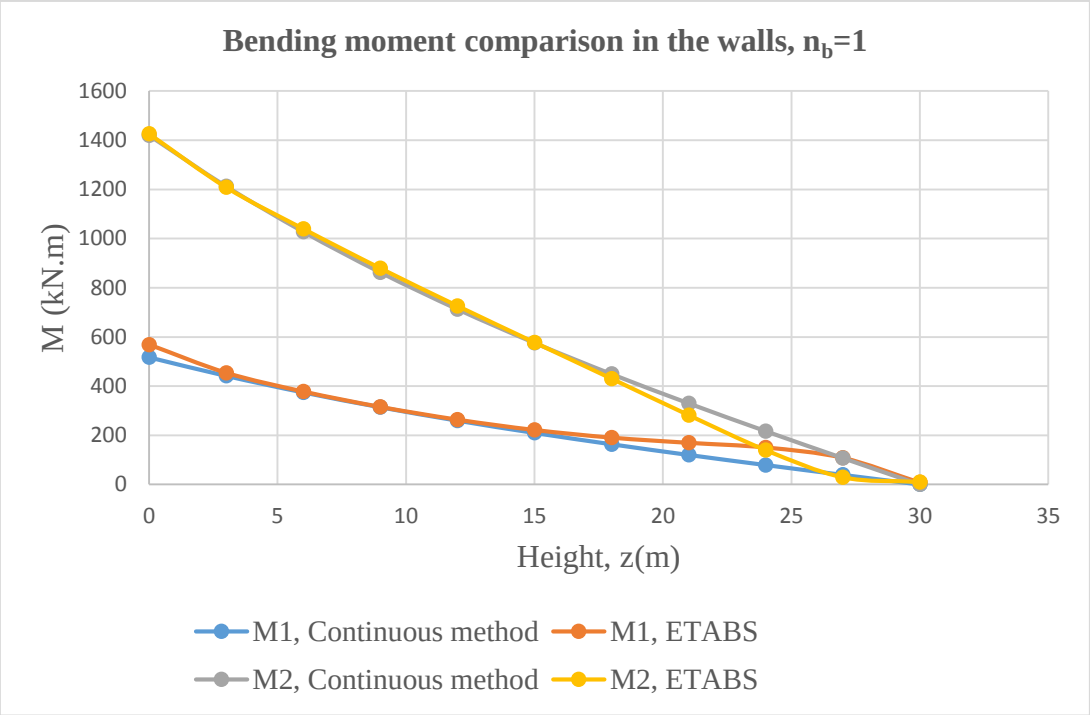

Figure 3.19 Bending moment comparison of in the walls, n_b=1

c. Shear flow in connecting beams, n_b=1

Table 3.5 Shear in connecting beams, n_b=1

z (m)	F_2	Q(z), Continuous method (kN)	Q(z) ETABS (kN)
0	0	0	0
3	0.133754	3.983719	3.5771
6	0.245697	7.317849	6.6014
9	0.338649	10.08634	9.1093
12	0.41495	12.35888	11.171
15	0.476521	14.19271	12.8433
18	0.524912	15.63398	14.176
21	0.561342	16.719	15.2161
24	0.586727	17.47506	16.0051
27	0.601706	17.92122	16.4925
30	0.606658	18.0687	13.124

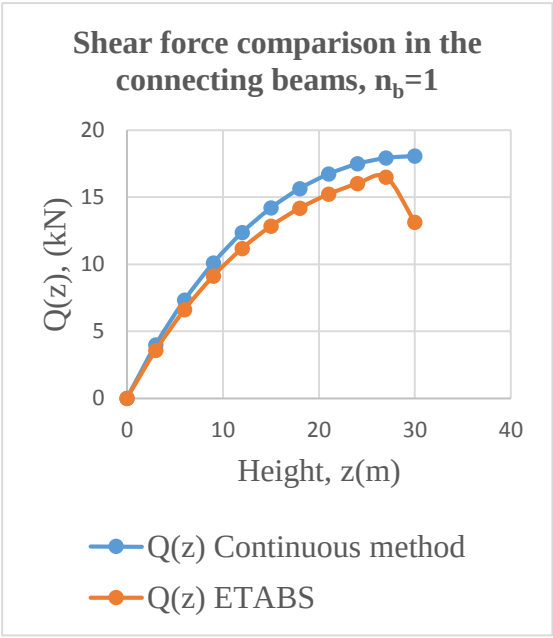

Figure 3.20 Shear force comparison in the connecting beams, n_b=1

d. Deflection, n_b=1

Table 3.6 Deflection, n_b=1

z (m)	F_3 (z)	x(z), Continuous method (m)	x(z), ETABS (m)
0	0	0	0
3	0.009801	2.51E-05	0.000035
6	0.037352	9.58E-05	0.000111
9	0.080072	0.000205	0.000223
12	0.135608	0.000348	0.000366
15	0.2018	0.000517	0.000534
18	0.276646	0.000709	0.000723
21	0.358268	0.000919	0.000931
24	0.444889	0.001141	0.001154
27	0.534804	0.001371	0.001393
30	0.626353	0.001606	0.001715

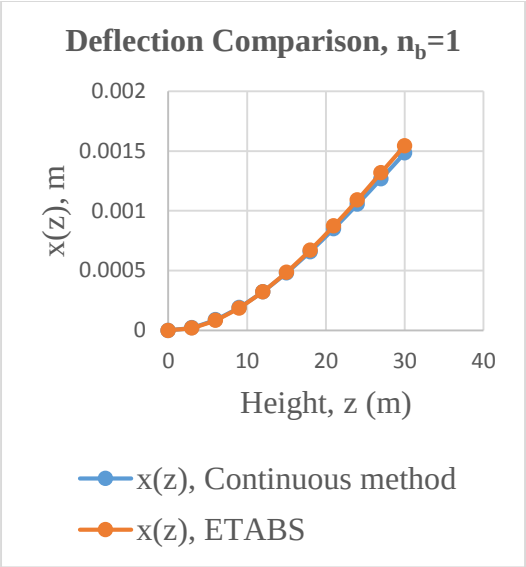

Figure 3.21 Deflection comparison, n_b=1

For cases of more than one beam per story, besides comparison with the FEM, from the improved equations an important observation can be made. i.e in each equation where α exists the number of beam term (n_b) exists and this term exists in root form ($\sqrt{n_b}$). So it is important to test if the curves developed for n_b>1 could have the same value with the curves for n_b=1 if α is changed into $\sqrt{n_b}\alpha$. So the responses are compared with their modified counterparts additionally.

Case II: Number of beams per story, n_b=2

For this case the modified α term will be $\alpha_2=\sqrt{2}*\alpha$.

a. Axial force in the walls, n_b=2

Table 3.7 Axial force in the walls, n_b=2

z (m)	N(z), Continuous method (kN)	N(z), Continuous method modified (kN)	N(z), ETABS (kN)
0	167.9319	167.9319	162.0223
3	164.9048	164.9048	163.374
6	156.6733	156.6733	154.508
9	144.3251	144.3251	142.1345
12	128.7398	128.7398	126.9172
15	110.6338	110.6338	109.4668
18	90.59623	90.59623	90.354
21	69.11891	69.11891	70.1192
24	46.62088	46.62088	49.2098
27	23.46971	23.46971	27.0951
30	0	0	-2.3172

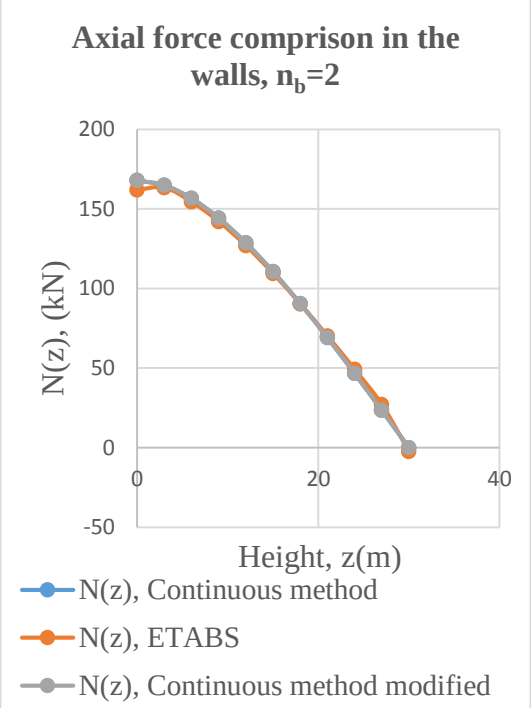

Figure 3.22 Axial force comparison in the walls, n_b=2

b. Bending moment in the walls, n_b=2

Table 3.8 Bending moment in the walls, n_b=2

z (m)	M_1, Continuous method (kN.m)	M_1, ETABS (kN.m)	M_2, Continuous method (kN.m)	M_2, ETABS (kN.m)
0	420.0264	470.5065	1152.552	1152.304
3	346.7707	360.2386	951.5388	953.6422
6	285.3303	289.6058	782.9463	800.1567
9	233.2363	235.1189	640.0003	661.2372
12	188.4914	191.0885	517.2204	536.0612
15	149.4693	155.7317	410.1437	421.2081
18	114.8323	130.5213	315.0998	310.8831
21	83.46401	118.06	229.0252	199.0413
24	54.41306	115.6544	149.3094	86.173
27	26.84495	99.9956	73.66253	-3.1535
30	9.49E-14	5.3361	2.6E-13	6.0285

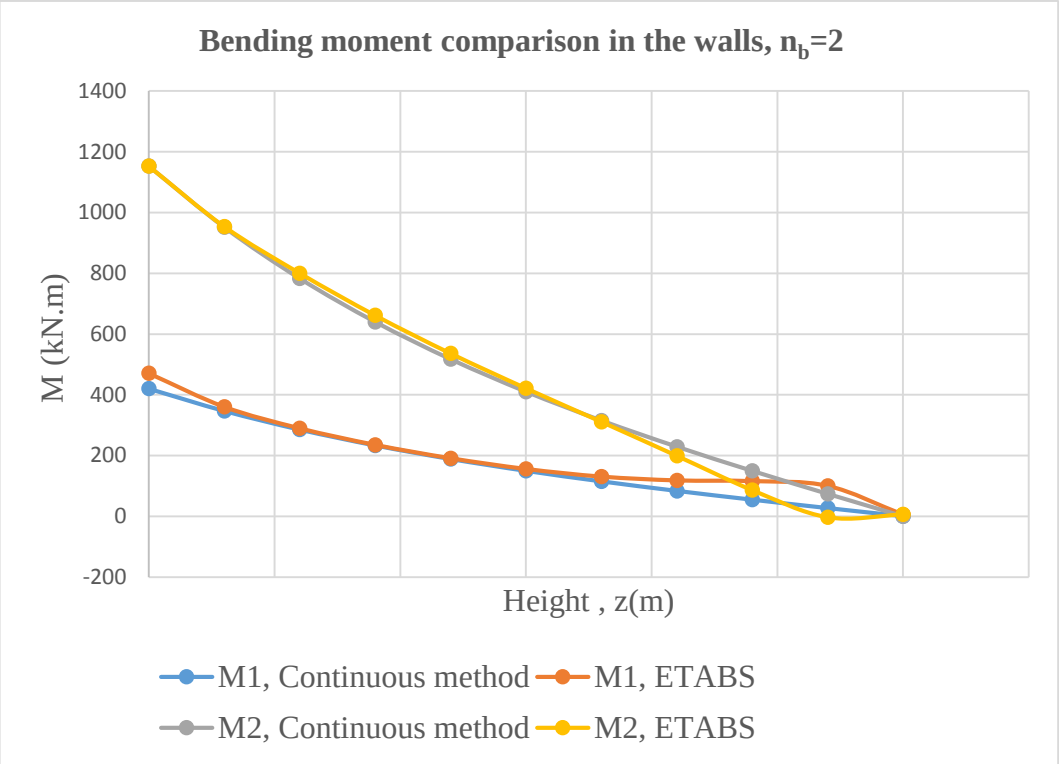

Figure 3.23 Bending moment comparison in the walls, n_b=2

c. Shear in connecting beams, n_b=2

Table 3.9 Shear in connecting beams, n_b=2

z (m)	Q(z), Continuous method (kN)	Q(z), Continuous method modified (kN)	Q(z) ETABS (kN)
0	0	0	1.4681
3	5.830716	5.830716	6.6261
6	10.45273	10.45273	10.7155
9	14.09928	14.09928	13.9429
12	16.95437	16.95437	16.4807
15	19.16207	19.16207	18.4544
18	20.83378	20.83378	19.9722
21	22.05386	22.05386	21.1429
24	22.88387	22.88387	22.0647
27	23.36569	23.36569	22.3653
30	23.52364	23.52364	8.7896

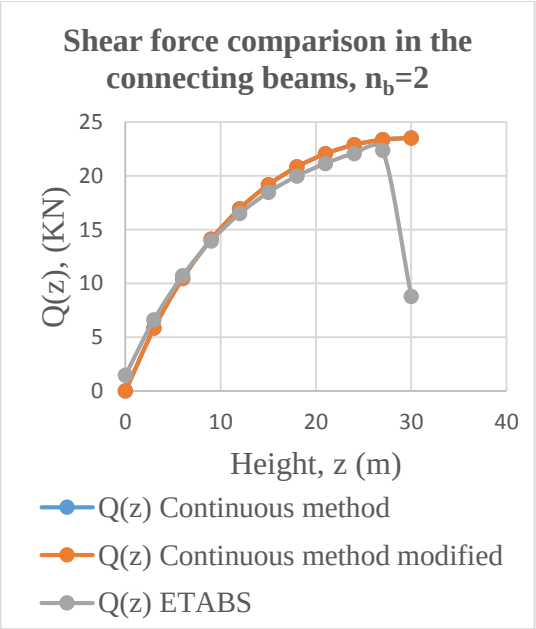

Figure 3.24 Shear force comparison in the connecting beams, n_b=2

d. Deflection, n_b=2

Table 3.10 Deflection, n_b=2

z (m)	x(z), Continuous method (m)	x(z), Continuous method modified (m)	x(z), ETABS (m)
0	0	0	0
3	2.04E-05	2.04E-05	0.00003
6	7.70E-05	7.70E-05	9.2E-05
9	0.00016	0.00016	0.00018
12	0.00028	0.00028	0.00029
15	0.00041	0.00041	0.00042
18	0.00056	0.00056	0.00057
21	0.00072	0.00072	0.00073
24	0.00089	0.00089	0.0009
27	0.00106	0.00106	0.00108
30	0.00124	0.00124	0.00134

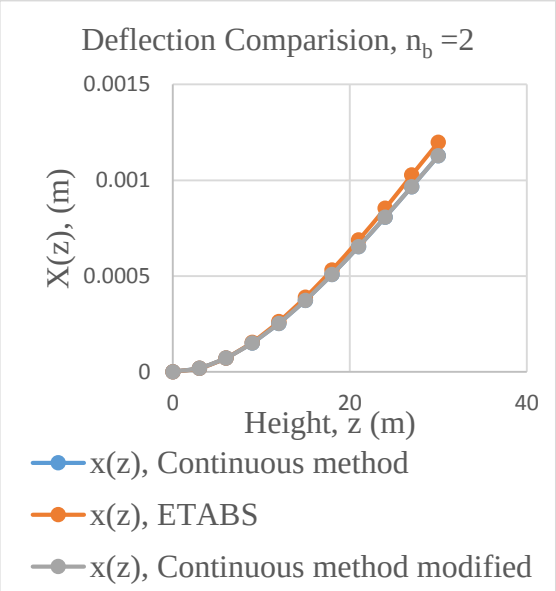

Figure 3.25 Deflection Comparison, n_b=2

Case III: Number of beams per story, n_b= 3

⇨ For this case also the modified α term will be $\alpha_3=\sqrt{3}*\alpha$.

a. Axial force in the walls for n_b=3

Table 3.11 Axial force in the walls, n_b=3

z (m)	N(z), Continuous method (kN)	N(z), Continuous method modified (kN)	N(z), ETABS (kN)
0	190.235	190.235	187.5996
3	186.5303	186.5303	187.514
6	176.6431	176.6431	176.5641
9	162.0825	162.0825	161.6318
12	144.003	144.003	143.6043
15	123.2922	123.2922	123.233
18	100.6381	100.6381	101.1703
21	76.58162	76.58162	77.9802
24	51.55686	51.55686	54.0258
27	25.92473	25.92473	28.365
30	0	0	-2.5307

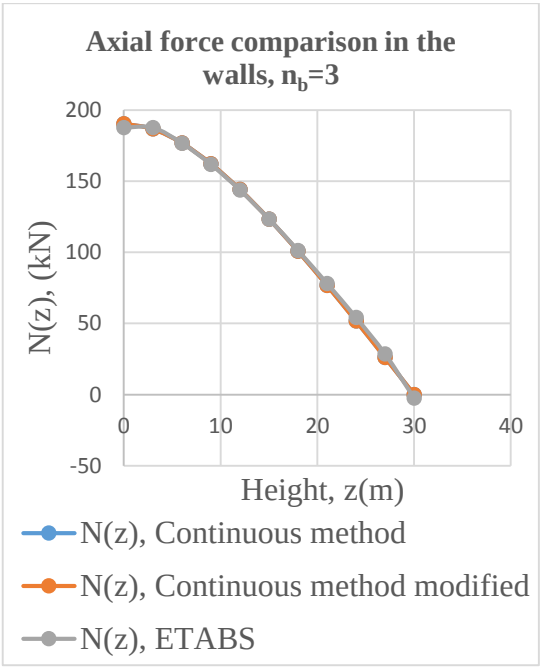

Figure 3.26 Axial force comparison in the walls, n_b=3

b. Bending moment in the walls, n_b=3

Table 3.12 Bending moment in the walls, n_b=3

z (m)	M_1, Continuous method (kN.m)	M_1, ETABS (kN.m)	M_2, Continuous method (kN.m)	M_2, ETABS (kN.m)
0	369.3917	411.5135	1013.611	993.89
3	297.6743	303.2335	816.8182	802.4633
6	239.9929	237.9055	658.5405	660.2195
9	192.9217	189.6685	529.3771	536.2127
12	153.8394	151.5995	422.1354	428.7661
15	120.731	121.28	331.2857	333.7749
18	92.03412	99.9532	252.5416	244.843
21	66.52143	91.154	182.5348	154.5365
24	43.20691	95.3726	118.5598	60.1911
27	21.27132	93.4975	58.3685	-16.5912
30	9.49E-14	6.0166	2.6E-13	6.1586

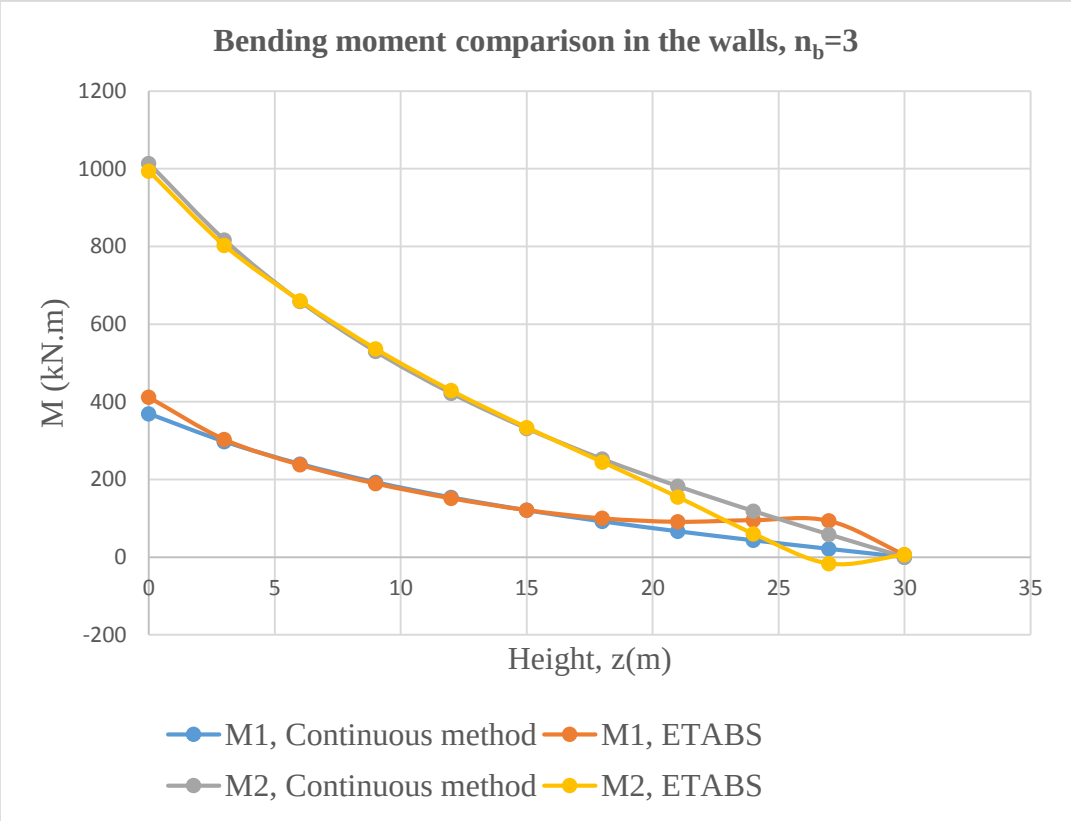

Figure 3.27 Bending moment comparison in the walls, n_b=3

c. Shear in connecting beams, n_b=3

Table 3.13 Shear force in connecting beams, n_b=3

z (m)	Q(z), Continuous method (kN)	Q(z), Continuous method modified (kN)	Q(z) ETABS (kN)
0	0	0	0.8891
3	7.082584	7.082584	6.8785
6	12.44328	12.44328	12.0334
9	16.48869	16.48869	15.9176
12	19.52566	19.52566	18.8538
15	21.78454	21.78454	21.0606
18	23.43667	23.43667	22.7083
21	24.60735	24.60735	23.9605
24	25.38539	25.38539	24.9902
27	25.8298	25.8298	25.5742
30	25.97428	25.97428	14.7334

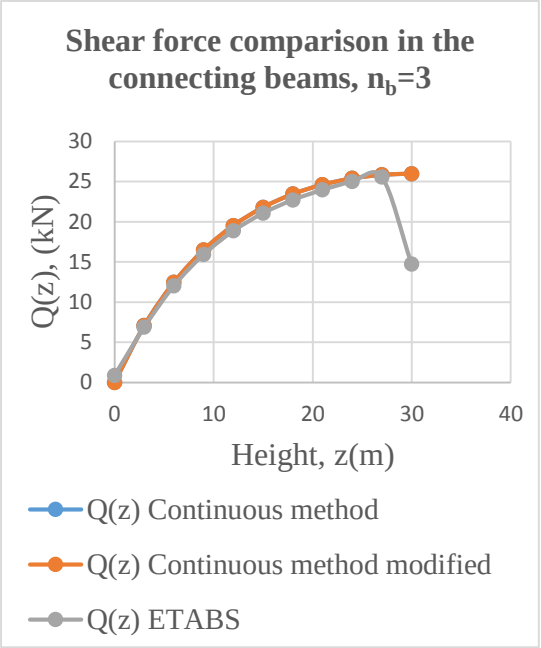

Figure 3.28 Shear force comparison in the connecting beams, n_b=3

d. Deflection, n_b=3

Table 3.14 Deflection, n_b=3

z (m)	x(z), Continuous method (m)	x(z), Continuous method modified (m)	x(z), ETABS (m)
0	0	0	0
3	1.78E-05	1.78E-05	2.8E-05
6	6.68E-05	6.68E-05	8.1E-05
9	0.00014	0.00014	0.00016
12	0.00024	0.00024	0.00025
15	0.00035	0.00035	0.00036
18	0.00047	0.00047	0.00048
21	0.00061	0.00061	0.00061
24	0.00075	0.00075	0.00075
27	0.0009	0.0009	0.0009
30	0.00105	0.00105	0.00113

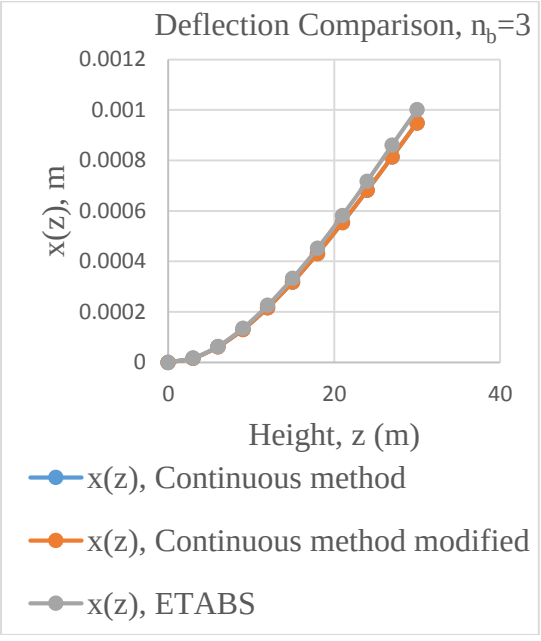

Figure 3.29 Deflection Comparison, n_b=3

From the numerical analysis of the CSW for the three cases, the following results are observed:

- The results of axial force from continuous method gives higher result (up to 5% greater) especially at the base. The variation arises due to the fact that at the base there's no beam or support directly below the opening. So a lower value from ETABs output is expected at the base. But at the top, values from ETABs are higher. One of the major differences between both methods is that, the axial force and the bending moment at the top of the walls are equal to zero according to the continuous method, though the FEM gives a nonzero value for the bending moment and axial force at the top of the walls.
- The variation of shear force also shows that results from continuous method gives up to 12% higher value than the ETABs value. The reason is that in continuous method, it is assumed that the maximum shear flow is constant throughout the height of a story though, the accurate shear force in a connecting beam is equal to the integration of the shear flow from $\frac{h}{(2)^{n_b}}$m above to$\frac{h}{(2)^{n_b}}$ m under the considered beam. And in all the 3 cases, ETABs gives a lower value since the top beam is subjected to only a shear flow from $\frac{h}{(2)^{n_b}}$m below.
- Another important comparison made is the values of responses were estimated using charts developed for number of beams 1, 2, 3 and also using chart for number of beam=1 with modification made for these chart as $\alpha=\sqrt{n_b} * \alpha$. As can be seen from the tables and graphs, curves and values of the results for the responses at each level (labeled under continuous method and continuous method modified) merge.

CHAPTER FOUR

APPLICATION TO THE DYNAMICS OF COUPLED SHEAR WALLS

4.1. Introduction

In this section, the application of the previously formulated equation to the dynamics of coupled shear walls is presented. The 'continuous' method of coupled shear wall analysis is extended into the regime of dynamics in which a method is proposed to estimate approximate value of the natural vibration frequency of the system. Since the formulation given previously is in terms of the deflection variables of the piers, it is readily adaptable for dynamic analysis by taking into account the inertia effect of the piers.

The coupled shear wall is treated as single degree of freedom (SDF) systems, which is called the generalized SDF systems. The analysis provides exact results for an assemblage of rigid bodies supported such that it can deflect in only one shape, but only approximate results for systems with distributed mass and flexibility. In the latter case, the approximate natural frequency is shown to depend on the assumed deflected shape (Chopra, 2000). Since the knowledge of the fundamental natural frequency is essential in seismic design by the spectrum technique; effort has been directed through the assumption of shape functions to arrive at a formulation for the expression of natural frequency.

4.2. Generalized SDF Systems

Consider, for example, the system of Fig. 4.1(a), consisting of a rigid, massless bar supported by a hinge at the left end with two lumped masses, a spring and a damper, attached to it, subjected to a time-varying external force p(t). Because the bar is rigid, its deflections can be related to a single generalized displacement z(t) through a shape function ψ(x) as shown, and can be expressed as:

$$u(x,t) = \psi(x)z(t) \qquad (4.1)$$

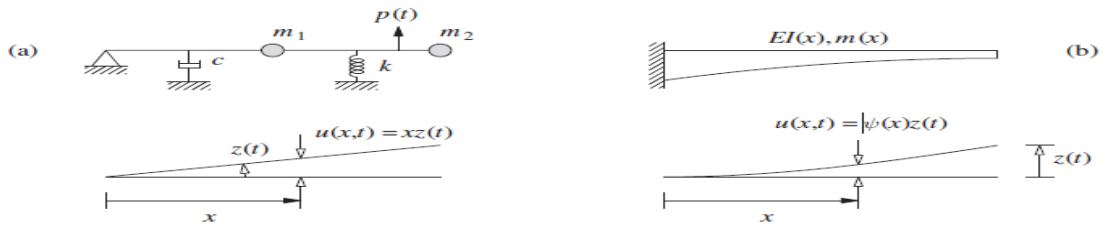

Figure 4.1 generalized SDF systems

Next consider, for example, the system of Fig. 4.1 (b) consisting of a cantilever beam with distributed mass. This system can deflect in an infinite variety of shapes, and for exact analysis it must be treated as an infinite-degree-of-freedom system. It is possible to obtain approximate results that are accurate to a useful degree for the lowest (also known as fundamental) natural frequency; however, by restricting the deflections of the beam to a single shape function ψ(x) that approximates the fundamental vibration mode. The deflections of the beam are then given by Eqn. 4.1, where the generalized coordinate z(t) is the deflection of the cantilever beam at a selected location—say the free end, as shown in Fig. 4.1(b).

The two systems of Fig. 4.1 are called generalized SDF systems because in each case the displacements at all locations are defined in terms of the generalized coordinate z(t) through the shape function ψ(x). It is shown that the equation of motion for a Generalized SDF system is of the form:

$$\tilde{m}\ddot{z} + \tilde{c}\dot{z} + \tilde{k}z = \tilde{p}(t) \qquad (4.2)$$

where $\tilde{m}$, $\tilde{c}$, $\tilde{k}$, and $\tilde{p}(t)$ are defined as the generalized mass, generalized damping, generalized stiffness, and generalized force of the system; these generalized properties are associated with the generalized displacement z(t) selected. Eqn. 4.2 is of the same form as the standard equation formulated for an SDF system with a single lumped Mass. Thus the analysis procedures and response results presented for lumped mass system can readily be adapted to determine the response z(t) of generalized SDF systems. With z(t) known, the displacements at all locations of the system are determined from Eqn. 4.1.This analysis procedure leads to the exact results for the system of Fig. 4.1(a) because the shape function ψ(x) could be determined exactly but provides only approximate results for the system of Fig. 4.1(b) because they are based on an assumed shape function.

4.3. Selection of Shape Function

The accuracy of the natural vibration frequency estimated using Rayleigh's quotient depends entirely on the shape function that is assumed to approximate the exact mode shape. In principle any shape may be selected that satisfies the displacement and force boundary conditions. It is suggested that an approximate shape function ψ(x) may be determined as the deflected shape due to static forces p(x) = m(x)ψ($\tilde{x}$), where ψ($\tilde{x}$) is any reasonable approximation of the exact mode shape.

In general, this procedure to select the shape function involves more computational effort than is necessary because Rayleigh's method gives excellent accuracy even if the shape function is mediocre. However, the preceding discussion does support the concept of determining the shape function from deflections due to a selected set of static forces. One common selection for these forces is the weight of the structure applied in an appropriate direction. For the cantilever tower it is the lateral direction (Fig. 4.2a). This selection is equivalent to taking $\psi(x) = 1$ in $p(x) = m(x)\,\ddot{\psi}(x)$.

Another selection includes several concentrated forces as shown in Fig. 4.2b.

The displacement and force boundary conditions are satisfied automatically if the shape function is determined from the static deflections due to a selected set of forces. This choice of shape function has the additional advantage that the strain energy can be calculated as the work done by the static forces in producing the deflections. Thus, the maximum strain energy of the system associated with the forces p(x) in Fig. 4.2a is:

$$E_{So} = \frac{1}{2}\int_o^L p(x)\,u(x)dx \qquad (4.3)$$

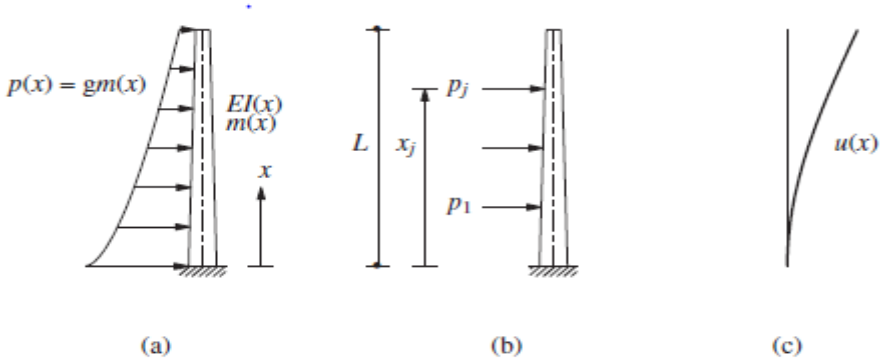

Figure 4.2 Shape function from deflections due to static forces

Equating this E_{So} to $E_{Ko} = \int_o^L \frac{1}{2} m(x)\,[\dot{u}(x)]^2$ with $\dot{u}_o(x) = \omega_n u_o(x)$ and dropping the subscript "o" gives:

$$\omega_n^2 = \frac{\int_o^L p(x)u(x)dx}{\int_o^L m(x)(u(x))^2 dx} \qquad (4.4)$$

For p(x) = gm(x) in Fig. 4.2a, Eqn. 4.3.2 becomes:

$$\omega_n^2 = g\,\frac{\int_o^L m(x)u(x)dx}{\int_o^L m(x)(u(x))^2 dx} \qquad (4.5)$$

Similarly, the maximum strain energy of the system associated with deflections u(x) due to the forces of Fig. 4.2b is:

$$\omega_n^2 = \frac{\sum P_j u(x_j)}{\int_o^L m(x)(u(x))^2 dx} \qquad (4.6)$$

4.3.1. Selection of Shape Function Based on the Provided Theory

For the coupled shear wall case the shape function may be selected based on the deflections of a coupled shear wall due to a unit lateral force at the top as:

$$u(z) = \frac{PH^3}{3EI} \times F_3(z)$$

If we select the generalized coordinate as the deflection of the top of the coupled shear wall, then:-

$$z(t) = u\,(H) = \frac{PH^3}{3EI} \times F_3(H) \qquad (4.7)$$

And

$$\psi(z) = \frac{F_3(z)}{F_3(H)}$$

where

$$F3(z) := \frac{3}{2}\frac{z^2}{H^2} - \frac{1}{2}\frac{z^3}{H^3} - \frac{3}{2}\frac{z^2}{H^2 k^2} + \frac{1}{2}\frac{z^3}{H^3 k^2} + \frac{3z}{H^3 nb\, k^4 \alpha^2} + \frac{3\sinh\left(\sqrt{nb}\, k\alpha H\right)\cosh\left(\sqrt{nb}\, k\alpha z\right)}{H^3 nb^{3/2} k^5 \alpha^3 \cosh\left(\sqrt{nb}\, k\alpha H\right)} - \frac{3\sinh\left(\sqrt{nb}\, k\alpha z\right)}{H^3 nb^{3/2} k^5 \alpha^3} - \frac{3\sinh\left(\sqrt{nb}\, k\alpha H\right)}{H^3 nb^{3/2} k^5 \alpha^3 \cosh\left(\sqrt{nb}\, k\alpha H\right)}$$

And

$$F_3(H) = \frac{\left(1 - 3\left(\frac{1}{3} + \frac{sinh\left(k\alpha H\sqrt{n_b}\right)}{k^3\alpha^3 H^3 n_b^{\frac{3}{2}} cosh\left(k\alpha H\sqrt{n_b}\right)} - \frac{1}{k^2\alpha^2 H^2 n_b}\right)\right)}{k^2}$$

Is from static analysis and is a function of the stiffness parameters k, αH and n_b.

Note: In the assumed shape function, the important thing is to assume shape function that satisfies the displacement and force boundary conditions. So the boundary conditions for the coupled shear walls become:

i. u(0) = 0

ii. $\dot{u}(0) = 0$

iii. $\ddot{u}(H) = 0$

In which the above assumed shape function satisfies the above displacement and force boundary conditions and is valid.

4.4. Natural Vibration Frequency of Coupled Shear Wall

Based on the assumed shape function, the expression for ω_n would be:

$$\omega_n{}^2 = \frac{\sum P_j u(z_j)}{\int_0^H m(z)[u(z)]^2 dz} \tag{4.8}$$

where

$$\sum P_j u(z_j) = Pu(H) =$$

$$\frac{1}{3}\,\frac{P^2 H^3 \left(1 - \frac{1}{k^2} + \frac{3}{H^2\, nb\, k^4\, \alpha^2} - \frac{3\sinh\left(\sqrt{nb}\, k\alpha H\right)}{H^3\, nb^{3/2}\, k^5\, \alpha^3 \cosh\left(\sqrt{nb}\, k\alpha H\right)}\right)}{E\, i}$$

And

$$\int_0^H m(z)[u(z)]^2 dz =$$

$$\begin{aligned}
&\frac{1}{420}\,\frac{1}{nb^{7/2} k^{11} \alpha^7 \left(\cosh\left(2\sqrt{nb}\, k\alpha H\right) + 1\right) E^2 i^2}\Big(\big(-1680\sqrt{nb}\, k\alpha H \\
&\quad + 1050\sinh\left(2\sqrt{nb}\, k\alpha H\right) + 840 H\alpha k^3 \sqrt{nb} + 11 H^7 \alpha^7 k^{11} nb^{7/2} - 22 H^7 \alpha^7 k^9 nb^{7/2} \\
&\quad + 11 H^7 \alpha^7 k^7 nb^{7/2} + 77 H^5 \alpha^5 k^7 nb^{5/2} - 77 H^5 \alpha^5 k^5 nb^{5/2} + 140 H^3 \alpha^3 k^3 nb^{3/2} \\
&\quad + 1680\sinh\left(\sqrt{nb}\, k\alpha H\right) - 840\sinh\left(2\sqrt{nb}\, k\alpha H\right) k^2 \\
&\quad + 560 H^3 \cosh\left(\sqrt{nb}\, k\alpha H\right) \alpha^3 k^3 nb^{3/2} + 140 H^3 \cosh\left(2\sqrt{nb}\, k\alpha H\right) \alpha^3 k^3 nb^{3/2} \\
&\quad + 11 H^7 \cosh\left(2\sqrt{nb}\, k\alpha H\right) \alpha^7 k^{11} nb^{7/2} - 22 H^7 \cosh\left(2\sqrt{nb}\, k\alpha H\right) \alpha^7 k^9 nb^{7/2} \\
&\quad + 11 H^7 \cosh\left(2\sqrt{nb}\, k\alpha H\right) \alpha^7 k^7 nb^{7/2} + 77 H^5 \cosh\left(2\sqrt{nb}\, k\alpha H\right) \alpha^5 k^7 nb^{5/2} \\
&\quad - 77 H^5 \cosh\left(2\sqrt{nb}\, k\alpha H\right) \alpha^5 k^5 nb^{5/2} - 560 H^3 \cosh\left(\sqrt{nb}\, k\alpha H\right) \alpha^3 k^5 nb^{3/2} \\
&\quad - 105 H^4 \sinh\left(2\sqrt{nb}\, k\alpha H\right) \alpha^4 k^6 nb^2 + 105 H^4 \sinh\left(2\sqrt{nb}\, k\alpha H\right) \alpha^4 k^4 nb^2 \\
&\quad - 420 H^2 \sinh\left(2\sqrt{nb}\, k\alpha H\right) \alpha^2 k^2 nb + 840 H\cosh\left(2\sqrt{nb}\, k\alpha H\right) \alpha k^3 \sqrt{nb} \\
&\quad - 1680 H\cosh\left(\sqrt{nb}\, k\alpha H\right) \alpha k\sqrt{nb} - 420 H\cosh\left(2\sqrt{nb}\, k\alpha H\right) \alpha k\sqrt{nb}\big)\, m P^2\Big)
\end{aligned}$$

The expressions for the numerator and denominator of Eqn. 4.8 are solved using mathematical software maple version 18.0 and the detail calculation is shown on Appendix 2.

After substituting and simplifying, the expression for natural frequency becomes:

$$\omega_n = \frac{F\omega_n}{H^2} \times \sqrt{\frac{EI}{M_{csw}}} \qquad (4.9)$$

where

$$M_{csw} = \frac{\gamma}{g} \times t\left(2d_1 + 2d_2 + \frac{n_b \times d_b \times b}{h}\right) \qquad (4.10)$$

$I = I_1 + I_2$

$F\omega_n$ is a factor which is a function of the stiffness parameters k, αH and n_b and it is plotted on Fig. 4.3. The mathematical manipulation to obtain this factor is also shown on Appendix 2 as done on maple18.0.

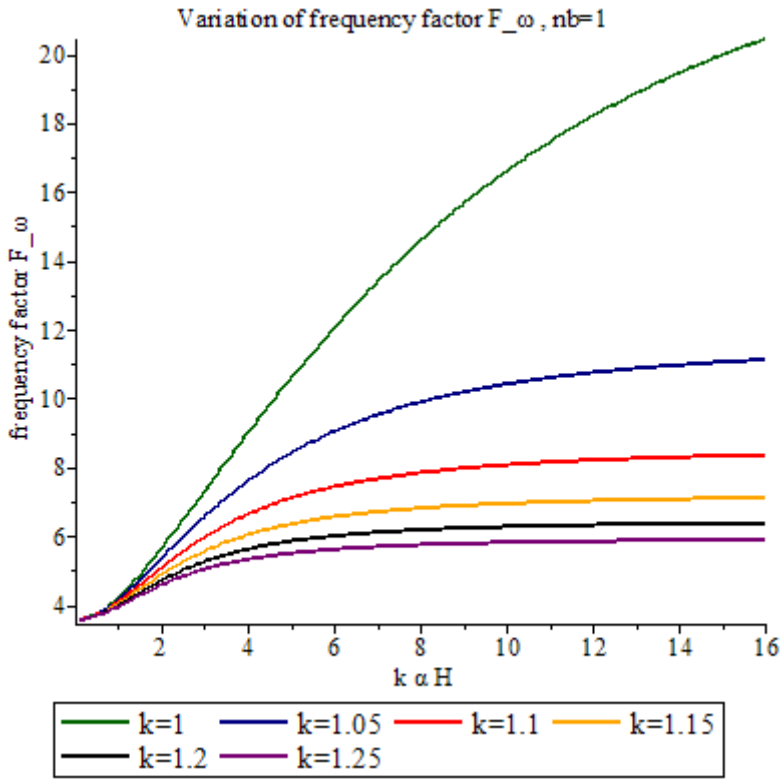

Figure 4.3 Variation of frequency factor F-ω for point load, n_b=1

4.5. Numerical Analysis

In this section, to verify the present method, first a case of coupled shear wall system with a single beam per story is illustrated. The analysis is then made for 21 model coupled shear walls using the proposed extended continuous medium method and three dimensional analysis of Building Systems (ETABS). The results are tabulated in this report.

4.5.1. Illustrative example

Material:

Concrete:

Modulus of elasticity, E = 30 GPa

Poisson's ratio, υ= 0.2

Concrete unit weight, γ = 25 kN/m^3

Shear wall section:

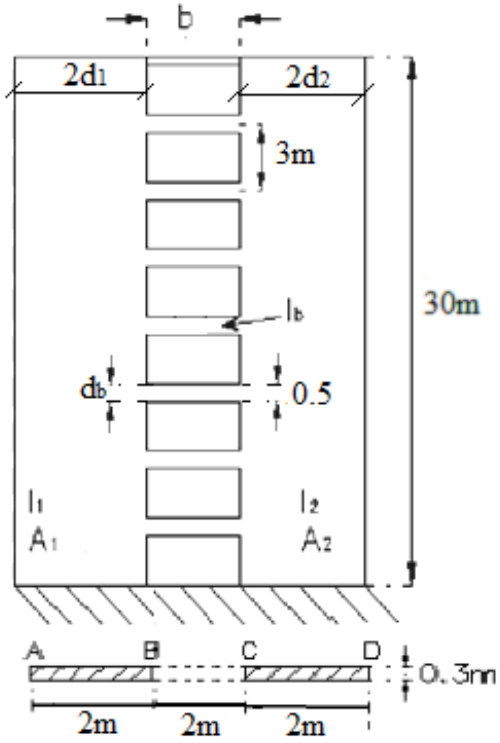

Figure 4.4 Sample CSW structure

a. Determine the area and the second moment of area of the connecting beams and the shear walls illustrated in Fig. 4.4.

Table 4.1 Properties of the coupled walls

H	[m]	30	**d_b**	[m]	0.4
l	[m]	2.5	**t_w=t_b**	[m]	0.3
2d_1	[m]	2	**h**	[m]	3
2d_2	[m]	2	**E**	[kN/m^2]	3E+07
b	[m]	0.5	**G**	[kN/m^2]	1.3E+07

Table 4.2 Cross sectional properties of connected beams and shear walls

A_1 (m^2)	0.6	**A_b (m^2)**	0.075
A_2 (m^2)	0.6	**I_b (m^4)**	0.00039
A (m^2)	1.2	**E (kN/m^2)**	3E+07
I_1 (m^4)	0.2	**G**	1.3E+07
I_2 (m^4)	0.2	**r**	0.07373
I (m^4)	0.4	**I_e**	0.00149

b. Determine the stiffness parameter kαH

k	**α**	**kαH**	**k^2**	**α^2**
1.10151	0.24325	8.03837	1.21333	0.05917

c. Determine the mass parameter, M_{csw}

$$M_{csw} = \frac{\gamma}{g} \times t(2d_1 + 2d_2 + \frac{n_b \times d_b \times b}{h})$$

$$M_{csw} = \frac{25000}{9.81} \times 0.3(2 + 2 + \frac{1 \times 0.4 \times 0.5}{3}) = 3109.07 kg/m$$

d. By using the curve in Fig. 4.3 for n_b=1, the natural frequency factor, $F\omega_n$=7.66 for value of kαH=8.044 and k=1.102.

e. Finally the natural vibration frequency, ω_n and natural vibration period, T_n will be respectively:

$$\omega_n = \frac{F\omega_n}{H^2} \times \sqrt{\frac{EI}{M_{csw}}}$$

$$\omega_n = \frac{7.661740284}{30^2} \times \sqrt{\frac{30 \times 10^9 \times 0.4}{3109.07}} = 16.73\ rad/sec$$

$$T_n = \frac{2\pi}{\omega_n} = \frac{2\pi}{16.73} = 0.376\ sec$$

4.5.2. Comparisons of results from continuous medium method and computer analysis using finite elements

For the comparison of the coupled shear wall structures, 21 geometries were selected so that the geometries (height of the building, connecting beams' width & depth, and wall width) are combined to give the stiffness parameter, kαH, within reasonable interval (i.e. if kαH is less than 1, the structure is considered to have negligible coupling action and behaves as an arrangement of linked walls. For values of kαH greater than about 8, the

coupling beams are considered to be stiff and the structural response is dominated by that of the wall piers as described by the factor k. *(*Kent et.al (2004))). So the CSW geometries are combined to give a value of kαH between the extremes to see the application range of the proposed method.

Table 4.3 Geometry of the sample coupled shear wall structures

Model No.	H (m)	$2d_1$ (m)	$2d_2$ (m)	b (m)	d_b (m)	$t_w=t_b$ (m)	h (m)	n_b	Mcsw (kg/m)	I (m^4)	E (Gpa)
1	30	2	2	0.5	0.25	0.3	3	1	3089.959	0.4	30
2	60	2	2	0.5	0.25	0.3	3	1	3089.959	0.4	30
3	30	2	2	0.5	0.25	0.3	3	2	3121.814	0.4	30
4	60	2	2	0.5	0.25	0.3	3	2	3121.814	0.4	30
5	30	2	2	0.5	0.25	0.3	3	3	3153.67	0.4	30
6	60	2	2	0.5	0.25	0.3	3	3	3153.67	0.4	30
7	30	3	4	2	0.5	0.3	3	1	5606.524	2.275	30
8	60	3	4	2	0.5	0.3	3	1	5606.524	2.275	30
9	30	3	4	2	0.5	0.3	3	2	5861.366	2.275	30
10	60	3	4	2	0.5	0.3	3	2	5861.366	2.275	30
11	30	3	4	2	0.5	0.3	3	3	6116.208	2.275	30
12	60	3	4	2	0.5	0.3	3	3	6116.208	2.275	30
13	90	3	3	1.5	0.5	0.3	3	1	4778.287	1.35	30
14	30	3	3	1.5	0.5	0.3	3	1	4778.287	1.35	30
15	21	3	3	1.5	0.5	0.3	3	1	4778.287	1.35	30
16	30	5	7	2.5	0.4	0.3	3	1	9429.154	11.7	30
17	30	5	7	2.5	0.4	0.3	3	2	9683.996	11.7	30
18	30	5	7	2.5	0.4	0.3	3	3	9938.838	11.7	30
19	60	5	7	2.5	0.4	0.3	3	1	9429.154	11.7	30
20	60	5	7	2.5	0.4	0.3	3	2	9683.996	11.7	30
21	60	5	7	2.5	0.4	0.3	3	3	9938.838	11.7	30

Table 4.4 Comparison of natural period

Model No.	Proposed method			ETABS 2015		
	$F\omega_n$	ω_n, Proposed method (rad/sec)	T_n, Proposed method (Sec)	ω_n, ETABS (rad/sec)	T_n (Sec)	% difference
1	7.787	17.051	0.368	17.0135	0.369	0.189
2	8.295	4.541	1.383	4.4913	1.399	1.147
3	8.109	17.664	0.356	17.5028	0.359	0.969
4	8.398	4.573	1.373	4.5142	1.392	1.354
5	8.231	17.840	0.352	17.6564	0.356	1.116
6	8.433	4.570	1.374	4.5075	1.394	1.414
7	6.808	26.391	0.238	25.0097	0.251	5.195

Model No.	Proposed method			ETABS 2015		
	$F\omega_n$	ω_n, Proposed method (rad/sec)	T_n, Proposed method (Sec)	ω_n, ETABS (rad/sec)	T_n (Sec)	% difference
8	8.616	8.351	0.752	7.9612	0.789	4.685
9	7.796	29.559	0.212	27.84	0.226	5.993
10	9.195	8.715	0.721	8.387	0.749	3.795
11	8.304	30.820	0.204	29.2182	0.215	5.228
12	9.428	8.748	0.718	8.4844	0.741	3.120
13	9.574	3.441	1.825	3.3572	1.872	2.508
14	7.869	25.456	0.247	24.2684	0.259	4.749
15	6.872	45.368	0.138	43.1992	0.145	4.536
16	4.506	30.548	0.206	29.0445	0.216	4.826
17	5.128	34.304	0.183	32.2283	0.195	6.118
18	5.583	36.863	0.170	34.5018	0.182	6.394
19	5.934	10.056	0.624	9.5699	0.657	4.948
20	6.805	11.380	0.552	10.7345	0.585	5.668
21	7.280	12.018	0.523	11.3687	0.553	5.509

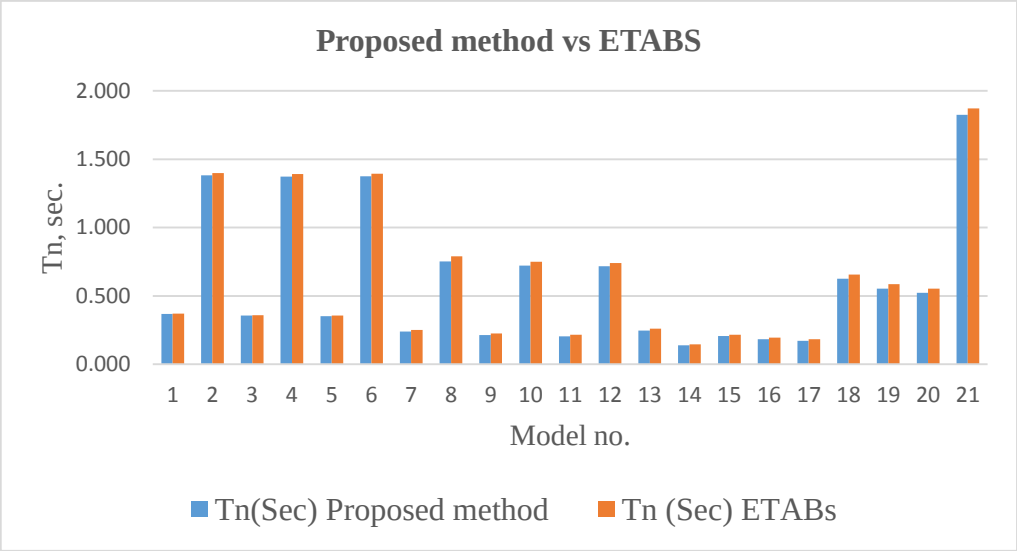

Figure 4.5 Proposed method vs ETABS

As can be observed from the chart and tables, the proposed method and the ETABS output give close results to each other with 0.2-6.5% difference.

CHAPTER FIVE

SUMMARY OF RESULTS AND DISCUSSION

In this chapter the findings are summarized and discussion on those results are made in combination with the provided theories for coupled shear walls.

5.1. Results of the extended continuous medium method

Based on the assumptions made, the governing differential equation for a system of coupled shear wall with multiple connecting beams in each story is derived. The equations are formulated in terms of axial force N and lateral deflection, x(z), with the beam parameter (n_b) included as follows:

$$\frac{d^2N(z)}{dz^2} - k^2\alpha^2 n_b N(z) = -\frac{n_b\alpha^2}{l} m(z) \text{ and}$$

$$\frac{d^4x(z)}{dz^4} - k^2\alpha^2 n_b \frac{d^2x(z)}{dz^2} = \frac{1}{EI}\left(\frac{d^2m(z)}{dz^2} - \alpha^2 n_b m(z)(k^2-1)\right)$$

The solution to the governing differential equation is computed by replacing the applied moment (which is due to point, uniformly distributed or triangularly distributed loads) and applying the boundary conditions. The responses found are expressed with factors F_1, F_2, F_3 and k_2 for axial force in the walls, shear force in the connecting beams, deflection at the top of the walls and stress in the walls respectively.

These factor are plotted for various height ratio (z/H) and stiffness factor kαH for number of connecting beams one up to five in each story in Appendix 1. The curves of each responses for various number of connecting beams in each story show identical shape and the only variation is the value of the factors change in some manner. These changes are shown under each responses in the solution to the GDE section (chapter 3, sub section 3.2) and the discussion on the effect of increasing the number of connecting beams on each responses are summarized in the subsequent section.

5.2. Results and discussions on effect of number of beam on structural responses

a) **Effect on axial force in the walls**: Considering Figs. 3.3, 3.4 and 3.5, two important points can be observed:-

- ✓ As the number of connecting beams in each story increase, the axial force factor F_1 also increases, at the base for all values of stiffness factors, kαH.

- ✓ Even if the axial force factor F_1 increase with number of connecting beams, the rate of increase is minimized and approaches to none at upper stories as the value of stiffness factor, kαH, increase.

In general, for low stiffness of coupling beams, increasing the number of connecting beams increases the axial force in the walls at all stories. But as the stiffness of the connecting beams increase its effect is minimal and is limited to only the base level.

b) **Effect on shear force in the connecting beams:** The variation of shear flow factor F_2 versus the height ratio and number of beams in a story has also been illustrated in Figs. 3.6 & 3.7 for various stiffness factor kαH. As can be seen from the curves,
   - ✓ The shear flow in the connecting beams is directly related to the stiffness parameter kαH amplified by number of beams. Which means that, increasing the stiffness or beam number leads to increasing shear flow in connecting beams.
   - ✓ Also the position of the most loaded connecting beam is always at the top for point load but the position of the most loaded beam lowers to the bottom stories for uniformly and triangularly distributed loads as the number of connecting beams increase as its effect as seen from point load is to amplify the stiffness factor kαH.

c) **Effect on deflection at top:** From the drawn charts in Appendix 1 for variation of deflection factor F_3, it is observed that the deflection factor F_3 is not only dependent on a single parameter kαH but also on wall parameter k for all number of connecting beams in each story. So the effect of increasing number of connecting beams on top deflection is drawn with respect to the two parameters (on Figs. 3.8 up to 3.12). From these charts also two important points are observed:-
   - ✓ As the value of wall parameter k increase, the deflection at the top also increase for all values of stiffness factor kαH and all number of connecting beams per story. Increasing the amount of k when the value of kαH remains constant means that, the value of α have been decreased. The value of α can be diminished by reducing the beam height which will have negative influence on coupling of the shear walls. As a result, the top deflection of the walls will be increased.
   - ✓ As the number of coupling beams in each story increase, the deflection factor F_3 decreases, especially the effect seen on low stiffness coupling beams. Meaning deflection at top decreases with increase in number of coupling beams in each story.

d) **Effect on stress in the walls:** The variation of k_1 and k_2 as a function of height ratio, kαH and number of beams has been illustrated in Fig. 3.14 & 3.15. As can be seen, in the higher level of the walls the composite action factor is larger which can be concluded that, coupling of the walls is more effective for the tall buildings. Furthermore, it can be seen that the value of composite action will be increased by increasing either the number of beams or the stiffness factor, kαH. Moreover, increasing the stiffness of coupling beams or number of beams after some point does not change the magnitude of composite factor greatly.

5.3. Result and discussion on comparison of results of computer analysis and continuous method

The comparison of the outputs from the continuous medium method and the computer analysis for the specified cases is shown at the end of chapter three and the variation of results is seen. In the following graphs the variation of responses with increased number of connecting beams with the two methods are summarized at critical locations (i.e. axial force and bending moment at the base of the walls, deflection at the top of the walls and shear force at the most loaded beam) and in both analysis methods effect of n_b follows the same pattern.

Also from the graphs as n_b increase the percentage variation between the two methods is minimized. i.e. for example the % of axial force variation lowers from 5%-1.5% as n_b increases from 1 up to 3. This is due to the fact that the higher the beam number the higher it approximates the actual case and assumption.

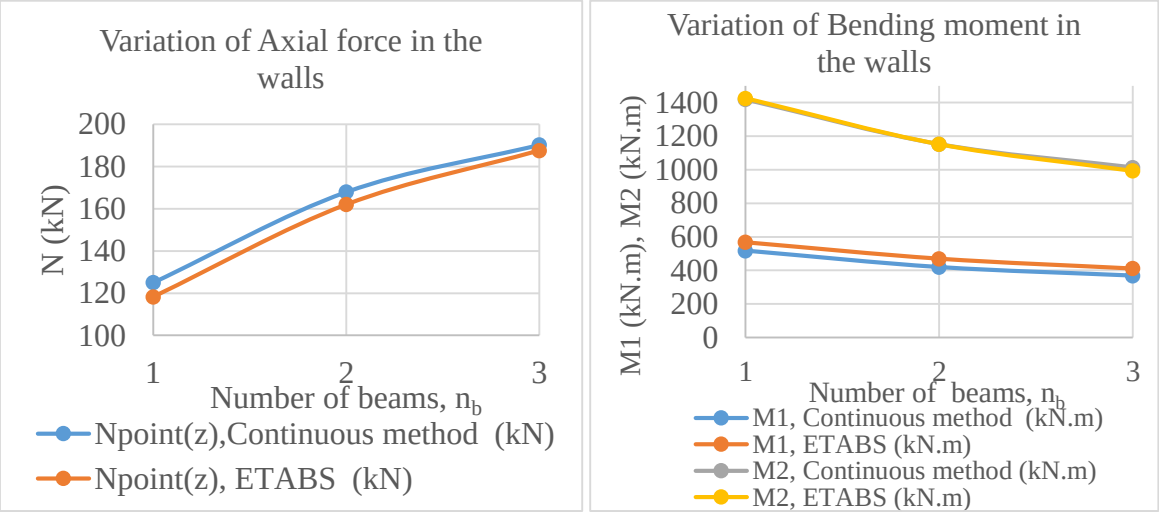

Figure 5.1 Comparison of Axial Force and Bending moment at the base of the walls

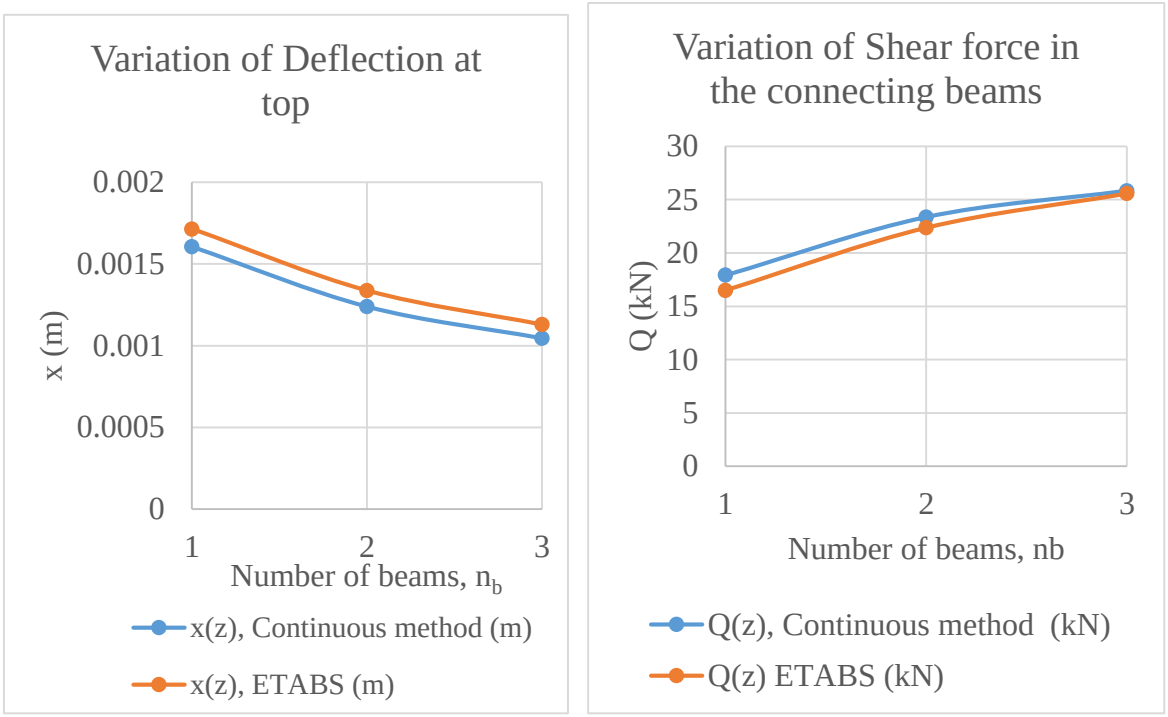

Figure 5.2 Comparison of deflection at top and shear force at the most loaded beam

In general it is known that the stiffness factor (kαH) depends on the walls dimensions, connecting beams' span, height of the connecting beams and the story height. This stiffness factor (kαH) will be increased by decreasing the walls dimensions, decreasing the length of the connecting beams, increasing the story height and increasing the height of the connecting beams. But without having to change this factor the overall stiffness of the coupled shear wall can be increased by increasing the number of connecting beams in each story. Especially if the individual connecting beams are relatively flexible originally.

CHAPTER SIX

CONCLUSIONS AND RECOMMENDATIONS

This chapter presents the answers to the main research questions and thereby the conclusions to this research.

6.1. Conclusions

The objective of this paper was to study the analysis and behaviour of coupled shear wall with multiple number of connecting beams in a story according to the continuous medium method. So based on the study, the following conclusions can be drawn:

- In this thesis the previous study about analysis of coupled shear walls according to continuous method has been revised. The obtained results are identical to the results given in other researches (A case for single connecting beams in each story).
- The behaviour of the coupled shear walls subjected to point loading at the top has been considered according to the continuous method for walls on rigid foundation with connecting beam greater than one in each story. The results have been given as some equations and curves from which the axial force in the walls, bending moment in the walls, shear force in the connecting beams and lateral deflection of the coupled walls system can be obtained.
- Based on the results of the formulated equations and plotted curves for multiple connecting beams in each story, it is observed that while using the continuous medium method one cannot speak about the individual component properties without having to affect the other components and this combined stiffness property is expressed in terms of the factor kαH for a coupled shear wall with a single beam in each story.
- So in the analysis of coupled shear walls with multiple connecting beams in each story, it is concluded that by modifying the combined stiffness property kαH, i.e. by multiplying the stiffness parameter α by the square root of number of beams per story that exists, the curves previously developed by A. Coull and Stafford smith for the factors F_1, F_2, F_3 and k_2 of a single connecting beam in each story can be read for a case of multiple connecting beams in each story without causing any variation on the structural responses.

⇨ So the results apply to the case of uniformly or triangularly distributed loads that arise due to wind or earthquake loads too.

- In addition a method to obtain natural frequency of the coupled shear wall system based on the generalized SDF system was proposed and comparison with ETABS 2015 result was made for 21 models of various coupled wall geometries. Based on the results it was observed that the results are within 0.2-6.5% for a range of wall stiffness parameter, kαH, between 1 and 16 (a range including low, intermediate and high coupling of the CSW). It means that the proposed method is simple and accurate enough to be used for preliminary analysis and design.

6.2. Recommendations

- Based on the result finding the continuous method can be used for wide range of coupled shear wall systems and it is apparent that the method could be extended for various cases that could arise due to functional requirements.
- Also for the dynamics of the coupled shear wall structure, it is implied that charts could be developed to formulate the generalized mass, generalized stiffness and generalized excitations for easy determination of dynamic responses.
- Another point is, as seen from the comparison of the continuous medium method and computer analysis using FEM for the cases taken, further research shall be made on analysis of CSW using FEM and the continuous medium method to clarify the difference between the two methods and their application relevance.

REFERENCES

[1] Beck H., 1956. Ein neues Berechnungsverfahren fuer gegliederte Scheiben, dargestellt am Beispiel der Vierendeeltraegers. Der Bauingenieur, Vol. 31, Heft 12, pp 436-443.

[2] Beck H., 1958. Ein Beitrag zur Berechnung regelmaessig gegliederter Scheibenll .Ingenieur-Archive, XXVI. Vol.

[3] Beck H., 1960. A discussion of Ref. 23 Der Bauingenieur, Vol.35, Heft 12, pp 481-482.

[4] Chaallal O., Gauthier, D. and Malenfane P., December 1996. Classification Methodology for Coupled Shear Walls. Journal of Structural Engineering Vol.122, No.12, pp 1453-1458.

[5] Chan H. B. B., April 1971. Static and Dynamic Analysis of Plane Coupled Shear Walls, MSc. Thesis, McMaster University.

[6] Chandran R., Kartha U.G. and Prabhakaran P., December 2014. A Comparative Study on Solid and Coupled Shear Wall. International Journal of Civil Engineering And Technology (IJCIET), Vol. 5, Issue 12, pp 117-133.

[7] Chitty L., October 1947. On The Cantilever Composed of A Number of Parallel Beams Interconnected By Cross Bars. The London, Edinburgh and Dublin Philosophical Magazine and Journal of Science. Vo1. 38, pp 685-699.

[8] Chopra A.K., 2000. Dynamics of Structures: Theory and Application in Earthquake Engineering. Prentice Hall, Eaglewood Cliffs, New Jersey.

[9] Coull A. and Choudhury J.R., February 1967. Stress And Deflection in Coupled Shear Walls ACI journal.

[10] Coull A. and Choudhury J.R., September 1967. Analysis of Coupled Shear Walls ACI journal.

[11] Coull A., and Irwin A. W., 1970. Analysis of Load Distribution in Multistory Shear Wall Structures. The Structural Engineer, Vol. 48, No. 8.

[12] Coull A. and Stafford S. B., "Analysis of Shear Wall Structures". Symposium on tall buildings with particular reference to shear wall structures, University of Southampton, April 1966, Oxford, Pergamon Press, 1967. pp 139-155.

[13] Gluck J. and Gellert M., 1972. Three Dimensional Lateral Load Analysis of Multistory Structures. Faculty of civil engineering, technion – Israel institute of technology.

[14] Hoenderkamp J.C.D., May 1983. A General Hand Method of Analysis for Tall Building Structures Subject To Lateral Loads. Department of Civil Engineering and App1ied Mechanics, McGill University Montreal, Quebec.

[15] Irwin A. W., and Heidebrecht A. C., 1971. Dynamic Response of Coupled Shear Wall Buildings. ASCE National Structural Engineering Meeting, Baltimore.

[16] Kanai K., Tajimi M, Osawa Y., and Kobayashi, H., 1968. Dynamic characteristics of Buildings with Pure Laminae-Type Construction. Architectural and Structural Engineering Series, Vol. 1, Earthquake Engineering, pp 111-122, Shokokusha, Tokyo, Japan.

[17] Kent A. H., Moulton J. D. and Robert L. C., March 2004. Parametric Study of Coupled Wall Behavior – Implications for the Design of Coupling Beams. Journal of Structural Engineering pp 480-488

[18] Li G. Q., and Choo B. S., 1995. Natural Frequency Evaluation of Coupled Shear Walls. *Struct. Engr., 73,* 301-304.

[19] Mukherjee P.R., and Coull A., 1973. Free Vibrations of Coupled Shear Walls. *Earthquake Eng. Struct. Dyn., 1*, 377-386. http://dx.doi.org/10.1002/eqe.4290010408

[20] Mukherjee P. R., and Coul, A., 1974. Free Vibrations of Coupled Shear Walls on Flexible base. *Proc.Instn.Civ.Engrs.*, *2*(57), 493-511. http://dx.doi.org/10.1680/iicep.1974.4028

[21] Paulay T., 1969. The Coupling of Shear Walls. Ph.D Thesis, University of Canterbury, Christ church, New Zealand, Volume 1.

[22] Reinhor A., Rutenberg A., Gluck J., February 1977. Dynamic Torsional Coupling in Asymmetric Building Structures. Publication no. 226.

[23] Rosman R., "Beitrag zur statischen Berechnung waagrecht belastete rQuerwaende bei Hochbauten". Der Bauingenieur, Part I, Vol. 35, Heft 4, 1960, pp 133-136, Part II, Vol. 37, Heft 1, 1962, pp 24-26, Part III, Vol. 37, Heft 8, 1962, pp 303-308.

[24] Sholeh M., February 2014. Investigation In to Behavior of Coupled Shear Walls By Means of Continuous Method. MSc. Thesis, Technical university of Delft.

[25] Skattum K.S., 1971. Dynamic Analysis of Coupled Shear Walls and Sandwich Beams. Earthquake Eng. Res. Lab., California Inst. of Technol., Pasadena, CA.

[26] Stafford S. B., and Coull A., 1991. Tall Building Structures- Analaysis And Design , Wiley and Interscience ,New York.

[27] Tani S., Sakurai J., and Iguch, M., 1969. An Approximate Method of Static and Dynamic Analysis of Core-Wall Buildings. Proceedings of the Fourth World Conference on Earthquake Engineering, Santiago, Chile.

[28] Tso W.K. and Biswas J.K., 1971. Seismic Analysis of Multi-Story Shear Wall Buildings. Civil Engineering and Engineering Mechanics Research Report, Faculty of Engineering, McMaster University, Canada.

[29] Tso W.K., and Chan H. B., February 1971. Dynamic Analysis of Plane Coupled Shear Walls. Journal of the Engineering Mechanics Division, ASCE, Vol. 97, No. EMl, Proc. Paper 7899, pp 33-48.

[30] Vuddandam R., Toutanji H. and Rodgers R., March 3, 2013. Approximate Solutions To Coupled Shear Walls On Fixed And Flexible Foundations. Modern applied Science, Vol.7, No.4.

[31] Wang Q., and Wang L.Y., 2005. Estimating Periods of Vibration of Buildings with Coupled Shear Walls. *J. Struct.Eng.*, *131*(12), 1931-35. http://dx.doi.org/10.1061/(ASCE)0733-9445(2005)131:12(1931)

APPENDIX 1: SOLVING THE GOVERNING DIFFERENTIAL EQUATION ON MAPLE

Deflection equation

$$\delta 1 := l \cdot \frac{dx}{dz};$$

$$l \left(\frac{d}{dz} x(z) \right)$$

$$\delta 2 := \frac{dN}{dz} \cdot \frac{b^3 \cdot h}{12 \cdot E \cdot Ie \cdot nb};$$

$$\frac{1}{12} \frac{\left(\frac{d}{dz} N(z) \right) b^3 h}{E \, Ie \, nb} \tag{2}$$

$$\delta 3 := -\frac{1}{E} \cdot \left(\frac{1}{A1} + \frac{1}{A2} \right) \int_0^z N(z) \, dz;$$

$$-\frac{\left(\frac{1}{A1} + \frac{1}{A2} \right) \left(\int_0^z N(z) \, dz \right)}{E} \tag{3}$$

$$\delta := \delta 1 + \delta 2 + \delta 3;$$

$$l \left(\frac{d}{dz} x(z) \right) + \frac{1}{12} \frac{\left(\frac{d}{dz} N(z) \right) b^3 h}{E \, Ie \, nb} - \frac{\left(\frac{1}{A1} + \frac{1}{A2} \right) \left(\int_0^z N(z) \, dz \right)}{E} \tag{4}$$

$$M1 := m(z) - \left(\frac{b}{2} + d1 \right) \cdot \int_z^H q(z) \, dz - Mb = E \cdot I1 \frac{d}{dz} \left(\frac{dx}{dz} \right);$$

$$m(z) - \left(\frac{1}{2} b + d1 \right) \left(\int_z^H q(z) \, dz \right) - Mb = E \, I1 \left(\frac{d^2}{dz^2} x(z) \right) \tag{5}$$

$$M2 := -\left(\frac{b}{2} + d2 \right) \cdot \int_z^H q(z) \, dz + Mb = E \cdot I2 \frac{d}{dz} \left(\frac{dx}{dz} \right);$$

$$-\left(\frac{1}{2} b + d2 \right) \left(\int_z^H q(z) \, dz \right) + Mb = E \, I2 \left(\frac{d^2}{dz^2} x(z) \right) \tag{6}$$

```
> (M1 + M2);
```

$$m(z) - \left(\frac{1}{2} b + d1 \right) \left(\int_z^H q(z) \, dz \right) - \left(\frac{1}{2} b + d2 \right) \left(\int_z^H q(z) \, dz \right) = E \, I1 \left(\frac{d^2}{dz^2} x(z) \right) + E \, I2 \left(\frac{d^2}{dz^2} x(z) \right) \tag{7}$$

```
> Sol1 := collect(M1 + M2, diff);
```

$$Sol1 := m(z) - \left(\frac{1}{2} b + d1 \right) \left(\int_z^H q(z) \, dz \right) - \left(\frac{1}{2} b + d2 \right) \left(\int_z^H q(z) \, dz \right) = (E \, I1 + E \, I2) \left(\frac{d^2}{dz^2} x(z) \right) \tag{8}$$

> $sol2 := collect\left(Sol1, \int_z^H q(z)\,dz\right);$

$$sol2 := (-b-d1-d2)\left(\int_z^H q(z)\,dz\right) + m(z) = (E\,I1 + E\,I2)\left(\frac{d^2}{dz^2}x(z)\right) \quad (9)$$

> $sol3 := algsubs((-b-d1-d2) = -l, sol2);$

$$sol3 := -\left(\int_z^H q(z)\,dz\right) l + m(z) = (E\,I1 + E\,I2)\left(\frac{d^2}{dz^2}x(z)\right) \quad (10)$$

> $sol4 := algsubs\left(\left(\int_z^H q(z)\,dz\right) = N(z), sol3\right);$

$$sol4 := -l\,N(z) + m(z) = (E\,I1 + E\,I2)\left(\frac{d^2}{dz^2}x(z)\right) \quad (11)$$

> $sol5 := collect\left(collect\left(algsubs\left(\left(\frac{d^2}{dz^2}x(z)\right) = \frac{-l\,N(z)+m(z)}{(EI1+EI2)}, \frac{d}{dz}\delta = 0\right), \frac{d^2}{dz^2}N(z)\right), N(z)\right);$

$$sol5 := -\frac{1}{12}\,\frac{1}{(EI1+EI2)\,E\,Ie\,nb\,A1\,A2}\left(\left(12\,A1\,A2\,E\,Ie\,l^2\,nb + 12\,A1\,EI1\,Ie\,nb + 12\,A1\,EI2\,Ie\,nb + 12\,A2\,EI1\,Ie\,nb + 12\,A2\,EI2\,Ie\,nb\right)N(z)\right) - \frac{1}{12}\,\frac{\left(-A1\,A2\,EI1\,b^3\,h - A1\,A2\,EI2\,b^3\,h\right)\left(\frac{d^2}{dz^2}N(z)\right)}{(EI1+EI2)\,E\,Ie\,nb\,A1\,A2} + \frac{m(z)\,l}{EI1+EI2} = 0 \quad (12)$$

> $eq1 := \frac{d^2}{dz^2}N(z) - N(z)\cdot\left(\frac{12\cdot Ie\cdot nb\cdot l^2}{b^3\cdot h\cdot i}\right)\cdot\left(1 + \frac{A\,i}{A1\cdot A2\cdot l^2}\right) = -\frac{m(z)\cdot l\cdot nb}{i}\cdot\left(\frac{12\cdot Ie}{b^3\cdot h}\right);$

$$eq1 := \frac{d^2}{dz^2}N(z) - \frac{12\,N(z)\,Ie\,nb\,l^2\left(1 + \frac{A\,i}{A1\,A2\,l^2}\right)}{b^3\,h\,i} = -\frac{12\,m(z)\,l\,nb\,Ie}{i\,b^3\,h} \quad (13)$$

> $eq := algsubs\left(\left(\frac{12\cdot Ie\cdot l}{b^3\cdot h\cdot i}\right) = \frac{\alpha^2}{l}, algsubs\left(\left(\frac{12\cdot Ie\cdot l^2}{b^3\cdot h\cdot i}\right) = \alpha^2, \left(algsubs\left(\left(1 + \frac{A\,i}{A1\cdot A2\cdot l^2}\right) = k^2, eq1\right)\right)\right)\right);$

$$eq := -N(z)\,nb\,k^2\,\alpha^2 + \frac{d^2}{dz^2}N(z) = -\frac{m(z)\,nb\,\alpha^2}{l} \quad (14)$$

> $eqdeflec1 := solve(algsubs(E\,I1 + E\,I2 = E\cdot i, sol4), N(z));$

$$eqdeflec1 := -\frac{\left(\frac{d^2}{dz^2}x(z)\right)E\,i - m(z)}{l} \quad (15)$$

> $eqdeflec2 := diff(eqdeflec1, z, z);$

$$eqdeflec2 := -\frac{\left(\frac{d^4}{dz^4}x(z)\right)E\,i - \left(\frac{d^2}{dz^2}m(z)\right)}{l} \quad (16)$$

```
> eqdeflec3 := diff(δ, z);
```

$$eqdeflec3 := l\left(\frac{d^2}{dz^2}x(z)\right) + \frac{1}{12}\,\frac{\left(\frac{d^2}{dz^2}N(z)\right) b^3 h}{E\,Ie\,nb} - \frac{\left(\frac{1}{A1}+\frac{1}{A2}\right)N(z)}{E} \tag{17}$$

```
> eqdeflec4 := algsubs(N(z) = eqdeflec1, algsubs(d^2/dz^2 N(z) = eqdeflec2, eqdeflec3));
```

$$eqdeflec4 := \frac{1}{12}\,\frac{1}{l\,E\,Ie\,nb\,A1\,A2}\left(-A1\,A2\,E\left(\frac{d^4}{dz^4}x(z)\right) b^3 h\,i + 12\,l^2\left(\frac{d^2}{dz^2}x(z)\right) E\,Ie\,nb\,A1\,A2 + A1\,A2\left(\frac{d^2}{dz^2}m(z)\right) b^3 h + 12\,A1\,E\,Ie\left(\frac{d^2}{dz^2}x(z)\right) i\,nb + 12\,A2\,E\,Ie\left(\frac{d^2}{dz^2}x(z)\right) i\,nb - 12\,A1\,Ie\,m(z)\,nb - 12\,A2\,Ie\,m(z)\,nb\right) \tag{18}$$

```
> ode1 := eqdeflec4 = 0;
```

$$ode1 := \frac{1}{12}\,\frac{1}{l\,E\,Ie\,nb\,A1\,A2}\left(-A1\,A2\,E\left(\frac{d^4}{dz^4}x(z)\right) b^3 h\,i + 12\,l^2\left(\frac{d^2}{dz^2}x(z)\right) E\,Ie\,nb\,A1\,A2 + A1\,A2\left(\frac{d^2}{dz^2}m(z)\right) b^3 h + 12\,A1\,E\,Ie\left(\frac{d^2}{dz^2}x(z)\right) i\,nb + 12\,A2\,E\,Ie\left(\frac{d^2}{dz^2}x(z)\right) i\,nb - 12\,A1\,Ie\,m(z)\,nb - 12\,A2\,Ie\,m(z)\,nb\right) = 0 \tag{19}$$

```
> ode2 := algsubs(-12 Ie/(b^3 h i E A2) - 12 Ie/(b^3 h i E A1) = -(k^2 - 1)·α^2/(i E),
    algsubs(12 Ie l^2/(b^3 h i) + 12 Ie/(b^3 h A2) + 12 Ie/(b^3 h A1) = k^2·α^2,
    collect(collect(expand((ode1)·(l·Ie·12/(h·b^3·i))), d^2/dz^2 x(z)), m(z))));
```

$$ode2 := m(z)\left(\frac{12\,l^2\,Ie}{E\,h\,b^3\,i^2} - \frac{k^2\,\alpha^2}{E\,i}\right) + \left(\frac{d^2}{dz^2}x(z)\right) k^2\,\alpha^2 + \frac{\frac{d^2}{dz^2}m(z)}{i\,E\,nb} - \frac{\frac{d^4}{dz^4}x(z)}{nb} = 0 \tag{20}$$

```
> ode3 := (d^4/dz^4 x(z)) - (d^2/dz^2 x(z)) k^2 α^2·nb = 1/(i E)·((d^2/dz^2 m(z)) - m(z) (k^2 - 1)·α^2·nb);
```

$$ode3 := \frac{d^4}{dz^4}x(z) - \left(\frac{d^2}{dz^2}x(z)\right) k^2\,\alpha^2\,nb = \frac{\frac{d^2}{dz^2}m(z) - m(z)\left(k^2-1\right)\alpha^2\,nb}{i\,E} \tag{21}$$

```
> m(z) := P·(H - z); d^2/dz^2 m(z);
```

$$m := z \to P\,(H - z)$$

$$0 \tag{22}$$

```
> dsolve(ode3, x(z));
```

$$x(z) = \frac{1}{k^2 i E}\left(\frac{E i \_C2\, e^{\sqrt{nb}\, k\alpha z}}{nb\,\alpha^2} + \frac{\_C1\, E i\, e^{-\sqrt{nb}\, k\alpha z}}{nb\,\alpha^2} + \frac{1}{2} H P k^2 z^2 - \frac{1}{6} P z^3 k^2 - \frac{1}{2} H P z^2 + \frac{1}{6} P z^3\right) + \_C3\, z + \_C4 \tag{23}$$

```
> ics := x(0) = 0, D(x)(0) = 0, D^(2)(x)(H) = 0, (D^(3)(x)(H) - nb·(k·α)^2·D(x)(H) = 1/(E i)
      ·((d/dz) m(z) - nb·α^2·(k^2 - 1)·∫_0^H m(z) dz));
```

$$ics := x(0) = 0,\ D(x)(0) = 0,\ D^{(2)}(x)(H) = 0,\ D^{(3)}(x)(H) - nb\,k^2\,\alpha^2\,D(x)(H) = \frac{-P - \frac{1}{2} nb\,\alpha^2\,(k^2-1)\,H^2 P}{E i} \tag{24}$$

```
> soldeflection := combine(convert(dsolve({ode3, ics}, x(z)), trig));
```

$$soldeflection := x(z) = \frac{1}{6}\,\frac{1}{k^5 i E nb^{5/2} \alpha^3 \cosh\left(\sqrt{nb}\, k\alpha H\right)}\left(3 H \cosh\left(\sqrt{nb}\, k\alpha H\right) nb^{5/2} P \alpha^3 k^5 z^2 - \cosh\left(\sqrt{nb}\, k\alpha H\right) nb^{5/2} P \alpha^3 k^5 z^3 - 3 H \cosh\left(\sqrt{nb}\, k\alpha H\right) nb^{5/2} P \alpha^3 k^3 z^2 + \cosh\left(\sqrt{nb}\, k\alpha H\right) nb^{5/2} P \alpha^3 k^3 z^3 + 6 P z k nb^{3/2} \alpha \cosh\left(\sqrt{nb}\, k\alpha H\right) + 6 \sinh\left(\sqrt{nb}\, k\alpha H - \sqrt{nb}\, k\alpha z\right) P nb - 6 \sinh\left(\sqrt{nb}\, k\alpha H\right) P nb\right) \tag{25}$$

```
> deflectionmax := expand(algsubs(z = H, soldeflection));
```

$$deflectionmax := x(H) = \frac{1}{3}\,\frac{H^3 P}{i E} - \frac{1}{3}\,\frac{H^3 P}{k^2 i E} + \frac{P H}{k^4 i \alpha^2 E nb} - \frac{\sinh\left(\sqrt{nb}\, k\alpha H\right) P}{E \alpha^3 i k^5 nb^{3/2} \cosh\left(\sqrt{nb}\, k\alpha H\right)} \tag{26}$$

```
> F3 := expand((3·E·i)/(P·H^3)·deflectionmax);
```

$$F3 := \frac{3 E i x(H)}{P H^3} = 1 - \frac{1}{k^2} + \frac{3}{H^2 k^4 \alpha^2 nb} - \frac{3 \sinh\left(\sqrt{nb}\, k\alpha H\right)}{H^3 \alpha^3 k^5 nb^{3/2} \cosh\left(\sqrt{nb}\, k\alpha H\right)} \tag{27}$$

```
> x(H) = (P·H^3)/(3·E·i)·F3;
```

$$x(H) = \left(x(H) = \frac{1}{3}\,\frac{H^3 P\left(1 - \frac{1}{k^2} + \frac{3}{H^2 k^4 \alpha^2 nb} - \frac{3 \sinh\left(\sqrt{nb}\, k\alpha H\right)}{H^3 \alpha^3 k^5 nb^{3/2} \cosh\left(\sqrt{nb}\, k\alpha H\right)}\right)}{i E}\right) \tag{28}$$

```
> Substituting y = k, x = k α H, r = nb :
> F3point := 1 - (1/y^2)·(3·((1/3) - 1/(r·x^2) + sinh(√r·x)/(r^(3/2)·x^3·cosh(√r·x))));
```

$$F3point := 1 - \frac{3\left(\frac{1}{3} - \frac{1}{r x^2} + \frac{\sinh\left(\sqrt{r}\, x\right)}{r^{3/2} x^3 \cosh\left(\sqrt{r}\, x\right)}\right)}{y^2} \tag{29}$$

```
> plot([subs(y=1, r=1, F3point), subs(y=1.05, r=1, F3point), subs(y=1.1, r=1, F3point),
  subs(y=1.15, r=1, F3point), subs(y=1.2, r=1, F3point), subs(y=1.25, r=1, F3point)],
  x=0..16, color=["DarkGreen", "NavyBlue", "Red", "Orange", "Black", "Niagara Purple"],
  legend=["k=1", "k=1.05", "k=1.1", "k=1.15", "k=1.2", "k=1.25"], title
  ="Variation of deflection factor F_3 for point load, nb=1", labels=["k α H",
  "Deflection force factor F_3"], labeldirections=["horizontal", "vertical"]); plot([subs(y
  =1, r=2, F3point), subs(y=1.05, r=2, F3point), subs(y=1.1, r=2, F3point), subs(y
  =1.15, r=2, F3point), subs(y=1.2, r=2, F3point), subs(y=1.25, r=2, F3point)], x=0
  ..16, color=["DarkGreen", "NavyBlue", "Red", "Orange", "Black", "Niagara Purple"],
  legend=["k=1", "k=1.05", "k=1.1", "k=1.15", "k=1.2", "k=1.25"], title
  ="Variation of deflection factor F_3 for point load, nb=2", labels=["k α H",
  "Deflection force factor F_3"], labeldirections=["horizontal", "vertical"]); plot([subs(y
  =1, r=3, F3point), subs(y=1.05, r=3, F3point), subs(y=1.1, r=3, F3point), subs(y
  =1.15, r=3, F3point), subs(y=1.2, r=3, F3point), subs(y=1.25, r=3, F3point)], x=0
  ..16, color=["DarkGreen", "NavyBlue", "Red", "Orange", "Black", "Niagara Purple"],
  legend=["k=1", "k=1.05", "k=1.1", "k=1.15", "k=1.2", "k=1.25"], title
  ="Variation of deflection factor F_3 for point load, nb=3", labels=["k α H",
  "Deflection force factor F_3"], labeldirections=["horizontal", "vertical"]); plot([subs(y
  =1, r=4, F3point), subs(y=1.05, r=4, F3point), subs(y=1.1, r=4, F3point), subs(y
  =1.15, r=4, F3point), subs(y=1.2, r=4, F3point), subs(y=1.25, r=4, F3point)], x=0
  ..16, color=["DarkGreen", "NavyBlue", "Red", "Orange", "Black", "Niagara Purple"],
  legend=["k=1", "k=1.05", "k=1.1", "k=1.15", "k=1.2", "k=1.25"], title
  ="Variation of deflection factor F_3 for point load, nb=4", labels=["k α H",
  "Deflection force factor F_3"], labeldirections=["horizontal", "vertical"]); plot([subs(y
  =1, r=5, F3point), subs(y=1.05, r=5, F3point), subs(y=1.1, r=5, F3point), subs(y
  =1.15, r=5, F3point), subs(y=1.2, r=5, F3point), subs(y=1.25, r=5, F3point)], x=0
  ..16, color=["DarkGreen", "NavyBlue", "Red", "Orange", "Black", "Niagara Purple"],
  legend=["k=1", "k=1.05", "k=1.1", "k=1.15", "k=1.2", "k=1.25"], title
  ="Variation of deflection factor F_3 for point load, nb=5", labels=["k α H",
  "Deflection force factor F_3"], labeldirections=["horizontal", "vertical"]);
```

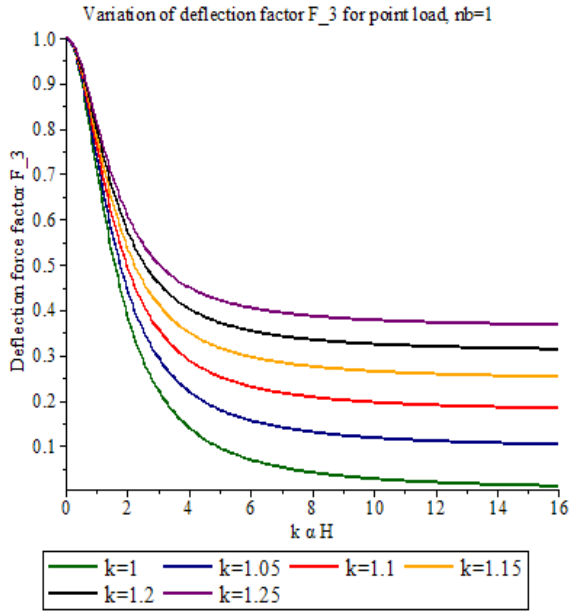

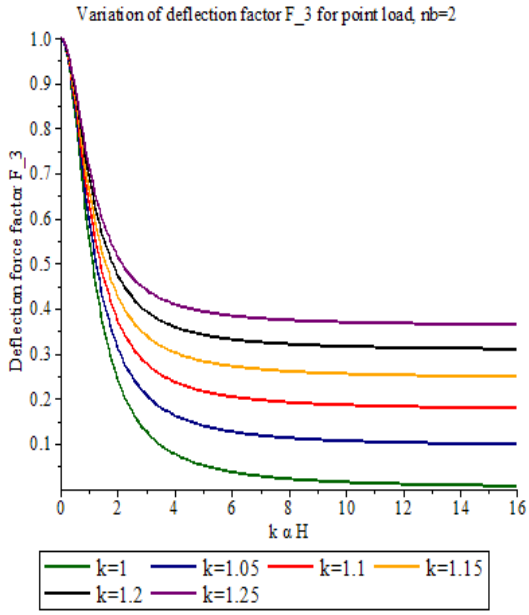

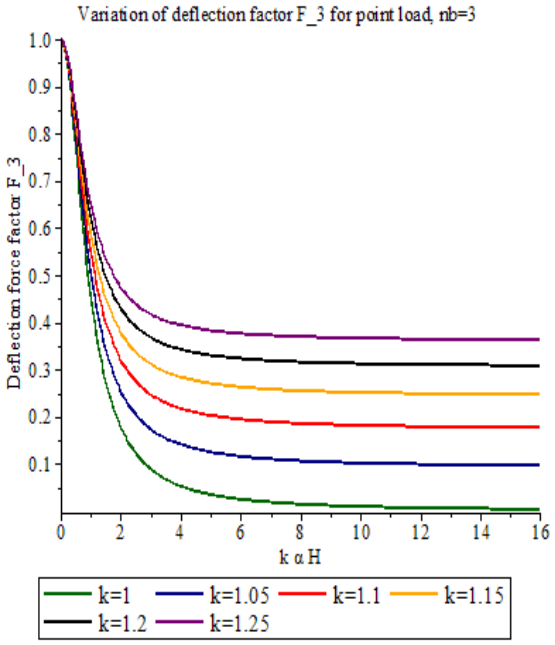

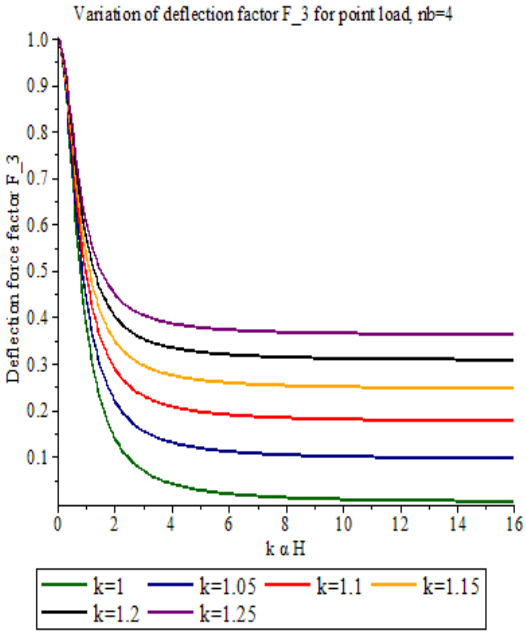

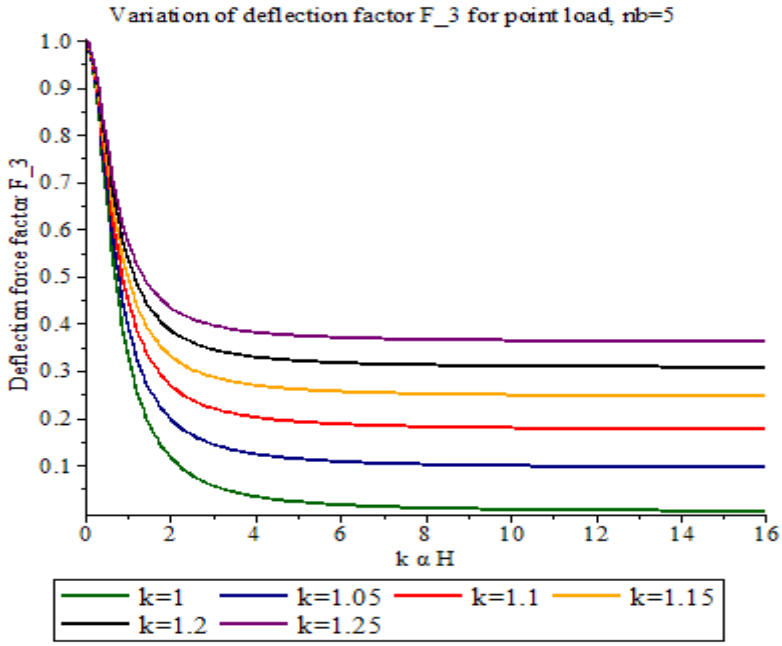

Axial force factor plots ($nb = 1$ to $nb = 5$)

> $ode := diff(N(z), z, z) - nb \cdot (k \cdot \alpha)^2 \cdot N(z) = -\frac{nb \cdot \alpha^2}{l} \cdot (P \cdot (H - z))$;

$$ode := \frac{d^2}{dz^2} N(z) - nb\, k^2\, \alpha^2\, N(z) = -\frac{nb\, \alpha^2\, P\, (H - z)}{l}$$

> $dsolve(ode)$;

$$N(z) = e^{\sqrt{nb}\, \alpha k z}\_C2 + e^{-\sqrt{nb}\, \alpha k z}\_C1 + \frac{P\, (H - z)}{k^2\, l}$$

```
> ics := N(H) = 0, D(N)(0) = 0;
```

$$ics := N(H) = 0,\ D(N)(0) = 0 \tag{33}$$

```
> convert(dsolve({ode, ics}), trig);
```

$$N(z) \tag{34}$$

$$= \frac{1}{2}\,\frac{1}{\cosh\left(\sqrt{nb}\,\alpha k H\right)\sqrt{nb}\,\alpha k^3 l}\left(\left(\cosh\left(\sqrt{nb}\,\alpha k z\right)\right.\right.$$

$$\left.\left.+\sinh\left(\sqrt{nb}\,\alpha k z\right)\right)\left(\cosh\left(\sqrt{nb}\,\alpha k H\right)-\sinh\left(\sqrt{nb}\,\alpha k H\right)\right)P\right)$$

$$-\frac{1}{2}\,\frac{1}{\cosh\left(\sqrt{nb}\,\alpha k H\right)\sqrt{nb}\,\alpha k^3 l}\left(\left(\cosh\left(\sqrt{nb}\,\alpha k z\right)\right.\right.$$

$$\left.\left.-\sinh\left(\sqrt{nb}\,\alpha k z\right)\right)P\left(\cosh\left(\sqrt{nb}\,\alpha k H\right)+\sinh\left(\sqrt{nb}\,\alpha k H\right)\right)\right)+\frac{P\,(H-z)}{k^2 l}$$

```
> Npointload
    := 1/2 * 1/(cosh(sqrt(nb)*alpha*k*H)*sqrt(nb)*alpha*k^3*l) * ((cosh(sqrt(nb)*alpha*k*z)
    + sinh(sqrt(nb)*alpha*k*z)) * (cosh(sqrt(nb)*alpha*k*H) - sinh(sqrt(nb)*alpha*k*H)) * P)
    - 1/2 * 1/(cosh(sqrt(nb)*alpha*k*H)*sqrt(nb)*alpha*k^3*l) * ((cosh(sqrt(nb)*alpha*k*z)
    - sinh(sqrt(nb)*alpha*k*z)) * P * (cosh(sqrt(nb)*alpha*k*H) + sinh(sqrt(nb)*alpha*k*H))) + P*(H-z)/(k^2*l);
```

$$Npointload := \tag{35}$$

$$\frac{1}{2}\,\frac{\left(\cosh\left(\sqrt{nb}\,\alpha k z\right)+\sinh\left(\sqrt{nb}\,\alpha k z\right)\right)\left(\cosh\left(\sqrt{nb}\,\alpha k H\right)-\sinh\left(\sqrt{nb}\,\alpha k H\right)\right)P}{\cosh\left(\sqrt{nb}\,\alpha k H\right)\sqrt{nb}\,\alpha k^3 l}$$

$$-\frac{1}{2}\,\frac{1}{\cosh\left(\sqrt{nb}\,\alpha k H\right)\sqrt{nb}\,\alpha k^3 l}\left(\left(\cosh\left(\sqrt{nb}\,\alpha k z\right)\right.\right.$$

$$\left.\left.-\sinh\left(\sqrt{nb}\,\alpha k z\right)\right)P\left(\cosh\left(\sqrt{nb}\,\alpha k H\right)+\sinh\left(\sqrt{nb}\,\alpha k H\right)\right)\right)+\frac{P\,(H-z)}{k^2 l}$$

```
> simplify(Npointload);
```

$$\frac{1}{\cosh\left(\sqrt{nb}\,\alpha k H\right)\sqrt{nb}\,\alpha k^3 l}\left(P\left(\cosh\left(\sqrt{nb}\,\alpha k H\right)\sqrt{nb}\,\alpha k H\right.\right. \tag{36}$$

$$-\cosh\left(\sqrt{nb}\,\alpha k H\right)\sqrt{nb}\,\alpha k z-\cosh\left(\sqrt{nb}\,\alpha k z\right)\sinh\left(\sqrt{nb}\,\alpha k H\right)$$

$$\left.\left.+\sinh\left(\sqrt{nb}\,\alpha k z\right)\cosh\left(\sqrt{nb}\,\alpha k H\right)\right)\right)$$

```
> algsubs(k*alpha*H*nb^(1/2) = y*r^(1/2), algsubs(k*alpha*z*nb^(1/2) = y*x*r^(1/2), k^2*l/(H*P) * (simplify(Npointload))));
```

$$\frac{1}{\cosh\left(y\sqrt{r}\right)\sqrt{nb}\,H k\alpha}\left(-\cosh\left(y\sqrt{r}\right)y x\sqrt{r}+\cosh\left(y\sqrt{r}\right)y\sqrt{r}\right. \tag{37}$$

$$\left.+\sinh\left(y x\sqrt{r}\right)\cosh\left(y\sqrt{r}\right)-\cosh\left(y x\sqrt{r}\right)\sinh\left(y\sqrt{r}\right)\right)$$

Substiuting $y = k\,\alpha\,H$, $x = \frac{z}{H}$, $r = nb$ **:**

```
> F1point := 1/(cosh(y*sqrt(r))*sqrt(r)*y) * (-cosh(y*sqrt(r))*y*x*sqrt(r) + cosh(y*sqrt(r))*y*sqrt(r)
    + sinh(y*x*sqrt(r))*cosh(y*sqrt(r)) - cosh(y*x*sqrt(r))*sinh(y*sqrt(r)));
```

$$F1point := \frac{1}{\cosh\left(y\sqrt{r}\right)\sqrt{r}\,y}\left(-\cosh\left(y\sqrt{r}\right)y x\sqrt{r}+\cosh\left(y\sqrt{r}\right)y\sqrt{r}\right. \tag{38}$$

$$\left.+\sinh\left(y x\sqrt{r}\right)\cosh\left(y\sqrt{r}\right)-\cosh\left(y x\sqrt{r}\right)\sinh\left(y\sqrt{r}\right)\right)$$

```
> plot([subs(y=1, r=1, F1point), subs(y=2, r=1, F1point), subs(y=3, r=1, F1point), subs(y
    =5, r=1, F1point), subs(y=10, r=1, F1point), subs(y=16, r=1, F1point)], x=0..1,
  color=["DarkGreen", "NavyBlue", "Red", "Orange", "Black", "Niagara Purple"], legend
  =["kαH=1", "kαH=2", "kαH=3", "kαH=5", "kαH=10", "kαH=16"], title=
  "Variation of axial force factor F_1 for point load, nb=1 ", labels=["z/H",
  "Axial force factor F_1"], labeldirections=["horizontal", "vertical"]); plot([subs(y=1, r
  =2, F1point), subs(y=2, r=2, F1point), subs(y=3, r=2, F1point), subs(y=5, r=2,
  F1point), subs(y=10, r=2, F1point), subs(y=16, r=2, F1point)], x=0..1, color
  =["DarkGreen", "NavyBlue", "Red", "Orange", "Black", "Niagara Purple"], legend
  =["kαH=1", "kαH=2", "kαH=3", "kαH=5", "kαH=10", "kαH=16"], title=
  "Variation of axial force factor F_1 for point load, nb=2 ", labels=["z/H",
  "Axial force factor F_1"], labeldirections=["horizontal", "vertical"]); plot([subs(y=1, r
  =3, F1point), subs(y=2, r=3, F1point), subs(y=3, r=3, F1point), subs(y=5, r=3,
  F1point), subs(y=10, r=3, F1point), subs(y=16, r=3, F1point)], x=0..1, color
  =["DarkGreen", "NavyBlue", "Red", "Orange", "Black", "Niagara Purple"], legend
  =["kαH=1", "kαH=2", "kαH=3", "kαH=5", "kαH=10", "kαH=16"], title=
  "Variation of axial force factor F_1 for point load, nb=3 ", labels=["z/H",
  "Axial force factor F_1"], labeldirections=["horizontal", "vertical"]); plot([subs(y=1, r
  =4, F1point), subs(y=2, r=4, F1point), subs(y=3, r=4, F1point), subs(y=5, r=4,
  F1point), subs(y=10, r=4, F1point), subs(y=16, r=4, F1point)], x=0..1, color
  =["DarkGreen", "NavyBlue", "Red", "Orange", "Black", "Niagara Purple"], legend
  =["kαH=1", "kαH=2", "kαH=3", "kαH=5", "kαH=10", "kαH=16"], title=
  "Variation of axial force factor F_1 for point load, nb=4 ", labels=["z/H",
  "Axial force factor F_1"], labeldirections=["horizontal", "vertical"]); plot([subs(y=1, r
  =5, F1point), subs(y=2, r=5, F1point), subs(y=3, r=5, F1point), subs(y=5, r=5,
  F1point), subs(y=10, r=5, F1point), subs(y=16, r=5, F1point)], x=0..1, color
  =["DarkGreen", "NavyBlue", "Red", "Orange", "Black", "Niagara Purple"], legend
  =["kαH=1", "kαH=2", "kαH=3", "kαH=5", "kαH=10", "kαH=16"], title=
  "Variation of axial force factor F_1 for point load, nb=5 ", labels=["z/H",
  "Axial force factor F_1"], labeldirections=["horizontal", "vertical"]);
```

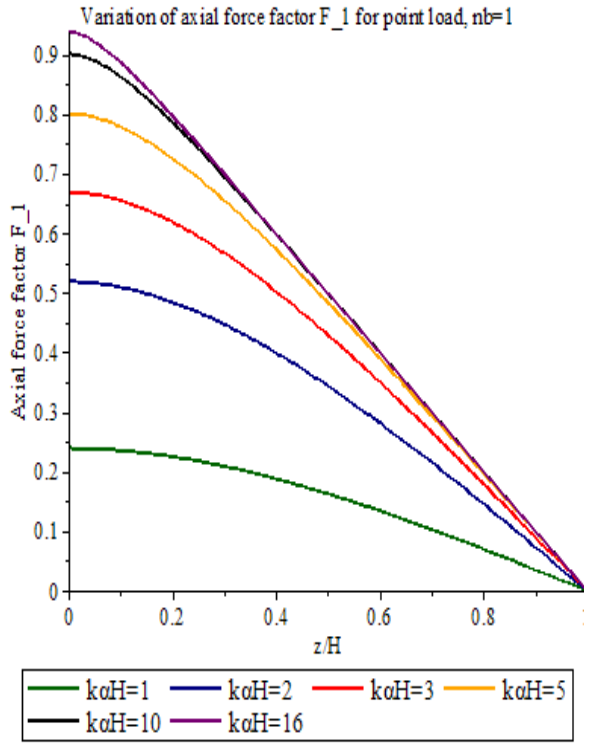

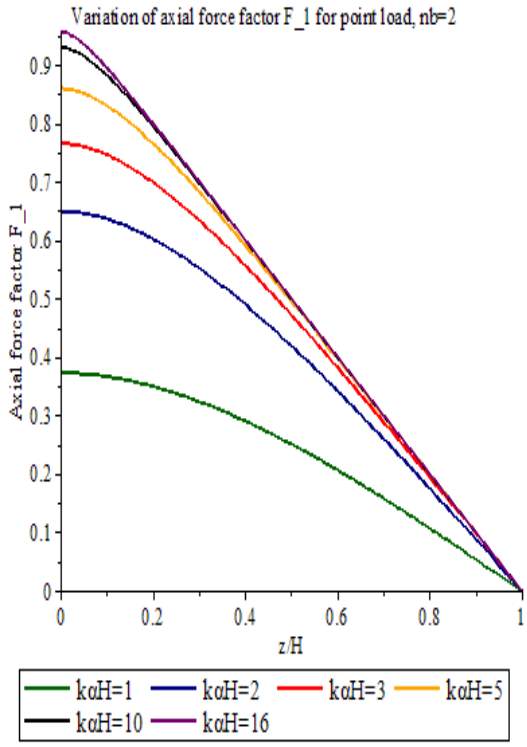

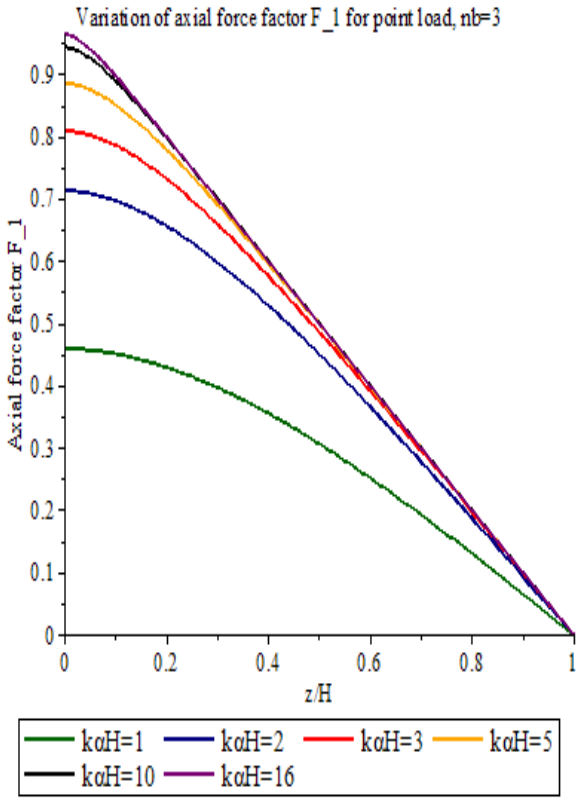
Variation of axial force factor F_1 for point load, nb=3
Axial force factor F_1
z/H
0
0.1
0.2
0.3
0.4
0.5
0.6
0.7
0.8
0.9
1
0.2
0.4
0.6
0.8
kαH=1
kαH=2
kαH=3
kαH=5
kαH=10
kαH=16

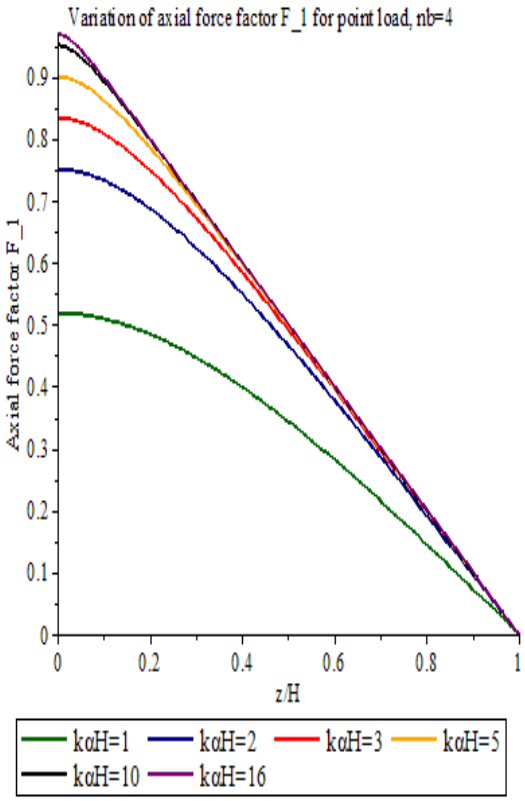
Variation of axial force factor F_1 for point load, nb=4
Axial force factor F_1
z/H
0
0.1
0.2
0.3
0.4
0.5
0.6
0.7
0.8
0.9
1
0.2
0.4
0.6
0.8
kαH=1
kαH=2
kαH=3
kαH=5
kαH=10
kαH=16

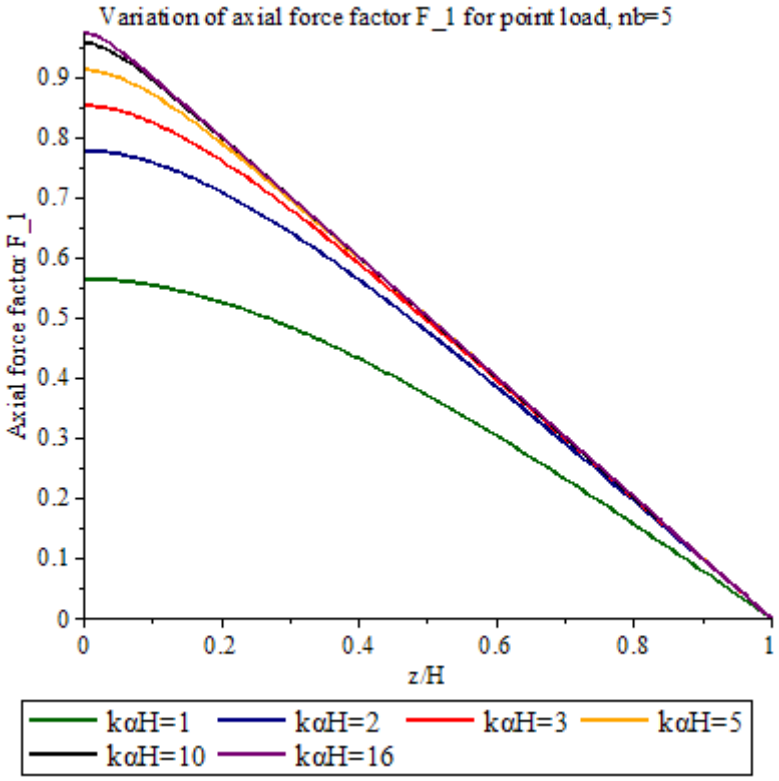
Variation of axial force factor F_1 for point load, nb=5
Axial force factor F_1
z/H
0
0.1
0.2
0.3
0.4
0.5
0.6
0.7
0.8
0.9
1
0.2
0.4
0.6
0.8
kαH=1
kαH=2
kαH=3
kαH=5
kαH=10
kαH=16

Shear flow factor plots in *the connecting medium* ($nb = 1$ to $nb = 5$) :

```
> qpoint := -diff(Npointload, z);
```

$$qpoint := -\frac{1}{2}\,\frac{1}{\cosh\left(\sqrt{nb}\,\alpha\,k\,H\right)\sqrt{nb}\,\alpha\,k^3\,l}\left(\left(\sinh\left(\sqrt{nb}\,\alpha\,k\,z\right)\sqrt{nb}\,\alpha\,k + \cosh\left(\sqrt{nb}\,\alpha\,k\,z\right)\sqrt{nb}\,\alpha\,k\right)\left(\cosh\left(\sqrt{nb}\,\alpha\,k\,H\right) - \sinh\left(\sqrt{nb}\,\alpha\,k\,H\right)\right)P\right) + \frac{1}{2}\,\frac{1}{\cosh\left(\sqrt{nb}\,\alpha\,k\,H\right)\sqrt{nb}\,\alpha\,k^3\,l}\left(\left(\sinh\left(\sqrt{nb}\,\alpha\,k\,z\right)\sqrt{nb}\,\alpha\,k - \cosh\left(\sqrt{nb}\,\alpha\,k\,z\right)\sqrt{nb}\,\alpha\,k\right)P\left(\cosh\left(\sqrt{nb}\,\alpha\,k\,H\right) + \sinh\left(\sqrt{nb}\,\alpha\,k\,H\right)\right)\right) + \frac{P}{k^2\,l} \tag{39}$$

```
> sim1 := simplify(convert(simplify(qpoint·k^2·l / P), trig));
```

$$sim1 := \frac{1}{\cosh\left(\sqrt{nb}\,\alpha\,k\,H\right)}\left(\sinh\left(\sqrt{nb}\,\alpha\,k\,z\right)\sinh\left(\sqrt{nb}\,\alpha\,k\,H\right) - \cosh\left(\sqrt{nb}\,\alpha\,k\,z\right)\cosh\left(\sqrt{nb}\,\alpha\,k\,H\right) + \cosh\left(\sqrt{nb}\,\alpha\,k\,H\right)\right) \tag{40}$$

```
> sim1 := 1/cosh(sqrt(nb) α k H) (sinh(sqrt(nb) α k z) sinh(sqrt(nb) α k H)
      - cosh(sqrt(nb) α k z) cosh(sqrt(nb) α k H) + cosh(sqrt(nb) α k H));
```

$$sim1 := \frac{1}{\cosh\left(\sqrt{nb}\,\alpha\,k\,H\right)}\left(\sinh\left(\sqrt{nb}\,\alpha\,k\,z\right)\sinh\left(\sqrt{nb}\,\alpha\,k\,H\right) - \cosh\left(\sqrt{nb}\,\alpha\,k\,z\right)\cosh\left(\sqrt{nb}\,\alpha\,k\,H\right) + \cosh\left(\sqrt{nb}\,\alpha\,k\,H\right)\right) \tag{41}$$

```
> F2 := algsubs(sqrt(nb) α k z = y·x·sqrt(r), algsubs(sqrt(nb) α k H = y·sqrt(r), sim1));
```

$$F2 := \frac{\sinh\left(y\,x\sqrt{r}\right)\sinh\left(y\sqrt{r}\right) - \cosh\left(y\,x\sqrt{r}\right)\cosh\left(y\sqrt{r}\right) + \cosh\left(y\sqrt{r}\right)}{\cosh\left(y\sqrt{r}\right)} \tag{42}$$

```
> plot([subs(y=1, r=1, F2), subs(y=2, r=1, F2), subs(y=3, r=1, F2), subs(y=5, r=1, F2),
      subs(y=10, r=1, F2), subs(y=16, r=1, F2)], x=0..1, color=["DarkGreen",
      "NavyBlue", "Red", "Orange", "Black", "Niagara Purple"], legend=["kαH=1", "kαH=2",
      "kαH=3", "kαH=5", "kαH=10", "kαH=16"], title
      ="Variation of shear flow factor F_2 for point load, nb=1 ", labels=["z/H",
      "shear flow factor F_2"], labeldirections=["horizontal", "vertical"]); plot([subs(y=1, r=2,
      F2), subs(y=2, r=2, F2), subs(y=3, r=2, F2), subs(y=5, r=2, F2), subs(y=10, r=2,
      F2), subs(y=16, r=2, F2)], x=0..1, color=["DarkGreen", "NavyBlue", "Red", "Orange",
      "Black", "Niagara Purple"], legend=["kαH=1", "kαH=2", "kαH=3", "kαH=5", "kαH=10",
      "kαH=16"], title="Variation of shear flow factor F_2 for point load, nb=2 ", labels
      =["z/H", "shear flow factor F_2"], labeldirections=["horizontal", "vertical"]);
      plot([subs(y=1, r=3, F2), subs(y=2, r=3, F2), subs(y=3, r=3, F2), subs(y=5, r=3,
      F2), subs(y=10, r=3, F2), subs(y=16, r=3, F2)], x=0..1, color=["DarkGreen",
      "NavyBlue", "Red", "Orange", "Black", "Niagara Purple"], legend=["kαH=1", "kαH=2",
      "kαH=3", "kαH=5", "kαH=10", "kαH=16"], title
      ="Variation of shear flow factor F_2 for point load, nb=3 ", labels=["z/H",
      "shear flow factor F_2"], labeldirections=["horizontal", "vertical"]); plot([subs(y=1, r=4,
      F2), subs(y=2, r=4, F2), subs(y=3, r=4, F2), subs(y=5, r=4, F2), subs(y=10, r=4,
      F2), subs(y=16, r=4, F2)], x=0..1, color=["DarkGreen", "NavyBlue", "Red", "Orange",
      "Black", "Niagara Purple"], legend=["kαH=1", "kαH=2", "kαH=3", "kαH=5", "kαH=10",
      "kαH=16"], title="Variation of shear flow factor F_2 for point load, nb=4 ", labels
      =["z/H", "shear flow factor F_2"], labeldirections=["horizontal", "vertical"]);
      plot([subs(y=1, r=5, F2), subs(y=2, r=5, F2), subs(y=3, r=5, F2), subs(y=5, r=5,
      F2), subs(y=10, r=5, F2), subs(y=16, r=5, F2)], x=0..1, color=["DarkGreen",
      "NavyBlue", "Red", "Orange", "Black", "Niagara Purple"], legend=["kαH=1", "kαH=2",
      "kαH=3", "kαH=5", "kαH=10", "kαH=16"], title
      ="Variation of shear flow factor F_2 for point load, nb=5 ", labels=["z/H",
      "shear flow factor F_2"], labeldirections=["horizontal", "vertical"]);
```

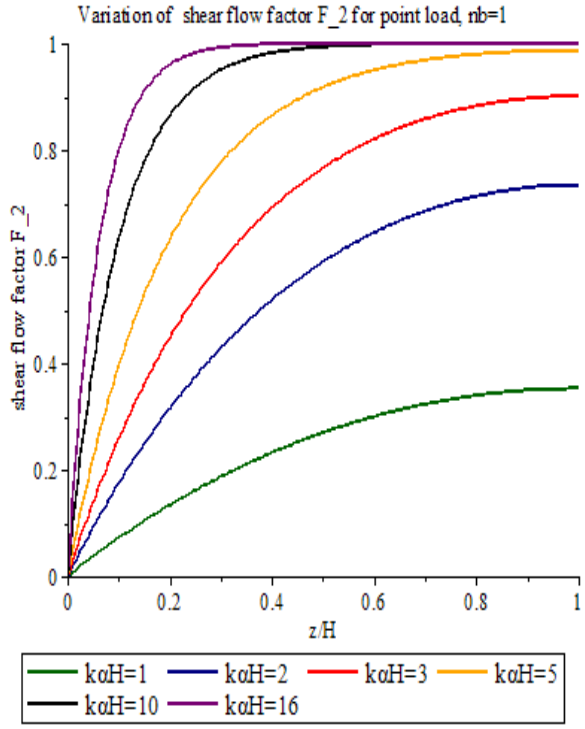
Variation of shear flow factor F_2 for point load, nb=1
shear flow factor F_2
z/H
0
0.2
0.4
0.6
0.8
1
kαH=1
kαH=2
kαH=3
kαH=5
kαH=10
kαH=16

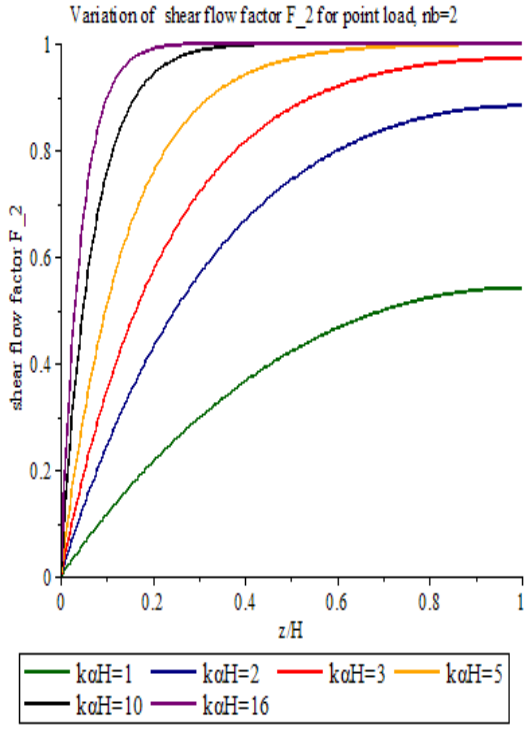
Variation of shear flow factor F_2 for point load, nb=2
shear flow factor F_2
z/H
0
0.2
0.4
0.6
0.8
1
kαH=1
kαH=2
kαH=3
kαH=5
kαH=10
kαH=16

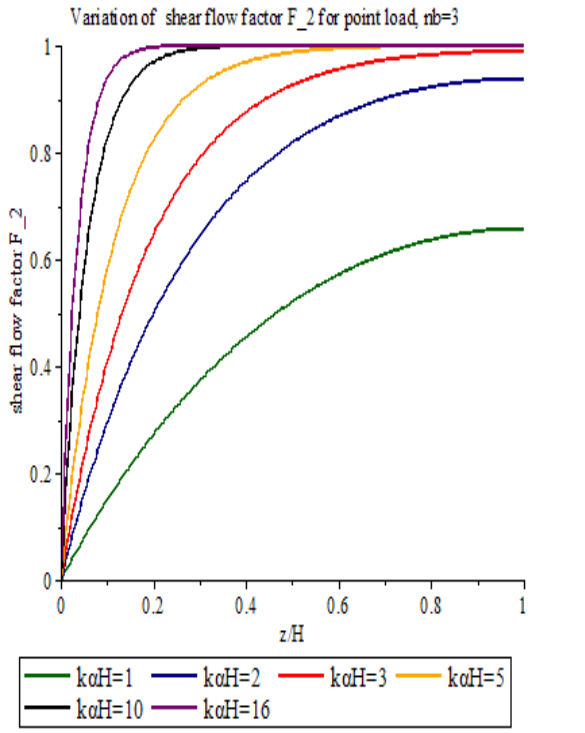
Variation of shear flow factor F_2 for point load, nb=3
shear flow factor F_2
z/H
0
0.2
0.4
0.6
0.8
1
kαH=1
kαH=2
kαH=3
kαH=5
kαH=10
kαH=16

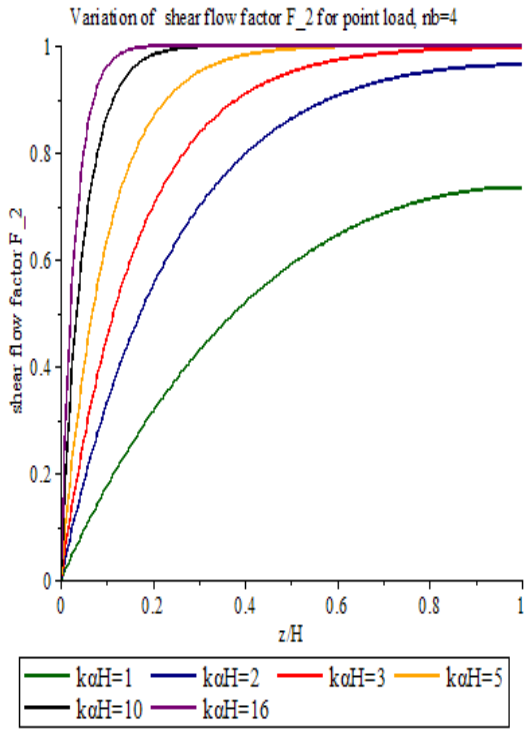
Variation of shear flow factor F_2 for point load, nb=4
shear flow factor F_2
z/H
0
0.2
0.4
0.6
0.8
1
kαH=1
kαH=2
kαH=3
kαH=5
kαH=10
kαH=16

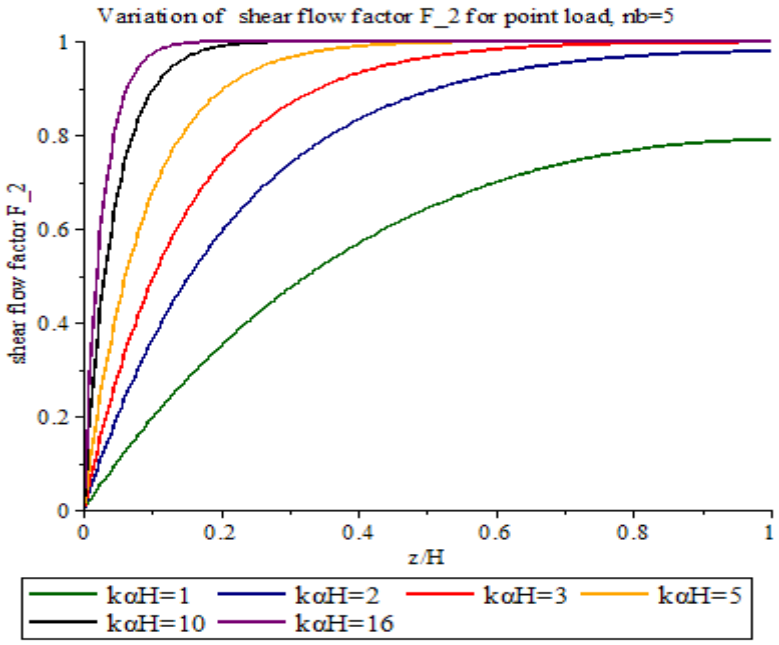

***Composite* and *individual canilever action factor plots* ($nb = 1$ to $nb = 5$) :**

$$> es1 := \frac{(P\cdot(H-z) - Npointload\cdot l)\cdot c1}{i} + \frac{Npointload}{A1};$$

$$es1 := \frac{1}{i}\left(\left(P\,(H-z)\right.\right. \tag{51}$$

$$-\left(\frac{1}{2}\,\frac{1}{\cosh\left(\sqrt{nb}\,\alpha k H\right)\sqrt{nb}\,\alpha k^3 l}\left(\left(\cosh\left(\sqrt{nb}\,\alpha k z\right)\right.\right.\right.$$

$$\left.\left.+\sinh\left(\sqrt{nb}\,\alpha k z\right)\right)\left(\cosh\left(\sqrt{nb}\,\alpha k H\right)-\sinh\left(\sqrt{nb}\,\alpha k H\right)\right)P\right)$$

$$-\frac{1}{2}\,\frac{1}{\cosh\left(\sqrt{nb}\,\alpha k H\right)\sqrt{nb}\,\alpha k^3 l}\left(\left(\cosh\left(\sqrt{nb}\,\alpha k z\right)\right.\right.$$

$$\left.\left.\left.-\sinh\left(\sqrt{nb}\,\alpha k z\right)\right)P\left(\cosh\left(\sqrt{nb}\,\alpha k H\right)+\sinh\left(\sqrt{nb}\,\alpha k H\right)\right)\right)+\frac{P\,(H-z)}{k^2 l}\right)l\Bigg)$$

$$c1\Bigg)$$

$$+\frac{1}{A1}\left(\frac{1}{2}\,\frac{1}{\cosh\left(\sqrt{nb}\,\alpha k H\right)\sqrt{nb}\,\alpha k^3 l}\left(\left(\cosh\left(\sqrt{nb}\,\alpha k z\right)\right.\right.\right.$$

$$\left.\left.+\sinh\left(\sqrt{nb}\,\alpha k z\right)\right)\left(\cosh\left(\sqrt{nb}\,\alpha k H\right)-\sinh\left(\sqrt{nb}\,\alpha k H\right)\right)P\right)$$

$$-\frac{1}{2}\,\frac{1}{\cosh\left(\sqrt{nb}\,\alpha k H\right)\sqrt{nb}\,\alpha k^3 l}\left(\left(\cosh\left(\sqrt{nb}\,\alpha k z\right)\right.\right.$$

$$\left.\left.\left.-\sinh\left(\sqrt{nb}\,\alpha k z\right)\right)P\left(\cosh\left(\sqrt{nb}\,\alpha k H\right)+\sinh\left(\sqrt{nb}\,\alpha k H\right)\right)\right)+\frac{P\,(H-z)}{k^2 l}\right)$$

> $es2 := \dfrac{P\cdot(H-z)}{\left(i+\dfrac{A1\cdot A2}{A}\cdot l^2\right)}\cdot\left(\dfrac{A2\cdot l}{A}+c1\right)\cdot\left(\dfrac{k2}{100}\right);$

$$es2 := \frac{1}{100}\,\frac{P\,(H-z)\left(\dfrac{A2\,l}{A}+c1\right)k2}{i+\dfrac{A1\,A2\,l^2}{A}} \tag{52}$$

> $es3 := \dfrac{P\cdot(H-z)\cdot c1}{i}\cdot\left(\dfrac{100-k2}{100}\right);$

$$es3 := \frac{P\,(H-z)\,c1\left(1-\dfrac{1}{100}\,k2\right)}{i} \tag{53}$$

> $es4 := (solve((es1 = es2+es3, k2)))\cdot\dfrac{(H-z)\cdot k\cdot\alpha\cdot\sqrt{nb}}{100};$

$$es4 := \frac{1}{A2\,A1\,l^2\cosh\left(\sqrt{nb}\,\alpha\,k\,H\right)k^2}\left(\left(A1\,A2\,l^2+A\,i\right)\left(\cosh\left(\sqrt{nb}\,\alpha\,k\,H\right)\sqrt{nb}\,\alpha\,k\,H\right.\right. \tag{54}$$
$$-\cosh\left(\sqrt{nb}\,\alpha\,k\,H\right)\sqrt{nb}\,\alpha\,k\,z-\cosh\left(\sqrt{nb}\,\alpha\,k\,z\right)\sinh\left(\sqrt{nb}\,\alpha\,k\,H\right)$$
$$\left.\left.+\sinh\left(\sqrt{nb}\,\alpha\,k\,z\right)\cosh\left(\sqrt{nb}\,\alpha\,k\,H\right)\right)\right)$$

> $expand\left(algsubs\left(\dfrac{i\cdot A}{l^2\cdot A1\cdot A2}=k^2-1, expand((4))\right)\right);$

$$m(z)-\frac{1}{2}\left(\int_z^H q(z)\,dz\right)b-\left(\int_z^H q(z)\,dz\right)d1-Mb=E\,I1\left(\frac{d^2}{dz^2}\,x(z)\right) \tag{55}$$

> $F5 := combine\left(-\dfrac{\cosh\left(\sqrt{nb}\,\alpha\,k\,z\right)\sinh\left(\sqrt{nb}\,\alpha\,k\,H\right)}{\cosh\left(\sqrt{nb}\,\alpha\,k\,H\right)}+\sinh\left(\sqrt{nb}\,\alpha\,k\,z\right), trig\right)$
$+factor\left(\sqrt{nb}\,\alpha\,k\,H-\sqrt{nb}\,\alpha\,k\,z\right);$

$$F5 := -\frac{\sinh\left(-\sqrt{nb}\,\alpha\,k\,z+\sqrt{nb}\,\alpha\,k\,H\right)}{\cosh\left(\sqrt{nb}\,\alpha\,k\,H\right)}+\sqrt{nb}\,\alpha\,k\,(H-z) \tag{56}$$

> $algsubs\left(\sqrt{nb}\,\alpha\,k\,z=\sqrt{r}\cdot y\cdot x, algsubs\left(\sqrt{nb}\,\alpha\,k\,H=\sqrt{r}\cdot x, F5\right)\right);$

$$\frac{\sinh\left(y\,x\sqrt{r}-x\sqrt{r}\right)}{\cosh\left(x\sqrt{r}\right)}+\sqrt{nb}\,\alpha\,k\,(H-z) \tag{57}$$

> $k2plot := \dfrac{100}{(1-y)\cdot\sqrt{r}\cdot x}\cdot\left(\dfrac{\sinh\left(\sqrt{r}\,y\,x-\sqrt{r}\,x\right)}{\cosh\left(\sqrt{r}\,x\right)}+(1-y)\cdot\sqrt{r}\cdot x\right);$

$$k2plot := \frac{100\left(\dfrac{\sinh\left(y\,x\sqrt{r}-x\sqrt{r}\right)}{\cosh\left(x\sqrt{r}\right)}+(1-y)\sqrt{r}\,x\right)}{(1-y)\sqrt{r}\,x} \tag{58}$$

> $k1plot := 100-k2plot;$

$$k1plot := 100-\frac{100\left(\dfrac{\sinh\left(y\,x\sqrt{r}-x\sqrt{r}\right)}{\cosh\left(x\sqrt{r}\right)}+(1-y)\sqrt{r}\,x\right)}{(1-y)\sqrt{r}\,x} \tag{59}$$

```
> with(plots):
> dualaxisplot(plot([subs(y=0, r=1, k2plot), subs(y=0.25, r=1, k2plot), subs(y=0.5, r=1,
      k2plot), subs(y=0.625, r=1, k2plot), subs(y=0.75, r=1, k2plot)], x=0..16, color
     =["DarkGreen", "NavyBlue", "Red", "Orange", "Black"], legend=["z/H=0", "z/H=0.25",
     "z/H=0.5", "z/H=0.625", "z/H=0.75"], labels=["kαH ",
     "k_2 percentage of composite cantilever action"], labeldirections=["horizontal",
     "vertical"]), plot([subs(y=0, r=1,-k1plot), subs(y=0.25, r=1,-k1plot), subs(y=0.5, r
     =1,-k1plot), subs(y=0.625, r=1,-k1plot), subs(y=0.75, r=1,-k1plot)], x=0..16, color
     =["DarkGreen", "NavyBlue", "Red", "Orange", "Black"], legend=["z/H=0", "z/H=0.25",
     "z/H=0.5", "z/H=0.625", "z/H=0.75"], labels=["kαH ",
     "(k_1 percentage of individual cantilever action)-1 "], labeldirections=["horizontal",
      "vertical"]), title
     ="variation of wall moment factor k_1 and k_2 for point load with nb, 1 ");
    dualaxisplot(plot([subs(y=0, r=2, k2plot), subs(y=0.25, r=2, k2plot), subs(y=0.5, r
     =2, k2plot), subs(y=0.625, r=2, k2plot), subs(y=0.75, r=2, k2plot)], x=0..16, color
     =["DarkGreen", "NavyBlue", "Red", "Orange", "Black"], legend=["z/H=0", "z/H=0.25",
     "z/H=0.5", "z/H=0.625", "z/H=0.75"], labels=["kαH ",
     "k_2 percentage of composite cantilever action"], labeldirections=["horizontal",
     "vertical"]), plot([subs(y=0, r=2,-k1plot), subs(y=0.25, r=2,-k1plot), subs(y=0.5, r
     =2,-k1plot), subs(y=0.625, r=2,-k1plot), subs(y=0.75, r=2,-k1plot)], x=0..16, color
     =["DarkGreen", "NavyBlue", "Red", "Orange", "Black"], legend=["z/H=0", "z/H=0.25",
     "z/H=0.5", "z/H=0.625", "z/H=0.75"], labels=["kαH ",
     "(k_1 percentage of individual cantilever action)-1 "], labeldirections=["horizontal",
      "vertical"]), title
     ="variation of wall moment factor k_1 and k_2 for point load with nb, 2 ");
    dualaxisplot(plot([subs(y=0, r=3, k2plot), subs(y=0.25, r=3, k2plot), subs(y=0.5, r
     =3, k2plot), subs(y=0.625, r=3, k2plot), subs(y=0.75, r=3, k2plot)], x=0..16, color
     =["DarkGreen", "NavyBlue", "Red", "Orange", "Black"], legend=["z/H=0", "z/H=0.25",
     "z/H=0.5", "z/H=0.625", "z/H=0.75"], labels=["kαH ",
     "k_2 percentage of composite cantilever action"], labeldirections=["horizontal",
     "vertical"]), plot([subs(y=0, r=3,-k1plot), subs(y=0.25, r=3,-k1plot), subs(y=0.5, r
     =3,-k1plot), subs(y=0.625, r=3,-k1plot), subs(y=0.75, r=3,-k1plot)], x=0..16, color
     =["DarkGreen", "NavyBlue", "Red", "Orange", "Black"], legend=["z/H=0", "z/H=0.25",
     "z/H=0.5", "z/H=0.625", "z/H=0.75"], labels=["kαH ",
     "(k_1 percentage of individual cantilever action)-1 "], labeldirections=["horizontal",
      "vertical"]), title
     ="variation of wall moment factor k_1 and k_2 for point load with nb, 3 ");
    dualaxisplot(plot([subs(y=0, r=4, k2plot), subs(y=0.25, r=4, k2plot), subs(y=0.5, r
     =4, k2plot), subs(y=0.625, r=4, k2plot), subs(y=0.75, r=4, k2plot)], x=0..16, color
     =["DarkGreen", "NavyBlue", "Red", "Orange", "Black"], legend=["z/H=0", "z/H=0.25",
     "z/H=0.5", "z/H=0.625", "z/H=0.75"], labels=["kαH ",
     "k_2 percentage of composite cantilever action"], labeldirections=["horizontal",
     "vertical"]), plot([subs(y=0, r=4,-k1plot), subs(y=0.25, r=4,-k1plot), subs(y=0.5, r
     =4,-k1plot), subs(y=0.625, r=4,-k1plot), subs(y=0.75, r=4,-k1plot)], x=0..16, color
     =["DarkGreen", "NavyBlue", "Red", "Orange", "Black"], legend=["z/H=0", "z/H=0.25",
     "z/H=0.5", "z/H=0.625", "z/H=0.75"], labels=["kαH ",
     "(k_1 percentage of individual cantilever action)-1 "], labeldirections=["horizontal",
      "vertical"]), title
     ="variation of wall moment factor k_1 and k_2 for point load with nb, 4 ");
    dualaxisplot(plot([subs(y=0, r=5, k2plot), subs(y=0.25, r=5, k2plot), subs(y=0.5, r
     =5, k2plot), subs(y=0.625, r=5, k2plot), subs(y=0.75, r=5, k2plot)], x=0..16, color
     =["DarkGreen", "NavyBlue", "Red", "Orange", "Black"], legend=["z/H=0", "z/H=0.25",
     "z/H=0.5", "z/H=0.625", "z/H=0.75"], labels=["kαH ",
     "k_2 percentage of composite cantilever action"], labeldirections=["horizontal",
     "vertical"]), plot([subs(y=0, r=5,-k1plot), subs(y=0.25, r=5,-k1plot), subs(y=0.5, r
     =5,-k1plot), subs(y=0.625, r=1,-k1plot), subs(y=0.75, r=5,-k1plot)], x=0..16, color
     =["DarkGreen", "NavyBlue", "Red", "Orange", "Black"], legend=["z/H=0", "z/H=0.25",
     "z/H=0.5", "z/H=0.625", "z/H=0.75"], labels=["kαH ",
     "(k_1 percentage of individual cantilever action)-1 "], labeldirections=["horizontal",
      "vertical"]), title
     ="variation of wall moment factor k_1 and k_2 for point load with nb, 5 ");
```

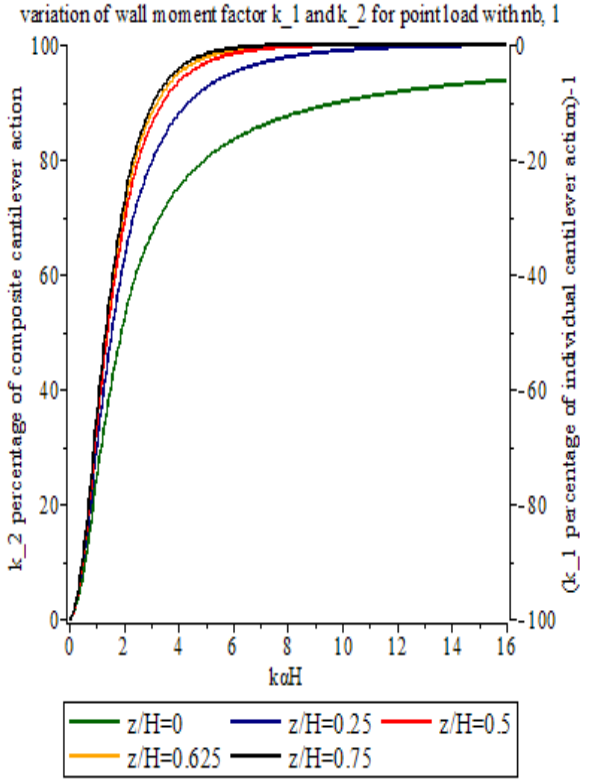
variation of wall moment factor k_1 and k_2 for point load with nb, 1
k_2 percentage of composite cantilever action
(k_1 percentage of individual cantilever action)-1
kαH
z/H=0
z/H=0.25
z/H=0.5
z/H=0.625
z/H=0.75

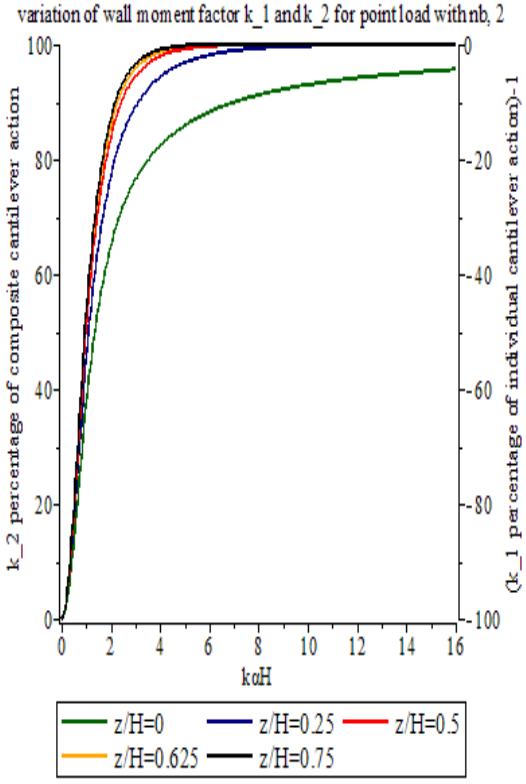
variation of wall moment factor k_1 and k_2 for point load with nb, 2
k_2 percentage of composite cantilever action
(k_1 percentage of individual cantilever action)-1
kαH
z/H=0
z/H=0.25
z/H=0.5
z/H=0.625
z/H=0.75

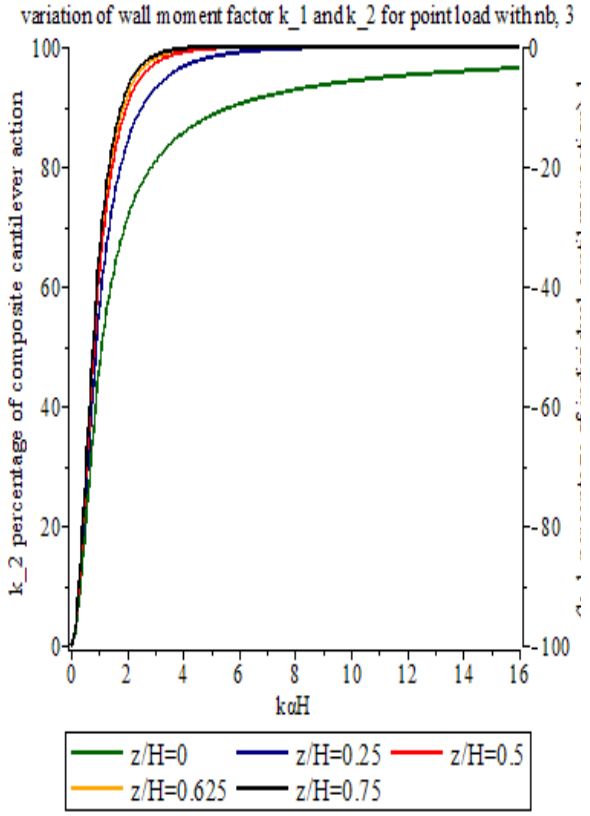
variation of wall moment factor k_1 and k_2 for point load with nb, 3
k_2 percentage of composite cantilever action
kαH
z/H=0
z/H=0.25
z/H=0.5
z/H=0.625
z/H=0.75

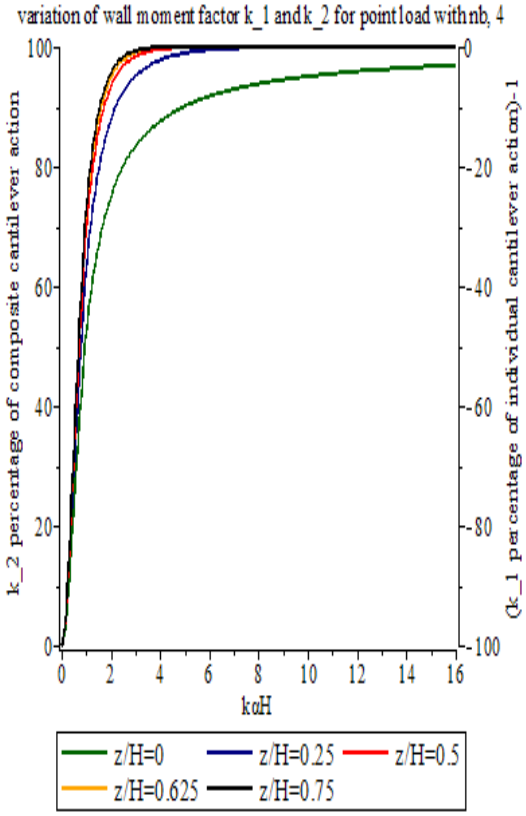
variation of wall moment factor k_1 and k_2 for point load with nb, 4
k_2 percentage of composite cantilever action
(k_1 percentage of individual cantilever action)-1
kαH
z/H=0
z/H=0.25
z/H=0.5
z/H=0.625
z/H=0.75

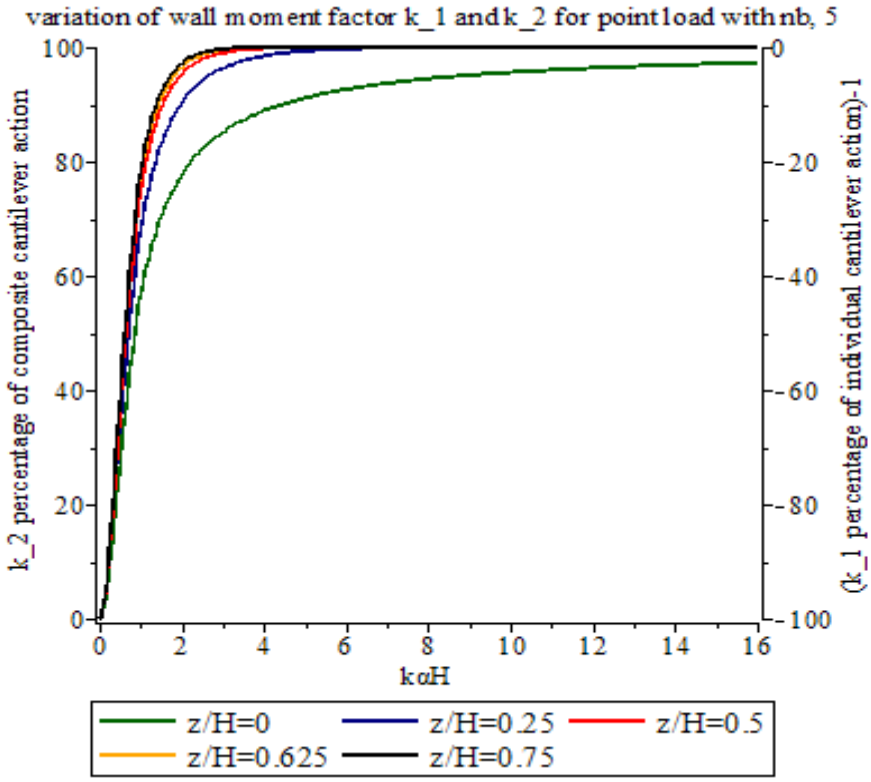
variation of wall moment factor k_1 and k_2 for point load with nb, 5
k_2 percentage of composite cantilever action
(k_1 percentage of individual cantilever action)-1
100
80
60
40
20
0
0
-20
-40
-60
-80
-100
0
2
4
6
8
10
12
14
16
kαH
z/H=0
z/H=0.25
z/H=0.5
z/H=0.625
z/H=0.75

APPENDIX 2: COMPUTATION OF NATURAL VIBRATION FREQUENCY FACTOR

```
> restart;
```

$$> x(z) := \frac{1}{6}\,\frac{1}{nb^{3/2}\,E\,i\,k^5\,\alpha^3\cosh\left(\sqrt{nb}\,k\,\alpha\,H\right)}\left(P\left(3\,H k^5 z^2 nb^{3/2}\alpha^3\cosh\left(\sqrt{nb}\,k\,\alpha\,H\right)\right.\right.$$
$$-z^3 k^5 nb^{3/2}\alpha^3\cosh\left(\sqrt{nb}\,k\,\alpha\,H\right)-3\,H z^2 nb^{3/2}\alpha^3 k^3\cosh\left(\sqrt{nb}\,k\,\alpha\,H\right)$$
$$+z^3 nb^{3/2}\alpha^3 k^3\cosh\left(\sqrt{nb}\,k\,\alpha\,H\right)+6\cosh\left(\sqrt{nb}\,k\,\alpha\,H\right)\alpha\,k\sqrt{nb}\,z+6\sinh\left(\sqrt{nb}\,k\,\alpha\,H\right.$$
$$\left.\left.-\sqrt{nb}\,k\,\alpha\,z\right)-6\sinh\left(\sqrt{nb}\,k\,\alpha\,H\right)\right)\right);$$

$$x(z) := \frac{1}{6}\,\frac{1}{nb^{3/2}\,E\,i\,k^5\,\alpha^3\cosh\left(\sqrt{nb}\,k\,\alpha\,H\right)}\left(P\left(3\,H k^5 z^2 nb^{3/2}\alpha^3\cosh\left(\sqrt{nb}\,k\,\alpha\,H\right)\right.\right. \tag{34}$$
$$-z^3 k^5 nb^{3/2}\alpha^3\cosh\left(\sqrt{nb}\,k\,\alpha\,H\right)-3\,H z^2 nb^{3/2}\alpha^3 k^3\cosh\left(\sqrt{nb}\,k\,\alpha\,H\right)$$
$$+z^3 nb^{3/2}\alpha^3 k^3\cosh\left(\sqrt{nb}\,k\,\alpha\,H\right)+6\cosh\left(\sqrt{nb}\,k\,\alpha\,H\right)\alpha\,k\sqrt{nb}\,z+6\sinh\left(\sqrt{nb}\,k\,\alpha\,H\right.$$
$$\left.\left.-\sqrt{nb}\,k\,\alpha\,z\right)-6\sinh\left(\sqrt{nb}\,k\,\alpha\,H\right)\right)\right)$$

```
> F3(z) := expand( (3·E·i)/(P·H^3) ·x(z) );
```

$$F3(z) := \frac{3}{2}\,\frac{z^2}{H^2}-\frac{1}{2}\,\frac{z^3}{H^3}-\frac{3}{2}\,\frac{z^2}{H^2 k^2}+\frac{1}{2}\,\frac{z^3}{H^3 k^2}+\frac{3\,z}{H^3\,nb\,k^4\,\alpha^2} \tag{35}$$
$$+\frac{3\sinh\left(\sqrt{nb}\,k\,\alpha\,H\right)\cosh\left(\sqrt{nb}\,k\,\alpha\,z\right)}{H^3\,nb^{3/2}\,k^5\,\alpha^3\cosh\left(\sqrt{nb}\,k\,\alpha\,H\right)}-\frac{3\sinh\left(\sqrt{nb}\,k\,\alpha\,z\right)}{H^3\,nb^{3/2}\,k^5\,\alpha^3}$$
$$-\frac{3\sinh\left(\sqrt{nb}\,k\,\alpha\,H\right)}{H^3\,nb^{3/2}\,k^5\,\alpha^3\cosh\left(\sqrt{nb}\,k\,\alpha\,H\right)}$$

```
> xdyn(z) := (P·H^3)/(3·E·i) ·F3(z);
```

$$xdyn(z) := \frac{1}{3}\,\frac{1}{E\,i}\left(P\,H^3\left(\frac{3}{2}\,\frac{z^2}{H^2}-\frac{1}{2}\,\frac{z^3}{H^3}-\frac{3}{2}\,\frac{z^2}{H^2 k^2}+\frac{1}{2}\,\frac{z^3}{H^3 k^2}+\frac{3\,z}{H^3\,nb\,k^4\,\alpha^2}\right.\right. \tag{36}$$
$$+\frac{3\sinh\left(\sqrt{nb}\,k\,\alpha\,H\right)\cosh\left(\sqrt{nb}\,k\,\alpha\,z\right)}{H^3\,nb^{3/2}\,k^5\,\alpha^3\cosh\left(\sqrt{nb}\,k\,\alpha\,H\right)}-\frac{3\sinh\left(\sqrt{nb}\,k\,\alpha\,z\right)}{H^3\,nb^{3/2}\,k^5\,\alpha^3}$$
$$\left.\left.-\frac{3\sinh\left(\sqrt{nb}\,k\,\alpha\,H\right)}{H^3\,nb^{3/2}\,k^5\,\alpha^3\cosh\left(\sqrt{nb}\,k\,\alpha\,H\right)}\right)\right)$$

```
> Px(H) := subs(z=H, xdyn(z))·P;
```

$$Px(H) := \frac{1}{3}\,\frac{P^2 H^3\left(1-\frac{1}{k^2}+\frac{3}{H^2\,nb\,k^4\,\alpha^2}-\frac{3\sinh\left(\sqrt{nb}\,k\,\alpha\,H\right)}{H^3\,nb^{3/2}\,k^5\,\alpha^3\cosh\left(\sqrt{nb}\,k\,\alpha\,H\right)}\right)}{E\,i} \tag{37}$$

```
> (H^3·F3(z))^2;
```

$$H^6\left(\frac{3}{2}\,\frac{z^2}{H^2}-\frac{1}{2}\,\frac{z^3}{H^3}-\frac{3}{2}\,\frac{z^2}{H^2 k^2}+\frac{1}{2}\,\frac{z^3}{H^3 k^2}+\frac{3\,z}{H^3\,nb\,k^4\,\alpha^2}\right. \tag{38}$$
$$+\frac{3\sinh\left(\sqrt{nb}\,k\,\alpha\,H\right)\cosh\left(\sqrt{nb}\,k\,\alpha\,z\right)}{H^3\,nb^{3/2}\,k^5\,\alpha^3\cosh\left(\sqrt{nb}\,k\,\alpha\,H\right)}-\frac{3\sinh\left(\sqrt{nb}\,k\,\alpha\,z\right)}{H^3\,nb^{3/2}\,k^5\,\alpha^3}$$
$$\left.-\frac{3\sinh\left(\sqrt{nb}\,k\,\alpha\,H\right)}{H^3\,nb^{3/2}\,k^5\,\alpha^3\cosh\left(\sqrt{nb}\,k\,\alpha\,H\right)}\right)^2$$

$$
> \int_0^H \left(H^6 \left(\frac{3}{2}\,\frac{z^2}{H^2} - \frac{1}{2}\,\frac{z^3}{H^3} - \frac{3}{2}\,\frac{z^2}{H^2 k^2} + \frac{1}{2}\,\frac{z^3}{H^3 k^2} + \frac{3\,z}{H^3\, nb\, k^4\, \alpha^2} \right.\right.
$$

$$
+ \frac{3\sinh\left(\sqrt{nb}\,k\,\alpha\,H\right)\cosh\left(\sqrt{nb}\,k\,\alpha\,z\right)}{H^3\, nb^{3/2}\, k^5\, \alpha^3 \cosh\left(\sqrt{nb}\,k\,\alpha\,H\right)} - \frac{3\sinh\left(\sqrt{nb}\,k\,\alpha\,z\right)}{H^3\, nb^{3/2}\, k^5\, \alpha^3}
$$

$$
\left.\left. - \frac{3\sinh\left(\sqrt{nb}\,k\,\alpha\,H\right)}{H^3\, nb^{3/2}\, k^5\, \alpha^3 \cosh\left(\sqrt{nb}\,k\,\alpha\,H\right)} \right)^2 \right) \mathrm{d}z;
$$

$$
\frac{3}{280}\,\frac{1}{nb^{13/2}\, k^{11}\, \alpha^7 \cosh\left(\sqrt{nb}\,k\,\alpha\,H\right)^2} \left(\left(1680\, H \cosh\left(\sqrt{nb}\,k\,\alpha\,H\right)^2 nb^{7/2}\, \mathrm{e}^{2\sqrt{nb}\,k\alpha H}\, \alpha\, k^3 \right.\right. \tag{39}
$$

$$
- 1680 \cosh\left(\sqrt{nb}\,k\,\alpha\,H\right) \sinh\left(\sqrt{nb}\,k\,\alpha\,H\right) \mathrm{e}^{2\sqrt{nb}\,k\alpha H}\, k^2\, nb^3
$$

$$
- 840\, H\, \mathrm{e}^{3\sqrt{nb}\,k\alpha H}\, k\,\alpha\, nb^{7/2} \cosh\left(\sqrt{nb}\,k\,\alpha\,H\right)^2
$$

$$
- 840\, H\, k\,\alpha\, nb^{7/2} \cosh\left(\sqrt{nb}\,k\,\alpha\,H\right)^2 \mathrm{e}^{2\sqrt{nb}\,k\alpha H}
$$

$$
- 840\, H^2 \sinh\left(\sqrt{nb}\,k\,\alpha\,H\right) nb^4\, k^2\, \alpha^2 \cosh\left(\sqrt{nb}\,k\,\alpha\,H\right) \mathrm{e}^{2\sqrt{nb}\,k\alpha H}
$$

$$
- 210\, H^4 \sinh\left(\sqrt{nb}\,k\,\alpha\,H\right) nb^5\, k^6\, \alpha^4 \cosh\left(\sqrt{nb}\,k\,\alpha\,H\right) \mathrm{e}^{2\sqrt{nb}\,k\alpha H}
$$

$$
+ 280\, H^3 \sinh\left(\sqrt{nb}\,k\,\alpha\,H\right) \mathrm{e}^{3\sqrt{nb}\,k\alpha H}\, nb^{9/2}\, k^5\, \alpha^3 \cosh\left(\sqrt{nb}\,k\,\alpha\,H\right)
$$

$$
+ 210\, H^4 \sinh\left(\sqrt{nb}\,k\,\alpha\,H\right) nb^5\, k^4\, \alpha^4 \cosh\left(\sqrt{nb}\,k\,\alpha\,H\right) \mathrm{e}^{2\sqrt{nb}\,k\alpha H}
$$

$$
- 280\, H^3 \sinh\left(\sqrt{nb}\,k\,\alpha\,H\right) \mathrm{e}^{3\sqrt{nb}\,k\alpha H}\, nb^{9/2}\, k^3\, \alpha^3 \cosh\left(\sqrt{nb}\,k\,\alpha\,H\right)
$$

$$
- 420\, H^2 \sinh\left(\sqrt{nb}\,k\,\alpha\,H\right) \mathrm{e}^{3\sqrt{nb}\,k\alpha H}\, nb^4\, k^4\, \alpha^2 \cosh\left(\sqrt{nb}\,k\,\alpha\,H\right)
$$

$$
+ 420\, H^2 \sinh\left(\sqrt{nb}\,k\,\alpha\,H\right) \mathrm{e}^{3\sqrt{nb}\,k\alpha H}\, nb^4\, k^2\, \alpha^2 \cosh\left(\sqrt{nb}\,k\,\alpha\,H\right)
$$

$$
+ 840\, H \sinh\left(\sqrt{nb}\,k\,\alpha\,H\right) \mathrm{e}^{3\sqrt{nb}\,k\alpha H}\, k\,\alpha\, nb^{7/2} \cosh\left(\sqrt{nb}\,k\,\alpha\,H\right)
$$

$$
+ 210\, \mathrm{e}^{4\sqrt{nb}\,k\alpha H}\, nb^3 \cosh\left(\sqrt{nb}\,k\,\alpha\,H\right)^2 + 840\, \mathrm{e}^{3\sqrt{nb}\,k\alpha H}\, nb^3 \cosh\left(\sqrt{nb}\,k\,\alpha\,H\right)^2
$$

$$
- 840\, \mathrm{e}^{3\sqrt{nb}\,k\alpha H}\, nb^3\, k^2 \cosh\left(\sqrt{nb}\,k\,\alpha\,H\right)^2
$$

$$
- 210 \sinh\left(\sqrt{nb}\,k\,\alpha\,H\right) \mathrm{e}^{4\sqrt{nb}\,k\alpha H}\, nb^3 \cosh\left(\sqrt{nb}\,k\,\alpha\,H\right)
$$

$$
- 840 \sinh\left(\sqrt{nb}\,k\,\alpha\,H\right) \mathrm{e}^{3\sqrt{nb}\,k\alpha H}\, nb^3 \cosh\left(\sqrt{nb}\,k\,\alpha\,H\right)
$$

$$
+ 2100 \sinh\left(\sqrt{nb}\,k\,\alpha\,H\right) nb^3 \cosh\left(\sqrt{nb}\,k\,\alpha\,H\right) \mathrm{e}^{2\sqrt{nb}\,k\alpha H}
$$

$$
+ 840\, nb^3\, k^2 \cosh\left(\sqrt{nb}\,k\,\alpha\,H\right)^2 \mathrm{e}^{\sqrt{nb}\,k\alpha H} - 1260\, H\, k\,\alpha\, nb^{7/2}\, \mathrm{e}^{2\sqrt{nb}\,k\alpha H}
$$

$$
+ 840 \sinh\left(\sqrt{nb}\,k\,\alpha\,H\right) \mathrm{e}^{3\sqrt{nb}\,k\alpha H}\, nb^3\, k^2 \cosh\left(\sqrt{nb}\,k\,\alpha\,H\right)
$$

$$
+ 840 \sinh\left(\sqrt{nb}\,k\,\alpha\,H\right) nb^3\, k^2 \cosh\left(\sqrt{nb}\,k\,\alpha\,H\right) \mathrm{e}^{\sqrt{nb}\,k\alpha H} - 105\, \mathrm{e}^{4\sqrt{nb}\,k\alpha H}\, nb^3
$$

$$
+ 840\, \mathrm{e}^{3\sqrt{nb}\,k\alpha H}\, nb^3 - 840\, nb^3\, \mathrm{e}^{\sqrt{nb}\,k\alpha H} - 210 \cosh\left(\sqrt{nb}\,k\,\alpha\,H\right)^2 nb^3
$$

$$
+ 280\, H^3\, nb^{9/2}\, k^3\, \alpha^3 \cosh\left(\sqrt{nb}\,k\,\alpha\,H\right)^2 \mathrm{e}^{\sqrt{nb}\,k\alpha H}
$$

$$
- 420\, H^2\, nb^4\, k^4\, \alpha^2 \cosh\left(\sqrt{nb}\,k\,\alpha\,H\right)^2 \mathrm{e}^{\sqrt{nb}\,k\alpha H}
$$

$$
+ 420\, H^2\, nb^4\, k^2\, \alpha^2 \cosh\left(\sqrt{nb}\,k\,\alpha\,H\right)^2 \mathrm{e}^{\sqrt{nb}\,k\alpha H}
$$

$$
- 840\, H \sinh\left(\sqrt{nb}\,k\,\alpha\,H\right) k\,\alpha\, nb^{7/2} \cosh\left(\sqrt{nb}\,k\,\alpha\,H\right) \mathrm{e}^{\sqrt{nb}\,k\alpha H}
$$

$$
- 280\, H^3\, nb^{9/2}\, k^5\, \alpha^3 \cosh\left(\sqrt{nb}\,k\,\alpha\,H\right)^2 \mathrm{e}^{\sqrt{nb}\,k\alpha H}
$$

$$
+ 420\, H^2\, \mathrm{e}^{3\sqrt{nb}\,k\alpha H}\, nb^4\, k^4\, \alpha^2 \cosh\left(\sqrt{nb}\,k\,\alpha\,H\right)^2
$$

$$
- 420\, H^2\, \mathrm{e}^{3\sqrt{nb}\,k\alpha H}\, nb^4\, k^2\, \alpha^2 \cosh\left(\sqrt{nb}\,k\,\alpha\,H\right)^2
$$

$$
+ 22\, H^7\, nb^{13/2}\, k^{11}\, \alpha^7 \cosh\left(\sqrt{nb}\,k\,\alpha\,H\right)^2 \mathrm{e}^{2\sqrt{nb}\,k\alpha H}
$$

$$
- 44\, H^7\, nb^{13/2}\, k^9\, \alpha^7 \cosh\left(\sqrt{nb}\,k\,\alpha\,H\right)^2 \mathrm{e}^{2\sqrt{nb}\,k\alpha H}
$$

$$
+ 22\, H^7\, nb^{13/2}\, k^7\, \alpha^7 \cosh\left(\sqrt{nb}\,k\,\alpha\,H\right)^2 \mathrm{e}^{2\sqrt{nb}\,k\alpha H}
$$

$$
+ 154\, H^5\, nb^{11/2}\, k^7\, \alpha^5 \cosh\left(\sqrt{nb}\,k\,\alpha\,H\right)^2 \mathrm{e}^{2\sqrt{nb}\,k\alpha H}
$$

$$
\begin{aligned}
&- 154\,H^5\,nb^{11/2}\,k^5\,\alpha^5\cosh\left(\sqrt{nb}\,k\alpha H\right)^2 e^{2\sqrt{nb}\,k\alpha H} \\
&- 280\,H^3\,e^{3\sqrt{nb}\,k\alpha H}\,nb^{9/2}\,k^5\,\alpha^3\cosh\left(\sqrt{nb}\,k\alpha H\right)^2 \\
&+ 280\,H^3\,e^{3\sqrt{nb}\,k\alpha H}\,nb^{9/2}\,k^3\,\alpha^3\cosh\left(\sqrt{nb}\,k\alpha H\right)^2 \\
&+ 280\,H^3\,nb^{9/2}\,k^3\,\alpha^3\cosh\left(\sqrt{nb}\,k\alpha H\right)^2 e^{2\sqrt{nb}\,k\alpha H} \\
&- 840\,H\,k\,\alpha\,nb^{7/2}\cosh\left(\sqrt{nb}\,k\alpha H\right)^2 e^{\sqrt{nb}\,k\alpha H} \\
&- 420\,H^2\sinh\left(\sqrt{nb}\,k\alpha H\right)nb^4\,k^4\,\alpha^2\cosh\left(\sqrt{nb}\,k\alpha H\right)e^{\sqrt{nb}\,k\alpha H} \\
&+ 420\,H^2\sinh\left(\sqrt{nb}\,k\alpha H\right)nb^4\,k^2\,\alpha^2\cosh\left(\sqrt{nb}\,k\alpha H\right)e^{\sqrt{nb}\,k\alpha H} \\
&- 280\,H^3\sinh\left(\sqrt{nb}\,k\alpha H\right)nb^{9/2}\,k^5\,\alpha^3\cosh\left(\sqrt{nb}\,k\alpha H\right)e^{\sqrt{nb}\,k\alpha H} \\
&+ 280\,H^3\sinh\left(\sqrt{nb}\,k\alpha H\right)nb^{9/2}\,k^3\,\alpha^3\cosh\left(\sqrt{nb}\,k\alpha H\right)e^{\sqrt{nb}\,k\alpha H} \\
&- 840\cosh\left(\sqrt{nb}\,k\alpha H\right)^2 e^{\sqrt{nb}\,k\alpha H}\,nb^3 + 105\,nb^3 \\
&- 840\cosh\left(\sqrt{nb}\,k\alpha H\right)\sinh\left(\sqrt{nb}\,k\alpha H\right)e^{\sqrt{nb}\,k\alpha H}\,nb^3 \\
&- 210\cosh\left(\sqrt{nb}\,k\alpha H\right)\sinh\left(\sqrt{nb}\,k\alpha H\right)nb^3\Big)\,e^{-2\sqrt{nb}\,k\alpha H}\Big)
\end{aligned}
$$

> $den := \dfrac{simplify(combine(convert(\mathbf{(39)}, trig)))\cdot m\cdot P^2}{(3\cdot E\cdot i)^2}$;

$$
\begin{aligned}
den := \frac{1}{420}\,&\frac{1}{nb^{7/2}\,k^{11}\,\alpha^7\left(\cosh\left(2\sqrt{nb}\,k\alpha H\right)+1\right)E^2\,i^2}\Big(\big(-1680\sqrt{nb}\,k\alpha H \\
&- 420\,H^2\sinh\left(2\sqrt{nb}\,k\alpha H\right)\alpha^2\,k^2\,nb + 840\,H\cosh\left(2\sqrt{nb}\,k\alpha H\right)\alpha\,k^3\sqrt{nb} \\
&- 1680\,H\cosh\left(\sqrt{nb}\,k\alpha H\right)\alpha\,k\sqrt{nb} - 420\,H\cosh\left(2\sqrt{nb}\,k\alpha H\right)\alpha\,k\sqrt{nb} \\
&+ 11\,H^7\cosh\left(2\sqrt{nb}\,k\alpha H\right)\alpha^7\,k^{11}\,nb^{7/2} - 22\,H^7\cosh\left(2\sqrt{nb}\,k\alpha H\right)\alpha^7\,k^9\,nb^{7/2} \\
&+ 11\,H^7\cosh\left(2\sqrt{nb}\,k\alpha H\right)\alpha^7\,k^7\,nb^{7/2} + 77\,H^5\cosh\left(2\sqrt{nb}\,k\alpha H\right)\alpha^5\,k^7\,nb^{5/2} \\
&- 77\,H^5\cosh\left(2\sqrt{nb}\,k\alpha H\right)\alpha^5\,k^5\,nb^{5/2} - 560\,H^3\cosh\left(\sqrt{nb}\,k\alpha H\right)\alpha^3\,k^5\,nb^{3/2} \\
&+ 560\,H^3\cosh\left(\sqrt{nb}\,k\alpha H\right)\alpha^3\,k^3\,nb^{3/2} + 140\,H^3\cosh\left(2\sqrt{nb}\,k\alpha H\right)\alpha^3\,k^3\,nb^{3/2} \\
&- 105\,H^4\sinh\left(2\sqrt{nb}\,k\alpha H\right)\alpha^4\,k^6\,nb^2 + 105\,H^4\sinh\left(2\sqrt{nb}\,k\alpha H\right)\alpha^4\,k^4\,nb^2 \\
&+ 11\,H^7\,\alpha^7\,k^{11}\,nb^{7/2} - 22\,H^7\,\alpha^7\,k^9\,nb^{7/2} + 11\,H^7\,\alpha^7\,k^7\,nb^{7/2} + 77\,H^5\,\alpha^5\,k^7\,nb^{5/2} \\
&- 77\,H^5\,\alpha^5\,k^5\,nb^{5/2} + 140\,H^3\,\alpha^3\,k^3\,nb^{3/2} + 840\,H\,\alpha\,k^3\sqrt{nb} + 1680\sinh\left(\sqrt{nb}\,k\alpha H\right) \\
&+ 1050\sinh\left(2\sqrt{nb}\,k\alpha H\right) - 840\sinh\left(2\sqrt{nb}\,k\alpha H\right)k^2\big)\,m\,P^2\Big)
\end{aligned}
\qquad \textbf{(40)}
$$

> $\omega sqr := simplify\left(combine\left(\dfrac{Px(H)}{den}\right)\right)$;

$$
\begin{aligned}
\omega sqr := \big(&140\,E\,\alpha^4\,i\,k^6\,nb^2\left(3\,H^3\cosh\left(\sqrt{nb}\,k\alpha H\right)\alpha^3\,k^5\,nb^{3/2}\right. \\
&+ H^3\cosh\left(3\sqrt{nb}\,k\alpha H\right)\alpha^3\,k^5\,nb^{3/2} - 3\,H^3\cosh\left(\sqrt{nb}\,k\alpha H\right)\alpha^3\,k^3\,nb^{3/2} \\
&- H^3\,nb^{3/2}\,\alpha^3\,k^3\cosh\left(3\sqrt{nb}\,k\alpha H\right) + 9\,H\cosh\left(\sqrt{nb}\,k\alpha H\right)\alpha\,k\sqrt{nb} \\
&\left.+ 3\,H\sqrt{nb}\,\alpha\,k\cosh\left(3\sqrt{nb}\,k\alpha H\right) - 3\sinh\left(\sqrt{nb}\,k\alpha H\right) - 3\sinh\left(3\sqrt{nb}\,k\alpha H\right)\right)\big)\Big/ \\
&\big(m\left(-1680\sqrt{nb}\,k\alpha H - 66\,H^7\cosh\left(\sqrt{nb}\,k\alpha H\right)nb^{7/2}\,\alpha^7\,k^9\right. \\
&- 22\,H^7\,nb^{7/2}\,\alpha^7\,k^9\cosh\left(3\sqrt{nb}\,k\alpha H\right) + 33\,H^7\cosh\left(\sqrt{nb}\,k\alpha H\right)nb^{7/2}\,\alpha^7\,k^7 \\
&\left.+ 11\,H^7\,nb^{7/2}\,\alpha^7\,k^7\cosh\left(3\sqrt{nb}\,k\alpha H\right) + 231\,H^5\cosh\left(\sqrt{nb}\,k\alpha H\right)nb^{5/2}\,\alpha^5\,k^7\right.
\end{aligned}
\qquad \textbf{(41)}
$$

$$+77\,H^5\,nb^{5/2}\,\alpha^5\,k^7\cosh\left(3\sqrt{nb}\,k\,\alpha\,H\right)-231\,H^5\cosh\left(\sqrt{nb}\,k\,\alpha\,H\right)nb^{5/2}\,\alpha^5\,k^5$$
$$-77\,H^5\,nb^{5/2}\,\alpha^5\,k^5\cosh\left(3\sqrt{nb}\,k\,\alpha\,H\right)-105\,H^4\,\alpha^4\,k^6\,nb^2\sinh\left(\sqrt{nb}\,k\,\alpha\,H\right)$$
$$-105\,H^4\,\alpha^4\,k^6\,nb^2\sinh\left(3\sqrt{nb}\,k\,\alpha\,H\right)+105\,H^4\,\alpha^4\,k^4\,nb^2\sinh\left(\sqrt{nb}\,k\,\alpha\,H\right)$$
$$+105\,H^4\,\alpha^4\,k^4\,nb^2\sinh\left(3\sqrt{nb}\,k\,\alpha\,H\right)-560\,H^3\,nb^{3/2}\,\alpha^3\,k^5\cosh\left(2\sqrt{nb}\,k\,\alpha\,H\right)$$
$$+140\,H^3\,nb^{3/2}\,\alpha^3\,k^3\cosh\left(3\sqrt{nb}\,k\,\alpha\,H\right)-420\,H^2\,\alpha^2\,k^2\,nb\sinh\left(\sqrt{nb}\,k\,\alpha\,H\right)$$
$$-420\,H^2\,\alpha^2\,k^2\,nb\sinh\left(3\sqrt{nb}\,k\,\alpha\,H\right)+2520\,H\cosh\left(\sqrt{nb}\,k\,\alpha\,H\right)\sqrt{nb}\,\alpha\,k^3$$
$$+840\,H\sqrt{nb}\,\alpha\,k^3\cosh\left(3\sqrt{nb}\,k\,\alpha\,H\right)-420\,H\sqrt{nb}\,\alpha\,k\cosh\left(3\sqrt{nb}\,k\,\alpha\,H\right)$$
$$+33\,H^7\cosh\left(\sqrt{nb}\,k\,\alpha\,H\right)nb^{7/2}\,\alpha^7\,k^{11}+11\,H^7\,nb^{7/2}\,\alpha^7\,k^{11}\cosh\left(3\sqrt{nb}\,k\,\alpha\,H\right)$$
$$-3780\,H\cosh\left(\sqrt{nb}\,k\,\alpha\,H\right)\alpha\,k\sqrt{nb}-1680\,H\cosh\left(2\sqrt{nb}\,k\,\alpha\,H\right)\alpha\,k\sqrt{nb}$$
$$+420\,H^3\cosh\left(\sqrt{nb}\,k\,\alpha\,H\right)\alpha^3\,k^3\,nb^{3/2}+560\,H^3\cosh\left(2\sqrt{nb}\,k\,\alpha\,H\right)\alpha^3\,k^3\,nb^{3/2}$$
$$-560\,H^3\,nb^{3/2}\,\alpha^3\,k^5+560\,H^3\,\alpha^3\,k^3\,nb^{3/2}+1050\sinh\left(\sqrt{nb}\,k\,\alpha\,H\right)$$
$$+1050\sinh\left(3\sqrt{nb}\,k\,\alpha\,H\right)+1680\sinh\left(2\sqrt{nb}\,k\,\alpha\,H\right)-840\,k^2\sinh\left(\sqrt{nb}\,k\,\alpha\,H\right)$$
$$-840\,k^2\sinh\left(3\sqrt{nb}\,k\,\alpha\,H\right)\Big)\Big)$$

> $Fωn := simplify\left(combine\left(((41))^{0.5}\cdot\left(\frac{m}{E\cdot i}\right)^{0.5}\right)\right);$

$Fωn :=$ **(42)**

$$11.83215957$$
$$\Big(\Big(E\,\alpha^4\,i\,k^6\,nb^2\left(3\,H^3\cosh\left(\sqrt{nb}\,k\,\alpha\,H\right)\alpha^3\,k^5\,nb^{3/2}\right.$$
$$+H^3\cosh\left(3\sqrt{nb}\,k\,\alpha\,H\right)\alpha^3\,k^5\,nb^{3/2}-3\,H^3\cosh\left(\sqrt{nb}\,k\,\alpha\,H\right)\alpha^3\,k^3\,nb^{3/2}$$
$$-H^3\,nb^{3/2}\,\alpha^3\,k^3\cosh\left(3\sqrt{nb}\,k\,\alpha\,H\right)+9\,H\cosh\left(\sqrt{nb}\,k\,\alpha\,H\right)\alpha\,k\sqrt{nb}$$
$$\left.+3\,H\sqrt{nb}\,\alpha\,k\cosh\left(3\sqrt{nb}\,k\,\alpha\,H\right)-3\sinh\left(\sqrt{nb}\,k\,\alpha\,H\right)-3\sinh\left(3\sqrt{nb}\,k\,\alpha\,H\right)\right)\Big)\Big/$$
$$\Big(m\left(-1680\sqrt{nb}\,k\,\alpha\,H-66\,H^7\cosh\left(\sqrt{nb}\,k\,\alpha\,H\right)nb^{7/2}\,\alpha^7\,k^9\right.$$
$$-22\,H^7\,nb^{7/2}\,\alpha^7\,k^9\cosh\left(3\sqrt{nb}\,k\,\alpha\,H\right)+33\,H^7\cosh\left(\sqrt{nb}\,k\,\alpha\,H\right)nb^{7/2}\,\alpha^7\,k^7$$
$$+11\,H^7\,nb^{7/2}\,\alpha^7\,k^7\cosh\left(3\sqrt{nb}\,k\,\alpha\,H\right)+231\,H^5\cosh\left(\sqrt{nb}\,k\,\alpha\,H\right)nb^{5/2}\,\alpha^5\,k^7$$
$$+77\,H^5\,nb^{5/2}\,\alpha^5\,k^7\cosh\left(3\sqrt{nb}\,k\,\alpha\,H\right)-231\,H^5\cosh\left(\sqrt{nb}\,k\,\alpha\,H\right)nb^{5/2}\,\alpha^5\,k^5$$
$$-77\,H^5\,nb^{5/2}\,\alpha^5\,k^5\cosh\left(3\sqrt{nb}\,k\,\alpha\,H\right)-105\,H^4\,\alpha^4\,k^6\,nb^2\sinh\left(\sqrt{nb}\,k\,\alpha\,H\right)$$
$$-105\,H^4\,\alpha^4\,k^6\,nb^2\sinh\left(3\sqrt{nb}\,k\,\alpha\,H\right)+105\,H^4\,\alpha^4\,k^4\,nb^2\sinh\left(\sqrt{nb}\,k\,\alpha\,H\right)$$
$$+105\,H^4\,\alpha^4\,k^4\,nb^2\sinh\left(3\sqrt{nb}\,k\,\alpha\,H\right)-560\,H^3\,nb^{3/2}\,\alpha^3\,k^5\cosh\left(2\sqrt{nb}\,k\,\alpha\,H\right)$$
$$+140\,H^3\,nb^{3/2}\,\alpha^3\,k^3\cosh\left(3\sqrt{nb}\,k\,\alpha\,H\right)-420\,H^2\,\alpha^2\,k^2\,nb\sinh\left(\sqrt{nb}\,k\,\alpha\,H\right)$$
$$-420\,H^2\,\alpha^2\,k^2\,nb\sinh\left(3\sqrt{nb}\,k\,\alpha\,H\right)+2520\,H\cosh\left(\sqrt{nb}\,k\,\alpha\,H\right)\sqrt{nb}\,\alpha\,k^3$$
$$+840\,H\sqrt{nb}\,\alpha\,k^3\cosh\left(3\sqrt{nb}\,k\,\alpha\,H\right)-420\,H\sqrt{nb}\,\alpha\,k\cosh\left(3\sqrt{nb}\,k\,\alpha\,H\right)$$
$$+33\,H^7\cosh\left(\sqrt{nb}\,k\,\alpha\,H\right)nb^{7/2}\,\alpha^7\,k^{11}+11\,H^7\,nb^{7/2}\,\alpha^7\,k^{11}\cosh\left(3\sqrt{nb}\,k\,\alpha\,H\right)$$
$$-3780\,H\cosh\left(\sqrt{nb}\,k\,\alpha\,H\right)\alpha\,k\sqrt{nb}-1680\,H\cosh\left(2\sqrt{nb}\,k\,\alpha\,H\right)\alpha\,k\sqrt{nb}$$
$$+420\,H^3\cosh\left(\sqrt{nb}\,k\,\alpha\,H\right)\alpha^3\,k^3\,nb^{3/2}+560\,H^3\cosh\left(2\sqrt{nb}\,k\,\alpha\,H\right)\alpha^3\,k^3\,nb^{3/2}$$
$$-560\,H^3\,nb^{3/2}\,\alpha^3\,k^5+560\,H^3\,\alpha^3\,k^3\,nb^{3/2}+1050\sinh\left(\sqrt{nb}\,k\,\alpha\,H\right)$$
$$+1050\sinh\left(3\sqrt{nb}\,k\,\alpha\,H\right)+1680\sinh\left(2\sqrt{nb}\,k\,\alpha\,H\right)-840\,k^2\sinh\left(\sqrt{nb}\,k\,\alpha\,H\right)$$
$$\left.-840\,k^2\sinh\left(3\sqrt{nb}\,k\,\alpha\,H\right)\right)\Big)\Big)^{1/2}\sqrt{\frac{m}{E\,i}}$$

```
> Fω
```

$$:= 0.1536644100\sqrt{77}\left(\left(x^4y^2r^2\left(\frac{1}{3}x\left(x^2(y-1)(y+1)r^{3/2}+3\sqrt{r}\right)\cosh(3\sqrt{r}x)-\sinh(3\sqrt{r}x)\right.\right.\right.$$
$$\left.+\left((y^2-1)x^3r^{3/2}+3\sqrt{r}x\right)\cosh(\sqrt{r}x)-\sinh(\sqrt{r}x)\right)\Big)\Big/\left(\left(\frac{1}{3}x\left(\frac{20}{11}x^2r^{3/2}\right.\right.\right.$$
$$\left.+\frac{1}{7}x^6(y-1)^2(y+1)^2r^{7/2}+x^4(y-1)(y+1)r^{5/2}+\sqrt{r}\left(\frac{120}{11}y^2-\frac{60}{11}\right)\right)$$
$$\cosh(3\sqrt{r}x)+\left(\frac{50}{11}-\frac{5}{11}x^4y^2r^2+\frac{5}{11}x^4r^2+\left(-\frac{20}{11}x^2r-\frac{40}{11}y^2\right)\right)\sinh(3\sqrt{r}x)$$
$$-\frac{80}{33}x\left(x^2(y-1)(y+1)r^{3/2}+3\sqrt{r}\right)\cosh(2\sqrt{r}x)+\frac{80}{11}\sinh(2\sqrt{r}x)$$
$$+\left(\frac{20}{11}x^3r^{3/2}+\left(\frac{1}{7}x^7y^4-\frac{2}{7}x^7y^2+\frac{1}{7}x^7\right)r^{7/2}+(x^5y^2-x^5)r^{5/2}+\left(\frac{120}{11}xy^2\right.\right.$$
$$\left.\left.-\frac{180}{11}x\right)\sqrt{r}\right)\cosh(\sqrt{r}x)+\left(\frac{50}{11}-\frac{5}{11}x^4y^2r^2+\frac{5}{11}x^4r^2+\left(-\frac{20}{11}x^2r\right.\right.$$
$$\left.\left.\left.\left.-\frac{40}{11}y^2\right)\right)\sinh(\sqrt{r}x)+\left(-\frac{80}{33}x^3y^2+\frac{80}{33}x^3\right)r^{3/2}-\frac{80}{11}\sqrt{r}x\right)\right)\right)\quad;$$

$$Fω := \quad \textbf{(43)}$$

$$0.1536644100\sqrt{77}\left(\left(x^4y^2r^2\left(\frac{1}{3}x\left(x^2(y-1)(y+1)r^{3/2}+3\sqrt{r}\right)\cosh(3\sqrt{r}x)-\sinh(3\sqrt{r}x)\right.\right.\right.$$
$$\left.+\left((y^2-1)x^3r^{3/2}+3\sqrt{r}x\right)\cosh(\sqrt{r}x)-\sinh(\sqrt{r}x)\right)\Big)\Big/\left(\frac{1}{3}x\left(\frac{20}{11}x^2r^{3/2}\right.\right.$$
$$\left.+\frac{1}{7}x^6(y-1)^2(y+1)^2r^{7/2}+x^4(y-1)(y+1)r^{5/2}+\sqrt{r}\left(\frac{120}{11}y^2-\frac{60}{11}\right)\right)$$
$$\cosh(3\sqrt{r}x)+\left(\frac{50}{11}-\frac{5}{11}x^4y^2r^2+\frac{5}{11}x^4r^2-\frac{20}{11}x^2r-\frac{40}{11}y^2\right)\sinh(3\sqrt{r}x)$$
$$-\frac{80}{33}x\left(x^2(y-1)(y+1)r^{3/2}+3\sqrt{r}\right)\cosh(2\sqrt{r}x)+\frac{80}{11}\sinh(2\sqrt{r}x)$$
$$+\left(\frac{20}{11}x^3r^{3/2}+\left(\frac{1}{7}x^7y^4-\frac{2}{7}x^7y^2+\frac{1}{7}x^7\right)r^{7/2}+(x^5y^2-x^5)r^{5/2}+\left(\frac{120}{11}xy^2\right.\right.$$
$$\left.\left.-\frac{180}{11}x\right)\sqrt{r}\right)\cosh(\sqrt{r}x)+\left(\frac{50}{11}-\frac{5}{11}x^4y^2r^2+\frac{5}{11}x^4r^2-\frac{20}{11}x^2r\right.$$
$$\left.\left.-\frac{40}{11}y^2\right)\sinh(\sqrt{r}x)+\left(-\frac{80}{33}x^3y^2+\frac{80}{33}x^3\right)r^{3/2}-\frac{80}{11}\sqrt{r}x\right)\Big)$$

```
> plot([subs(y=1.01, r=1, Fω), subs(y=1.05, r=1, Fω), subs(y=1.1, r=1, Fω), subs(y=1.15,
  r=1, Fω), subs(y=1.2, r=1, Fω), subs(y=1.25, r=1, Fω)], x=.1 .. 16, color
  =["DarkGreen", "NavyBlue", "Red", "Orange", "Black", "Niagara Purple"], legend=["k=1",
  "k=1.05", "k=1.1", "k=1.15", "k=1.2", "k=1.25"], title
  ="Variation of frequency factor Fω, for point load, nb=1", labels=["k αH",
  "frequency factor Fω"], labeldirections=["horizontal", "vertical"]);
```

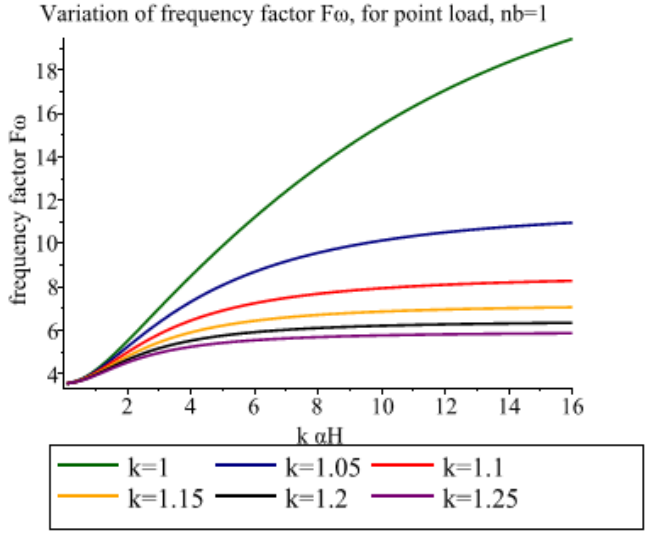

APPENDIX 3: REPRESENTATIVE MODEL AND RESULT OUTPUT

Sample model for the illustrative example and its result outputs for the given loading:

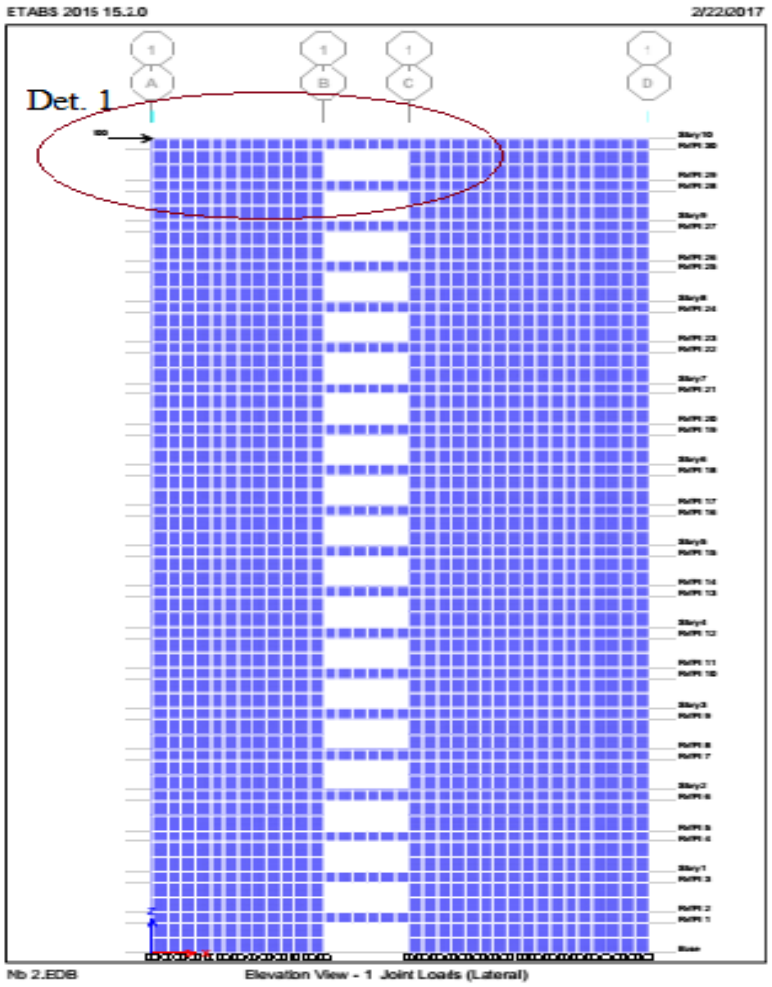

Detail 1

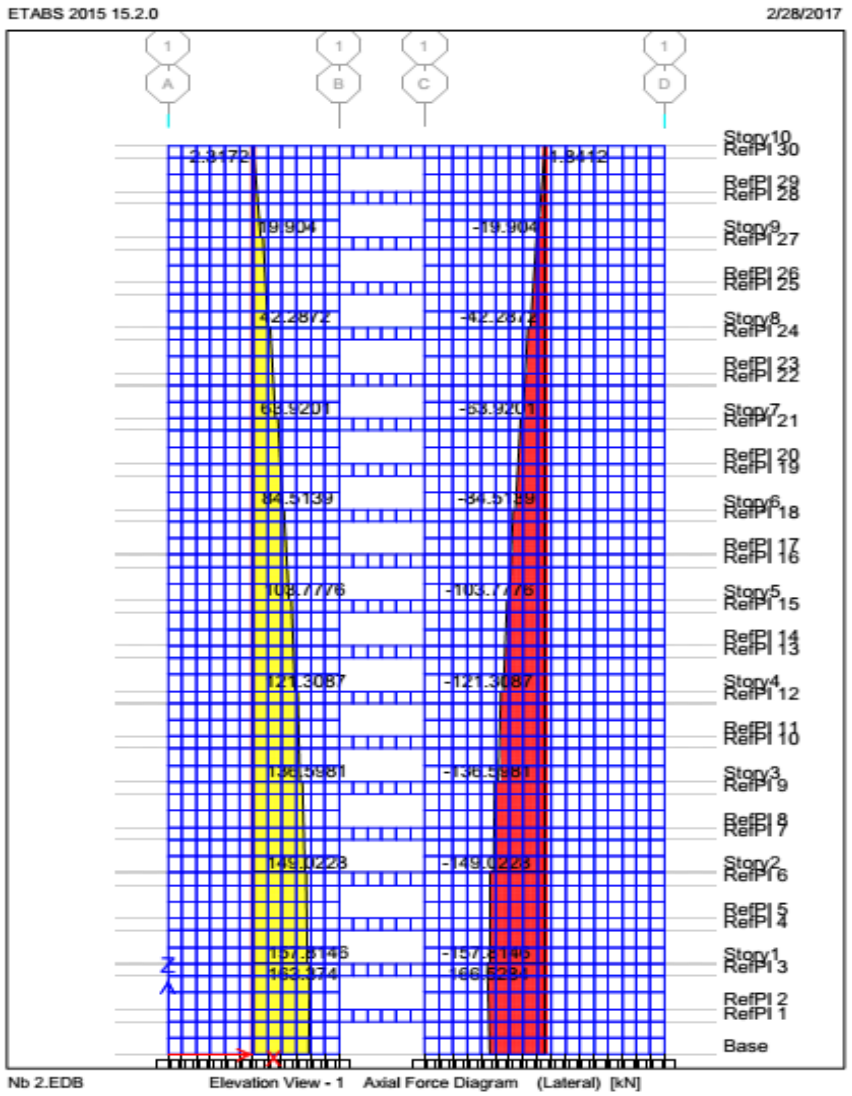

ETABs output for axial force in walls

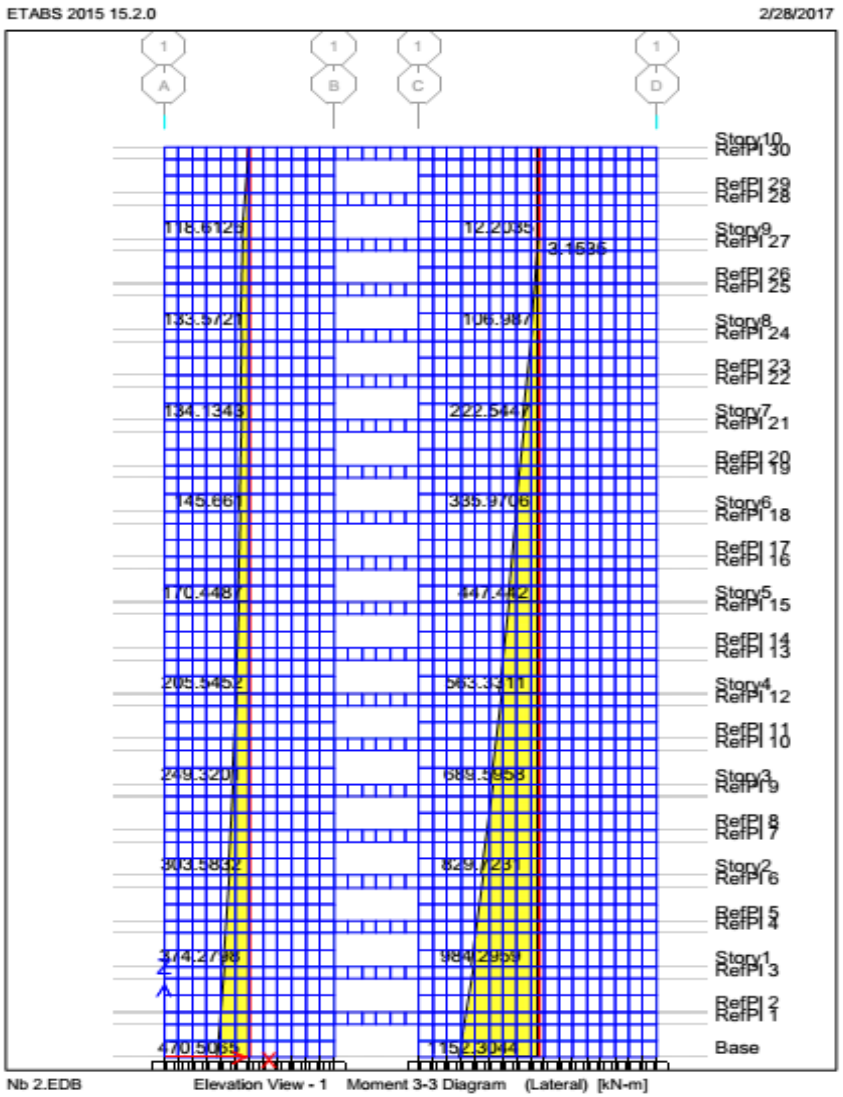

ETABs output for bending moment in walls

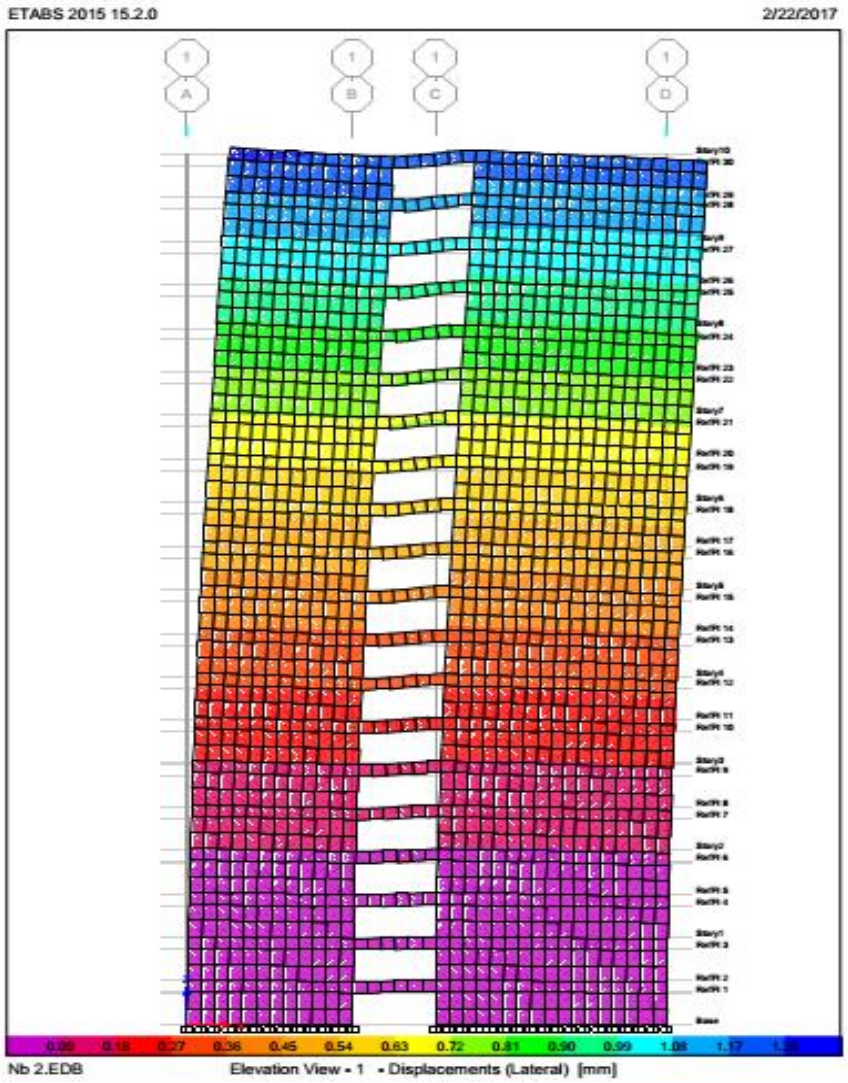

ETABs output for deflection of the coupled shear walls

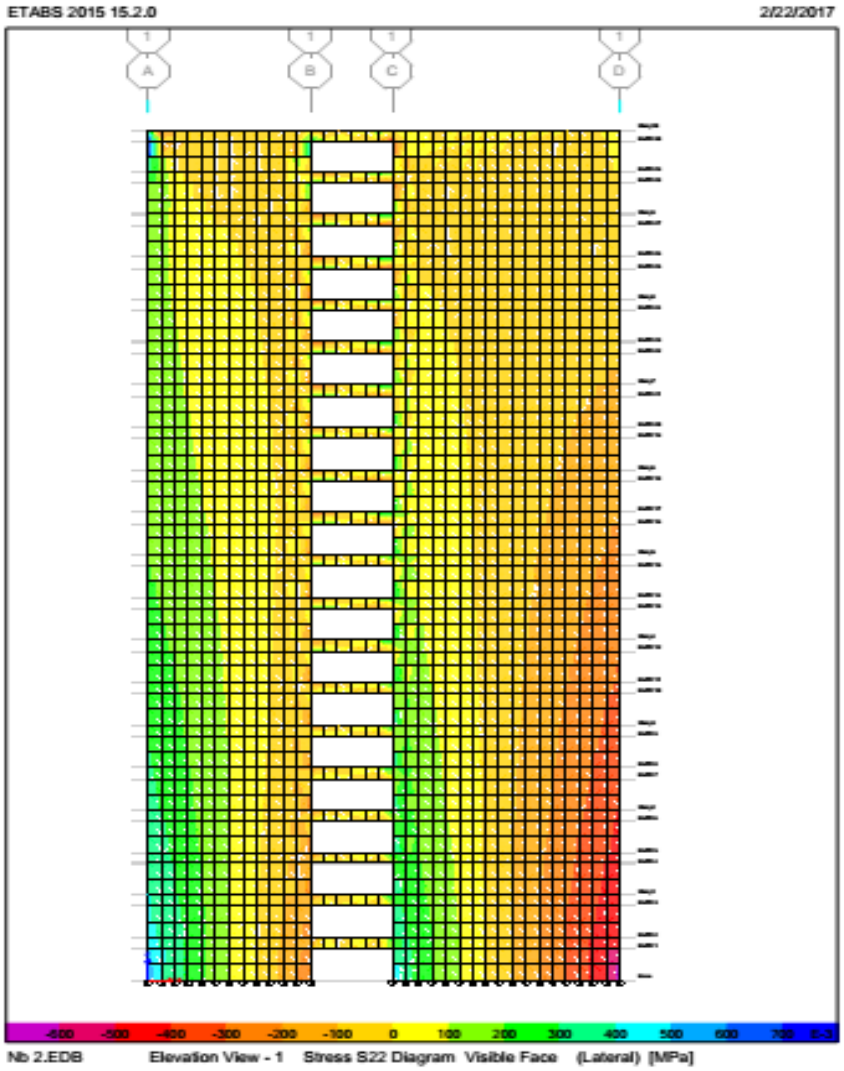

ETABs output for Stress in the walls

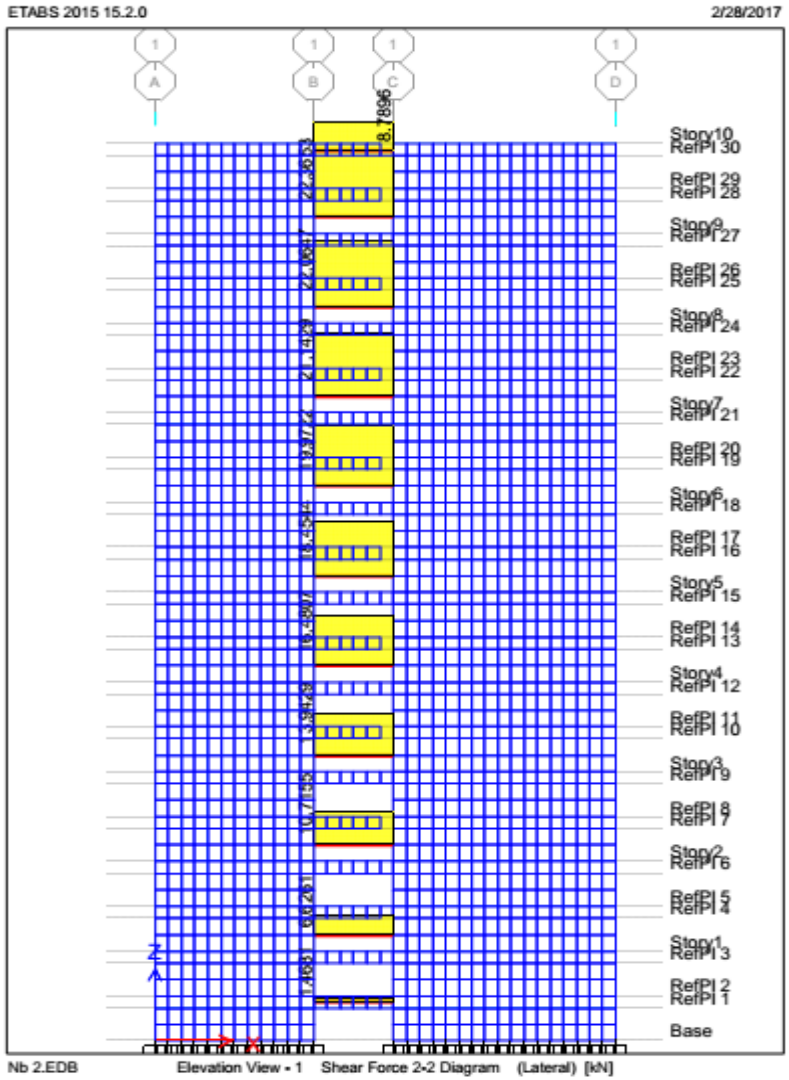

Shear force in the spandrels

This Page Is Left Blank Intentionally